LONG-TERM ASSESSMENT OF
PASSENGER GROUND TRANSPORTATION
SYSTEM TECHNOLOGY

Prepared for

Federal Railroad Administration
U.S. Department of Transportation

CONTRACT NO. DOT-FR-9097

by

Department of Mechanical Engineering
Massachusetts Institute of Technology

1. Report No. DOT/FRA/ORD-82/48	2. Government Accession No.	3. Recipient's Catalog No.
4. Title and Subtitle LONG TERM ASSESSMENT OF PASSENGER GROUND TRANSPORTATION SYSTEM TECHNOLOGY		5. Report Date February 1982
		6. Performing Organization Code
7. Author(s) David N. Wormley and James H. Goldie		8. Performing Organization Report No.
9. Performing Organization Name and Address Department of Mechanical Engineering Massachusetts Institute of Technology Cambridge, MA 02139		10. Work Unit No. (TRAIS)
		11. Contract or Grant No. DOT-FR-9097
12. Sponsoring Agency Name and Address Federal Railroad Administration U.S. Department of Transportation Washington, D.C. 20590		13. Type of Report and Period Covered FINAL REPORT, 8/79-1/82
		14. Sponsoring Agency Code

15. Supplementary Notes

16. Abstract

In this study advanced intercity ground transportation has been reviewed to establish the present status and future directions of worldwide technology development. The study has focused in detail on noncontacting types of suspension and propulsion technology while citing significant developments in the last decade of advanced, conventional rail systems placed into intercity revenue service.

A limited analytical and experimental evaluation of hybrid types of systems employing noncontacting propulsion with conventional rail systems has been performed. A linear induction motor propulsion system for rail vehicles which utilizes conventional rail as the reaction rail has been studied using analytical models validated with scale model experimental test data for thrust normal force, efficiency and power factor.

17. Key Words Noncontacting Suspension Propulsion, Linear Induction Motors, Magnetic Suspensions	18. Distribution Statement Document is available to the public through the National Technical Information Service, Springfield, VA 22161		
19. Security Classif. (of this report) UNCLASSIFIED	20. Security Classif. (of this page) UNCLASSIFIED	21. No. of Pages	22. Price

Form DOT F 1700.7 (8-72)   Reproduction of completed page authorized

-i-

The objective of this study is to provide basic information to planners in Government, State, and industry, to facilitate their assessment of the available options for future passenger transportation systems. To this end, advanced intercity passenger ground transportation research has been reviewed to establish the present status and future directions of worldwide technology development. While the study has focused primarily upon advanced noncontacting types of suspension and propulsion, recent significant improvements in intercity, passenger rail transportation have been noted. The study has also included a limited analysis and experimental evaluation (using an existing scale-model laboratory test facility at MIT) of hybrid propulsion/suspension systems which utilize linear electric motor technology operating on conventional rails.

Systems employing noncontacting suspension and propulsion have attracted worldwide attention for the past two decades because of their potential to accommodate guideway irregularities and to operate at high speeds, favoring increased productivity and anticipated low maintenance with the elimination of wheels. While early effort considered both air cushion and magnetic systems, at the present time development effort is focused primarily on magnetically levitated systems employing electric propulsion. A major barrier to the deployment of these systems has been the uncertainty associated with development of a new technology.

One of the primary factors limiting the introduction of new systems is the need for large investments of capital. This has resulted in an interest in hybrid systems, because these systems have the potential to utilize existing rail infrastructure with elements of noncontacting technology to reduce large initial capital investment and yet gain the operational benefits of the new technology.

The two most significant current development projects in intercity magnetically levitated systems directed to eventual deployment of revenue service systems are:

(1) The Federal Republic of West Germany system which incorporates an electromagnetic suspension vehicle operating on an active track. Test vehicles employing magnetic suspension and propulsion elements have been tested at 250 km/hr. Prototype vehicle/guideway tests are planned for 1982.

(2) A Japanese National Railway system which employs an electrodynamic system operating on an active track. An experimental vehicle has been operated at speeds in excess of 500 km/hr.

Both systems are at the stage of prototype vehicle/guideway test and evaluation, and many of the major technical feasibility issues for these systems are addressed. Application assessment studies of these magnetic systems are continuing and are also currently in progress in Canada for an intercity system and in Britain for airport access.

In the the United States the level of activity concerning non-contacting suspension and propulsion systems has decreased in the last five years with very little current activity.

The study has also cited the development for revenue service of advanced rail passenger intercity systems in the last decade including the Japanese National Railroad Shinkansen Line, the British Advanced Passenger Train, and the French Tres Grande Vitesse which is planned to operate at 300 km/hr. All these systems operate on electrified lines. The development of advanced high-speed rail systems has provided a possible alternative to noncontacting systems for operation in the 200-300 km/hr range.

A limited evaluation of hybrid systems employing noncontacting linear motor technology to provide and/or supplement the propulsion/braking of wheeled vehicles operating on conventional rails has been performed using an existing scale-model laboratory test facility. The use of noncontacting propulsion/braking forces, not limited by wheel/rail adhesion,and coupled with the attractive force generated by the linear induction motor between the vehicle and the rail, enhances the capability to operate under adverse weather conditions and on grades, as well as decreases the possibility of derailment. The experimental test data and application analysis have determined the size, weight, and power requirements for a linear induction motor-propelled light rail vehicle. The analysis has indiciated that the thrust/braking forces required in a light rail vehicle can be proviced by a linear induction motor. The combined weight of the propulsion system and associated power conditioning unit considered in the analysis approaches 20 percent of vehicle weight for operating speeds of 250 km/hr.

METRIC CONVERSION FACTORS

Approximate Conversions to Metric Measures

Symbol	When You Know	Multiply by	To Find	Symbol
LENGTH				
in	inches	*2.5	centimeters	cm
ft	feet	30	centimeters	cm
yd	yards	0.9	meters	m
mi	miles	1.6	kilometers	km
AREA				
in²	square inches	6.5	square centimeters	cm²
ft²	square feet	0.09	square meters	m²
yd²	square yards	0.8	square meters	m²
mi²	square miles	2.6	square kilometers	km²
	acres	0.4	hectares	ha
MASS (weight)				
oz	ounces	28	grams	g
lb	pounds	0.45	kilograms	kg
	short tons (2000 lb)	0.9	tonnes	t
VOLUME				
tsp	teaspoons	5	milliliters	ml
Tbsp	tablespoons	15	milliliters	ml
fl oz	fluid ounces	30	milliliters	ml
c	cups	0.24	liters	l
pt	pints	0.47	liters	l
qt	quarts	0.95	liters	l
gal	gallons	3.8	liters	l
ft³	cubic feet	0.03	cubic meters	m³
yd³	cubic yards	0.76	cubic meters	m³
TEMPERATURE (exact)				
°F	Fahrenheit temperature	5/9 (after subtracting 32)	Celsius temperature	°C

*1 in = 2.54 (exactly). For other exact conversions and more detailed tables, see NBS Misc. Publ. 286, Units of Weights and Measures, Price $2.25, SD Catalog No. C13.10:286.

Approximate Conversions from Metric Measures

Symbol	When You Know	Multiply by	To Find	Symbol
LENGTH				
mm	millimeters	0.04	inches	in
cm	centimeters	0.4	inches	in
m	meters	3.3	feet	ft
m	meters	1.1	yards	yd
km	kilometers	0.6	miles	mi
AREA				
cm²	square centimeters	0.16	square inches	in²
m²	square meters	1.2	square yards	yd²
km²	square kilometers	0.4	square miles	mi²
ha	hectares (10,000 m²)	2.5	acres	
MASS (weight)				
g	grams	0.035	ounces	oz
kg	kilograms	2.2	pounds	lb
t	tonnes (1000 kg)	1.1	short tons	
VOLUME				
ml	milliliters	0.03	fluid ounces	fl oz
l	liters	2.1	pints	pt
l	liters	1.06	quarts	qt
l	liters	0.26	gallons	gal
m³	cubic meters	35	cubic feet	ft³
m³	cubic meters	1.3	cubic yards	yd³
TEMPERATURE (exact)				
°C	Celsius temperature	9/5 (then add 32)	Fahrenheit temperature	°F

°F -40   0   32   40   98.6   80   120   160   200   212
°C -40 -20   0   20   37   40   60   80   100

TABLE OF CONTENTS

LIST OF FIGURES

LIST OF TABLES

1. INTRODUCTION

1.1 BACKGROUND

In the past decade considerable worldwide attention has been directed to advanced intercity ground transportation systems. Early in the decade effort could be categorized as directed to:

(1) Tracked, Levitated Vehicle Systems (TLV)
TLV systems include magnetically and air levitated, guided and propelled systems operating on decicated passive or active guideway systems.

(2) Conventional Rail Systems (CR)
CR systems constitute conventional trains running on passive steel rails.

TLV systems have been considered as a promising transportation option for the future. For low-speed (less than 100 km/hr) urban vehicles, the advantages of physical simplicity, low-noise levels, low-unit loadings on guideways, and associated low guideway maintenance costs and the ability to move laterally in and out of off-line stations are attractive and when combined, offer the potential for the operation of quiet, clean, effective systems. For intercity high speeds (150-500 km/hr), these vehicles have potentially high performance in terms of accommodating guideway irregularities while maintaining passenger comfort, have propulsion systems that are not limited by wheel-rail adhesion limits and offer enhanced safety and reduced maintenance cost compared with conventional vehicles. High speed also offers increased capacity and productivity in terms of increased utilization of labor and capital.

Research in TLV and CR systems has been extensive as described in the references [1-63].* During the decade, significant research efforts in the technical development of TLV were undertaken by the United States, Japan, West Germany, Britain and Canada. Today, major research efforts continue in Japan and West Germany to develop revenue service systems while application studies for TLV systems are being conducted in Britain and Canada. [1] The most advanced current development programs are being pursued in Japan and West Germany.

Also during the decade several significant advances in conventional rail systems have occurred with the highly effective JNR Shinkansen Line, [48] the British Advanced Passenger Train (APT) and the French Tres Grande Vitesse (TGV), [47] which will operate at 300 km/hr.

Several studies have been conducted in assessing the relative merits of CR and TLV systems for specific sites, including the West Germany study for a new route between Hanover and Kassel, [52] the Canadian study [51] for a new link between Montreal and Toronto, and the United States study for the Northeast Corridor. [50] In these

---

*Numbers in [ ] refer to references listed in the bibliography.

studies the economics of implementing a new technology and its new technology and its new infrastructure were weighed against the benefits from potentially reduced maintenance and increased speeds.

According to thestudy of the Northeast Corridor [50] for an annual traffic growth of 5 percent after the year 2000, a noncontacting system cruising at 360 km/hr breaks even at a lower fare than does a conventional system cruising at 215 km/hr. The study also indicated that the uncertainty of projecting capital and operating costs for a new technology necessitates further research before detailed comparisons between TLV and CR systems can be made with respect to a specific route.

In the evaluation of high-speed systems it has been shown that while productivity in terms of the utilization of equipment and labor increase with increasing vehicle speeds, the energy requirements of high-speed vehicles also increase. As vehicle speeds increase above the range of 50-80 km/hr, aerodynamic drag effects become more significant than rolling resistance of wheeled vehicles and are the dominant loss in levitated vehicles. The power required by a higher speed vehicle increases approximately as the cube of the velocity, thus a vehicle operating at speeds of 400 km/hr as a power loss which is eight times that of a vehicle operating at 200 km/hr. In the study of the Northeast Corridor application, the energy penalty associated with high-speed systems has been assessed. The study has determined that a net reduction in petroleum energy use can be achieved if the introduction of a new high-speed ground system diverts sufficient passenger traffic from automobiles and aircraft to high-speed ground transportation. The number of passengers diverted depends significantly upon the total transportation system from origin to destination including local transportation services. [20]

The primary factors limiting the introduction of new high-speed systems have been related to:

    (1)   the normal uncertainty associated with the development of a new technology

    (2)   the need for large capital investment to establish new systems

In the United States the level of technical research in large scale TLV systems has decreased in the last few years and emphasis has focused more on conventional rail systems. Along with this reorientation, interest has developed in assessing combinations of TLV and CR technology to determine if improved performance may result from incorporating non-contacting propulsion methods with conventional rail systems to form hybrid types of systems which may utilize conventional track and gain the benefits of noncontacting propulsion.

1.2 RESEARCH OBJECTIVES

In this study three research objectives have been addressed:

    (1)   Assessment of the TLV Technology Base

           The literature describing the present status of

the development of TLV systems worldwide has been re-
viewed to establish the present level of the technology.
In addition a detailed review of the noncontacting
propulsion systems literature with specific emphasis
on the linear induction motor (LIM) has been performed
to establish the level of technology and potential for
application of the technology to conventional systems.

(2) Development of Performance Data for Hybrid Noncontacting
Propulsion Systems/Rail Vehicle-Track Systems

The second objective of the study has been to
develop basic analyses corroborated by experimental re-
sults to predict the forces developed in noncontacting
types of propulsion systems which may be incorporated in
CR vehicles operating on conventional rail.

(3) Application Evaluation of Noncontacting Propulsion In
Conventional Rail Applications

The third objective of the study has been to determine
the potential of utilizing noncontacting propulsion in
conventional rail applications. Application to rail
car systems at suburban and intercity speeds has been
assessed.

The results of the research directed to these objectives are
summarized in the following section.

1.3 SUMMARY

The review of the technology status for TLV systems is described
in Chapter 2. Although early TLV research was directed to both air
cushion and magnetically levitated systems, recent worldwide re-
search has concentrated on magnetically levitated systems. Two
countries are continuing research directed to revenue service
intercity TLV systems:

(1) Japan is developing a superconducting electrodynamic
suspension system vehicle operating on an active track.
Experimental vehicles have been operated on a test
track at speeds above 500 km/hr.

(2) West Germany is developing a system incorporating an
electromagnetic suspension vehicle operating on an
active track. Vehicle tests of the system are planned
in 1982. Prototype test vehicles employing electro-
magnetic suspension have been operated at speeds in
excess of 250 km/hr.

The study has also identified a number of lower speed TLV systems
either in passenger service or planned for passenger service in
localized urban areas.

A detailed review of the use of noncontacting propulsion systems
for transportation vehicle propulsion has been conducted. Non-
contacting propulsion systems thrust, power factors, and effic-
iencies have been cited, as well as laboratory experimental measure-

ment of performance. The evaluation of a full-scale urban rail transit vehicle using linear induction motor propulsion in Canada has been summarized.

An analysis has been utilized in Chapter 3, building upon techniques described in the literature, to predict the thrust, normal force, efficiency, and power factor for a noncontacting linear induction motor propulsion unit interacting with either a steel track or with an aluminum clad steel track. The analysis provides a basis for performance evaluation of a LIM incorporated in a CR vehicle.

A test facility has been utilized to experimentally measure the performance of a LIM interacting with a steel and an aluminum clad rail. Normal, lateral, and longitudinal LIM forces were measured over a wide range of operating speeds. The experimental data have agreed with the analysis described in Chapter 3.

A study of the application of the LIM to CR vehicles has been described in Chapter 5. In the study CR track is considered as the LIM reaction rail. As a part of the study the size, weight, and power requirements for a LIM propelling a light rail vehicle are computed for several vehicle operating speeds.

2. REVIEW OF ADVANCED SYSTEM TECHNOLOGY

2.1 ADVANCED VEHICLE SYSTEMS

In the last two decades, considerable research has been devoted to development of advanced ground transportation systems. Comprehensive reviews of these developments are given in references [1-6]. A summary of developments for advanced transportation systems is contained in Table 2.1. The status of the systems, listed in Table 2.1, is described below in terms of high-speed and low-speed systems.

2.1.1 High Speed Systems

Considerable attention has been devoted to air cushion vehicles with prototype vehicles built and tested in the United States, Britain, France, and West Germany, as indicated in the first entries in Table 2.1. France has demonstrated vehicles capable of 430 km/hr. In the early 1970's, West Germany built and tested the nearly identical air cushion TR03 and magnetic suspension TR02 vehicles. In the comparison, the magnetically levitated vehicle had superior performance with respect to power, noise, and maintenance. On the basis of these tests, the West German activity in air cushion vehicles stopped and effort concentrated on magnetic suspensions. Somewhat independent of the West German results, the governments of the United States, Britain and France also have terminated air cushion system development for intercity applications, largely because of the substantial investment required by implementation of a new ground transportation technology and the potential improvements envisioned for conventional rail.

The group of entries in Table 2.1 cite magnetically levitated systems. An overview of magnetic suspension and propulsion systems is contained in Table 2.2. Two basic types of suspension are indicated: the repulsion suspension and the attractive suspension. The repulsive scheme or electrodynamic suspension (EDS) employs on-board superconducting magnets that interact with passive guideway conductors for suspension and sequentially excited windings in the guideways for thrust (air core LSM). The attractive suspension technique or electromagnetic suspension (EMS) utilizes feedback-controlled electromagnets and ferromagnetic rails to create suspension forces. Propulsion is usually provided by an on-board linear induction motor (LIM) or an active track iron core linear synchronous motor (LSM).

Attractive suspension (EMS) methods have been studied for many years worldwide. Vehicle systems built in Germany and Japan have demonstrated the feasibility of using feedback control to overcome the fundamental instability of this suspension technique and to maintain a small track-vehicle magnet gap (1-3 cm). Furthermore, Japanese HSST-02 [8,9,10] and the West German KOMET M [1] have shown the advantages of a secondary suspension between the vehicle and its magnets [11], including improved ride quality and the maintenance of a small, constant air gap. The KOMET M also revealed that each suspension magnet should have its own controller. Simplicity (modular structure), reliability (chance of overall suspension failure reduced), and reduction of levitation power re-

-5-

TABLE 2.1

SUMMARY OF ADVANCED TRANSPORTATION SYSTEMS

SYSTEM	PLACE	DATE	SPEED	SIZE	SUSPENSION	PROPULSION	REMARKS
RTV 31	England, Tracked Hovercraft Ltd. (THL)	1973	Tested to 172 km/hr	22 tons, 22.1 m long	Air Cushion	SLIM (single-sided linear induction motor)	Experimental, no passengers
01 Experimental Aerotrain	France, Sociéte-de l'Aerotrain	Testing begun in 1965	Tested to 345 km/hr	10.4 m long	Air Cushion	Aircraft engine & propeller; later aircraft turbojet engine; solid fuel rocket boosters	
02 Experimental Aerotrain	France, Societe-de l'Aérotrain	1969	Reached an average speed of 411 km/hr during testing		Air Cushion	Turbojet Engine	
Suburban	France, Societe-de l'Aérotrain	Tested in 1969	Designed cruising speed of 180 km/hr	12 tons, 14.3 m long	Air Cushion	LIM	Commercial prototype, seat 44.

SYSTEM	PLACE	DATE	SPEED	SIZE
I-80	France, Sociéte-de l'Aerotrain	1969	Designed cruising speed of 250 km/hr	N.A.
I-80 high-speed aerotrain	France, Sociéte-de l'Aerotrain	1973	Reached 430 km/hr	N.A.
TR-03	Germany, Krauss-Maffei (KM)	Testing began 1972	Designed maximum speed of 140 km/hr	9.6 tons, 11.7 m long
TLRV	U.S., Grumman Aerospace	Testing began 1973	Reached 147 km/hr with aeropropulsion	15.4 tons, 15.6 m long
PTACV	U.S., Rohr Industries	Built in 1973	Reached 232 km/hr	29.6 tons, 28.6 m long

SUSPENSION	PROPULSION	REMARKS
Air Cushion	Shrouded tur- boprop system	Commercial proto- type, 80 pass
Air Cushion	N.A.	High-speed pro- pulsion was added to create this vehicle.
Air Cushion	LIM	Used for compari- son with similar magnetically levitated vehicle, the TR02: maglev shown preferable
Air Cushion	Turbofan engines; later used a LIM	Only one of two planned LIMs was ever installed
Air Cushion	DLIM (double-sided linear induc- tion motor)	Full-scale proto- type, 60 pass.

SYSTEM	PLACE	DATE	SPEED
TT1	Val~, Otis Transportation Technology Division	First demonstrated at TRANSPO '72	Maximum speed of 43.6 km/hr
EML-50	Japan, Japanese National Railways	N.A.	Tested to 40 km/hr
HSST-01	Japan, Japan Air Lines	Designed 1973; first tested 1975	Tested to 308 km/hr
HSST-02	Japan, Japan Air Lines	1976	Tested to 100 km/hr (limited by track length)

-8-

SIZE	SUSPENSION	PROPULSION	REMARKS
	Air Cushion	LIM	Operating system at Duke Univ. Med. Center; low speed automated system
1.8 tons, 2.8 m long	EMS, separate electromagnets for lift and guidance	SLIM, passive track	Built to test control system for the suspension system
1.0 tons, 4 m long, 2 seats	EMS, combined lift and guidance	SLIM, passive track	Tested high speed performance of suspension and propulsion system; tested control of vehicle-rail contact with skids at high speeds
800 kg, 6.84 m long, 7-9 seats	EMS combined lift and guidance	SLIM, passive track	JAL planned an 80-seat HSST proto- type vehicle but HSST program terminated; HSST program in- tended to improve airport access

SYSTEM	PLACE	DATE	SPEED	SIZE
ROMAG	U.S.; Rohr Industries	Exhibited TRANSPO '72	Bottom supported vehicle tested to 56 km/hr; top supported vehicle tested to 48 km/hr	N.A.
Magnet-mobil	West Germany, Messerschmitt -Bölkow- Blohm (MBB)	Demonstrated to public 1971	Designed and tested to 90 km/hr	7 tons
TR02	W. Germany, KM	Demonstrated 1971	Designed and tested to 164 km/hr	11 tons, 11.7 m long

SUSPENSION	PROPULSION	REMARKS
EMS, combined suspension and propulsion using LIM	SLIM, passive truck	Utilized the SLIM normal and lateral forces to provide suspension; SLIM operates at low slip, low power factor to provide large attractive normal force; employs a transistor inverter for power conditioning for SLIM; Boeing uses system for its Mag Transit low-speed AGT system.
EMS, separate lift and guidance	DLIM, passive track	
EMS, combined L/G	DLIM, passive track	Used for comparison with TRO3, an air cushion vehicle, to determine if maglev is preferable

	PLACE	DATE	SPEED	SIZE
TR04	W. Germany, KM	N.A.	Designed maximum speed of 250 km/hr.	16.5 tons, 15.0 m long
TR05	W. Germany, Transrapid EMS	Demonstrated in 1979	Operated up to 75 km/hr	26 m long, 68 pass.
TR06	W. Germany, Transrapid EMS	Initial testing proposed 1982	Designed for maximum speed of 400 km/hr	EMS, same as TR05
KOMET	W. Germany MBB	Tested 1976	Tested to 400 km/hr.	10 tons, 8.5 m long

-10-

SUSPENSION	PROPULSION	REMARKS
EMS, combined L/G	DLIM, passive truck	DLIM reaction rail horizontal; intended to test system components under realistic conditions
EMS, electro-magnets provide lift and propulsion, separate electro-magnets provide guidance	Iron core LSM, active track	Each electromagnet is independently sprung and controlled; called the "magnetic wheel" configuration; intended as a low speed demonstration at the International Transportation Exposition in Hamburg
Iron core LSM, active track		On-board linear generator for non-contacting power pickup
EMS, separate L/G	Hot water rocket	

SYSTEM	PLACE	DATE	SPEED
KOMET M	W. Germany, MBB	Tested in 1977	Tested to 400 km/hr.
TU02	W. Germany KM	Testing began in 1973	Low speeds
SRI sled	U.S., Stanford Research Institute	Constructed and tested 1971-1973	Tested to 42 km/hr
Magneplane	U.S., M.I.T.		
EET-01	W. Germany, Siemens		
EET-02	W. Germany, Siemens	Tested in 1979	

SIZE	SUSPENSION	PROPULSION	REMARKS
12 tons	EMS, separate L/G	Hot water rocket	Independently sprung and controlled suspension magnets
N.A.	EMS, combined L/G	LIM, passive track	12 pass. prototype of program to develop a low-speed maglev system
296 kg, 4.25 m long	EDS	towed	
small scale model	EDS	air core LSM, active track	
	EDS	LIM, passive track	Tested cryostats
	EDS	air core LSM, active track	Concluded re-pulsive suspension research in W. Germany

SYSTEM	PLACE	DATE	SPEED	SIZE
ML-100	Japan, Japan National Railway (JNR)	Built 1972	Tested to 60 km/hr.	
ML-100A	Japan, Japan National Railway (JNR)	Testing began 1975	Tested to 60 km/hr	3,600 kg, 5 m long
ML-500	Japan, JNR	Tested 1979	Tested to 517 km/hr	10,000 kg, 13.5 m long
ML-500R	Japan, JNR	Tested in 1979		
MLU-001-01	Japan, JNR	Tested in 1981	Tested to 216 km/hr.	9 tons, 13 m long

SUSPENSION	PROPULSION	REMARKS
EDS, sliding shoe guidance	DLIM, passive track	Demonstrated good ride quality, stability, and large gap for repulsive suspension
EDS	Air core LSM, active track	Propulsion and lateral guidance combined, expected deficiency in damping confirmed
EDS	Air core LSM, active track	Research vehicle, no pass. inverted-tee track, cryostats for SCM cooling
EDS	Air core LSM, active track	A refrigerator was added to ML-500 to create ML-500R for SCM cooling
EDS	Air core LSM, active track	8 pass; U-shaped guideway; eventual application to high-speed intercity transport; I-shaped SCM's integrate lift, guidance and propulsion

SYSTEM	PLACE	DATE	SPEED
Intermediate Capacity Transport System (ICTS)	Canada, Urban Transportation Development Corporation (UTDC)	Program began 1975; testing began 1978	Cruise speed 72 km/hr.
VEC	France, Cytec Inc.	N.A.	Maximum speed of 32 km/hr.
Telebus	France, French General Electric Company	Tested 1977-1979	Design speed of 10 m/sec
TGV	France	1981	Designed for 300 km/hr.

SIZE	SUSPENSION	PROPULSION	REMARKS
14.3 tons, 12.7 m long, 28 seats	Steel wheel/ rail	SLIM, passive track	83 pass. capacity for typical vehicle; different vehicle sizes possible; automated (AGT), modularized, high capacity-small headway, low speed
N.A.	N.A.	Moving belts, LIM- driven chains	Demonstrated in Paris; AGT system for short-distance, low-speed appli- cations, small headway
40 pass. test vehicle	Steel wheel/ rail	LIM, active track	Elevated guideway; copper, U-shaped, vehicle-mounted LIM reaction rail, low speed
8-car trains with a 386 pass. capacity	Wheel/rail		Will climb 16 de- gree grades; 4- minute headways possible

SYSTEM	PLACE	DATE	SPEED
C-Bahn	W. Germany, DEMAG & MBB	Development began 1969	8-12 m/sec for existing vehicles
H-Bahn	W. Germany, Siemens & DUWAG	Development began 1973, testing began 1977	Maximum design speed 50 km/hr.
M-Bahn	W. Germany, Magnetbahn	Testing began 1976	N.A.

SIZE	SUSPENSION	PROPULSION	REMARKS
Varied vehicle con-figuration	Wheel/rail	DLIM, passive track	AGT system, low speed, modulariza-tion; many vehicle configurations possible; high capacity-small head-way system, elevated
Varied vehicle con-figuration	Rubber tire	Support wheels, SLIM, or gear units in guide-way	AGT system, low speed, modular-ization, intended for medium city public transit; a feeder system for intercity transporta-tion, or airport transportation, ele-vated
6.3 m long, 16 seats	Wheels for lateral guidance, lift by on-board permanent magnets and wheels	Iron core LSM, active track	40 pass. capacity vehicles; on-board permanent magnets, reduced vehicle weight, guideway structure weight and propul-sion power require-ments according to developers, elevated AGT system

SYSTEM	PLACE	DATE	SPEED	SIZE
WEDway	U.S., Disney Productions	Began operation, Disneyworld 1975	Average speed 8 km/hr	N.A.

SUSPENSION	PROPULSION	REMARKS
Wheel/rail	SLIM, active track	AGT low-speed system; proposed as people mover at Houston International Airport

TABLE 2.2: MAGLEV SYSTEM CONFIGURATIONS

TYPE	GUIDEWAY	PROPULSION	GUIDEWAY POWER CONDITIONING	ON-BOARD POWER CONDITIONING	CRITICAL ON-BOARD SUBSYSTEMS
Attraction (EMS)	Passive Track	DLIM SLIM LSHM	NONE	Power and Control (VVVF PCU)	Power Collector (brush/rail, electric arc)
	Active Track	Iron Core LSM	LSM Power and Control	NONE	NONE
Repulsion (EDS)	Active Track	Air Core LSM	LSM Power and Control	NONE	Cryogenics (cryostat and/or refrigerator)

quirements (a result of the reduced air gap) were the primary advantages of this decentralized approach to magnet control. The West German TR05 [2,12] and the proposed TR06 [2] employ decentralized independently sprung magnets. At present, the Japanese attractive suspension development (JAL) has been terminated.

While substantial progress in demonstrating the feasibility of attractive suspension technology has been made, several technical problems still exist. For those systems that utilize a passive truck, areas of future effort include:

(1) Reliability and maintenance of power pickup equipment, especially at high speeds.

(2) Weight of the on-board power conditioning unit (PCU).

Brush-rail devices are the most obvious method of power collection. They have been proven up to high speeds. Alternatives include use of an electric arc for power transmission to the vehicle. [13] Wear is a concern in both methods; and the feasibility of wind gust extinction exists for the electric arc. On-board power conditioning weight can be reduced by the availability of wayside d.c. power, eliminating the need for on-board rectification. Consequently d.c. power distribution is being considered for passive track systems. Furthermore, research is being performed to reduce the weight of thyristor and transistor inverters. The Electric Power Systems Engineering Laboratory at MIT is doing a study to determine the optimal EMS vehicle system with respect to minimization of SLIM and PCU weight. [14] Parameter variation with simple but valid models is being used to explore the various tradeoffs. The newer transistor inverter, utilized in ROMAG, will be included in the final design.

Attractive suspension techniques that employ an active track present a different set of technical issues:

(1) Methods for activating only the portions of the guideway (block lenghts) being traversed by a vehicle

(2) Methods for providing the necessary frequencies and high voltages to the guideway

West Germany is actively pursuing these areas in its Transrapid program. There is still debate over the fundamental chocie between the active and the passive track. It is discussed in some detail in a following section since it is closely tied to the choice between the LIM and the LSM.

Repulsion suspension (EDS) techniques have also been studied worldwide. In recent research, West Germany and Japan have built and tested EDS vehicle systems. The principal benefits of EDS are its large operating air gap (~10 cm) and its inherent stability. It utilizes magnetic fields developed by on-board superconducting magnets. As the vehicle traverses the guideway conductor, currents which provide levitation are induced in the guideway.

-17-

Induced currents in the guideway increase as vehicle speed increases, causing the air gap to increase with speed. Despite the successful demonstration of EDS systems, West Germany has terminated its EDS development to concentrate on EMS vehicles. Consequently, Japan (JNR) is the leader in repulsive maglev, whereas Germany is the leader in attractive maglev.

The problems of applying repulsive suspension systems to commercial transport are:

(1) The induced guideway currents produce drag as well as lift, increasing the propulsion power requirements.

(2) The suspension is inherently undamped and provides little stiffness.

(3) The on-board cryogenic hardware for cooling the superconducting magnets is heavy.

The JNR is continuing development of high-speed repulsive vehicle systems. [1,2,5,15] JNR has developed configurations (null flux) to reduce drag and increase damping. It has successfully demonstrated an on-board refrigerator with its ML-500R vehicle. [2,6,16,17] An even lighter and more compact refrigerator has been installed on its newly constructed MLU-001 vehicle [2,6,16], which has been constructed to accommodate passengers. The liquid helium cryostats used on earlier vehicles were incapable of cooling the superconducting magnets long enough for commercial application. Research into higher critical temperature superconductors and lighter cryogenic equipment is continuing. The repulsive suspension development effort by JNR has been impressive. The ML-500 vehicle achieved a record 517 km/hr at the end of 1979.

2.1.2 Low-Speed Systems

In the last few years, considerable attention has been directed to the application of noncontacting suspension and propulsion techniques to automated low-speed transportation. At low-speeds some of the difficulties associated with high-speeds become less critical. Furthermore, most of the benefits of noncontacting suspension and propulsion may also be realized at low speeds. For example, power pick-up equipment for passive track systems is available in current technology for moderate speeds. Also, on-board power conditioning is considerably lighter for the power levels required at low speeds. Although some of the low speed vehicles employ noncontacting suspension and propulsion, most use wheels for support and guidance and a linear motor (noncontacting) for propulsion. In particular, the linear induction motor (LIM), compatible with a passive track, is attractive for low-speed systems.

The emphasis of low-speed systems has been on automation and small headways. This approach, known as Automated Guideway Transit (AGT), has pursued automation, in order to eliminate the cost of vehicle operators.

The Canadian Urban Transportation Development Corporation (UTDC) hasdeveloped the Intermediate Capacity Transportation System. (ICTS) [2,18] for urban transit. The intent is to create a capacity level higher than other surface modes. Development and testing have been conducted since 1975, and commercial application to Hamilton, Ontario, is planned. The ICTS vehicle, capable of holding 83 passengers, employs two SLIMs for propulsion and steel wheels and rails for support and guidance. With efficient auto- mation techniques, ICTS will achieve a capacity of 15,000 passen- gers/hr with headways of 50-60 sec, and a cruise speed of 45 km/hr.

In France, Cytec Inc. has developed and demonstrated an AGT system, VEC, for low-speed urban travel. [2] Moving belts and LIM-driven chains provide vehicle propulsion. Small vehicles with a maximum speed of 32 km/hr. provide service with headways as short as 2 seconds.

Telebus, developed by the French General Electric Company, utilizes a U-shpaed, vehicle-mounted copper reaction rail that interacts with guideway SLIM windings for propulsion. [2] Steel wheels and rails provide support and guidance. Testing of a 40-passenger, 10 m/s prototype was performed between 1977-1979.

West Germany has been studying three low-speed urban transport systems: the C-Bahn, the H-Bahn, and the M-Bahn. The C-Bahn [2] employs an elevated guideway, which has been standardized to in- clude many vehicle configurations. This system, tested at Hagen and an installation at the District Hospital complex in Ziegenhain, utilizes double sided LIMs for propulsion and wheels for support and guidance. Automation techniques provide small headway, high- capacity transport. The city of Hamburg has proposed an oper- ational demonstration system. The H-Bahn [2], another AGT system, has been developed and tested by Siemens at the Erlangen test track since 1977. Wheels provide support and guidance, whereas propul- sion may be provided either by a SLIM or by motor driven wheels. A modular approach permits this choice in the method of propulsion and also a variation in vehicle configuration. The M-Bahn [2] elevated AGT system, developed by Magnetbahn, utilizes an active truck LSM with onboard permanent magnets. This system has under- gone extensive testing since 1976 in Braunschweig. The LSM gives static lift, while wheels provide vertical and lateral restoring forces. The M-Bahn will be installed as transport at the Hamburg Industrial Fair in 1982-1983. The system will have seven trains of three vehicles, each with a capacity of 40 passengers.

The United States has studied four vehicle systems for low-speeds applications. Since 1968, the Transportation Technology Division of the Otis Elevator Company has been developing a LIM propelled, air cushion AGT system. [2] It was demonstrated at Transpo 72 near Washington, D.C., and has been installed at the Duke Medical Center. It could be applied to any activity center such as a business district. The WEDway People Mover [2] is an active track LIM-propelled system developed by Disney Productions for Walt Disney World. This system uses four passenger vehicles in five- car trains. The Houston International Airport has selected the WEDway system to upgrade and extend its people mover system. The

Boeing Company is continuing work on ROMAG, originally developed by Rohr, a system that employs the LIM for suspension as well as propulsion. The Boeing System, termed Mag Transit [2,19], is an extension of the technology of the ROMAG system to various AGT applications. The General Motors Research Laboratory has built and tested a LIM-propelled, magnetically suspended vehicle [2], to study the practical problems of longitudinal position and magnet control of a personal rapid transit system.

The British Railways Research Division have built a 2,700 kg vehicle and test track in 1976 to study the application of magnetic sus-pension techniques to urban transport. [2] Such a system may be built to provide a link between Birmingham Airport and Birmingham International Railway Station. The University of Sussex built a 1-ton vehicle [2,20], to study the feasibility of attractive sus-pension systems for low-speed transport.

A review of current research activities in the field of non-contacting suspension and propulsion has been prepared. [2] Much of the work is directed toward the development of alternative linear motors. This research is discussed in the following section. The work in West Germany concerning the use of on-board permanent mag-nets is very promising and is discussed below.

Researchers at the University of Braunschweig have proposed using rare earth cobalt permanent magnets in place of conventional electromagnets [21] to provide the necessary static lift. Control coils are used to vary the field strength, in order to maintain stability. However, the static load is achieved without any dissipative coil losses. There are several anticipated benefits:

(1) Reduced power losses

(2) Smaller control coils, reducing the coil time constant and permitting a smaller controller

(3) Permanent magnetic material has a low permittivity, increasing the effective magnetic gap and reducing sensitivity of suspension forces to air gap variation.

2.2   LINEAR MOTOR SUSPENSION AND PROPULSION

2.2.1   Linear Motor Research and Development

Efforts to develop new high-speed ground transportation tech-nologies since the middle 1960's have led to research in the use of the linear induction motor (LIM) for vehicle propulsion and, more recently, for vehicle suspension. Initial interest in the LIM grew from its compatibility with noncontacting suspension sys-tems, since it requires no mechanical contact with the guideway. Many studies including analytical and experimental investigations have been performed, utilizing belts and wheels to simulate motion along a track. [2,22,23,24,25,26] A review and list of refer-ences of experimental LIM studies is contained in reference [27]. Many of the vehicles included in Table 2.1 employ the LIM, demon-strating the capability of the LIM to propel a full-sized vehicle.

A principal asset of the LIM is that it permits use of a simple guideway. The vehicle is powered, while the track contains a passive conductor. The use of a passive track is significant, because the guideway represents the largest portion of the capital cost for a new ground transportation system. However, experience with the LIM has shown that the LIM has an inherently low power factor for practical operating conditions. Consequently, the West German Transrapid program has adopted the iron core linear synchronous motor (LSM) for its most recent vehicles. The iron core LSM, which utilizes an active track, has the following features:

(1) The iron core LSM can operate practically at a higher power factor than the LIM.

(2) The LSM-active track system avoids the problem of high-speed power pickup faced by the LIM-passive track scheme.

(3) The LSM-active track system does not require the heavy on-board power conditioning equipment needed by the LIM-passive track scheme.

(4) Lift can be readily incorporated into the LSM function, as demonstrated by the TR05 vehicle.

(5) The LSM-active track scheme does not require wayside power rails as does the LIM-passive track system.

The third point is tempered somewhat by the anticipated development of light, high-power transistor inverters and d.c. power distribution, eliminating the need for on-board rectification. Furthermore, PCU weight is less critical at the power levels of the low speed AGT system receiving increasing attention. With reference to the fourth point, the LIM produces forces, in addition to thrust, that could provide suspension. Considerable interest has developed in this possibility, as discussed below.

Researchers have recently developed alternative linear motors that permit the synchronous motor to be used with passive track systems. The primary alternative is the linear synchronous homopolar motor (LSHM), a short stator motor which requires both a.c. and d.c. windings on the vehicle-mounted portion and a passive ferromagnetic, notched track. Rummich [28] performed LSHM analytical work followed by analytical and experimental work by Levi at the Polytechnic Institute of New York. [29,30] General Electric has built and tested an LSHM [31] and observed an end effect similar to the LIM end effect.

An analytical-experimental study at the University of Toronto [32] has achieved reasonable agreement between theory and analysis. It suggests that the eddy current losses from the LSHM end effect is relatively small for a practical length motor providing the thrust for an urban transit vehicle. Consequently, track lamination may not be necessary. Furthermore, the study concludes that a full size LSHM could achieve a power factor of 0.72, despite experimental

values around 0.4. Researchers at the University of Manchester
in England are developing a variation of the LSHM which utilizes
a zigzag-shaped reaction rail. [2] At Queen's University in Canada,
a transverse laminated LSHM was built and tested. [2,33]

Researchers at Queen's University indicate that the transverse
flux configuration is preferable since it allows track and arma-
ture core lamination, reduces truck and core weight, and allows
satisfactory cooling of the windings. The LSHM has the potential
capability of providing vehicle suspension and propulsion. Addi-
tional linear motors being studied for application to vehicles are
listed below:

(1) Heterpolar transverse flux linear synchronous
     motor at Bath University in England [2,34]

(2) Segmental rotor (rail) linear reluctance motor
     at the University of Sussex in England [2,35]

(3) Hybrid flux reluctance motors at Brush Electrical
     Machines, Ltd., in England. [2]

(4) Linear d.c. motor (LDCM) by the Japan National
     Railway (JNR) in Japan [2,36,37]

(5) Air core linear synchronous motor using vehicle-
     mounted samarium-cobolt permanent magnets at the
     University of Toronto in Canada [2,38]

(6) Double excited linear synchronous motor (DELSYM)
     utilizing permanent magnet excitation at the
     University of Braunschweig in West Germany [39]

Professor Weh of the University of Braumschweig indicates that the
DELSYM concept can result in a passive track configuration with
comparable force densities and higher power factors and effic-
iencies than the LIM.

2.2.2 Linear Induction Motor Studies

The linear induction motor (LIM) produces forces that can be used
for vehicle suspension and propulsion. The ROMAG system [40] is
the only system listed in Table 2.1 in which the LIM provides sus-
pension as well as propulsion. It is a system worth noting be-
cause it eliminates the need for separate SLIM reaction rail and
suspension electromagnets. Boeing Aerospace Company has acquired
rights to the ROMAG system technology and is continuing development
of this concept for low-speed urban vehicles. [19]

The extension of the ROMAG concept to high speed (500 km/h) was
proposed by Rohr in 1974 and led to a MITRE-designed wheel experi-
ment conducted at Queen's University in Canada, sponsored by the
U.S. Department of Transportation. [24,41] The results suggested
that the reactive power requirement of a LIM used in the combined
suspension-propulsion configuration was high enough to require a
prohibitively large power conditioning unit (PCU) at high speed.

MITRE concluded that the SLIM normal force could be used for lateral guidance with a reasonable size PCU, and lift would have to be provided by separate electromagnets.

Concurrent with its LSHM research, General Electric built a four-pole SLIM and test facility. [23] Power factor, efficiency, flux, thrust, normal force, lateral force, pitch torque and yaw torque were all measured at various slips, offsets, frequencies and gaps. The results were compared to the predictions of a mesh matrix model.

Other recent studies have investigated conventional rail applications of the LIM. [42] Table 2.3 lists some of the specific uses proposed for the LIM.

The primary use of booster-retarders is to control the speed of freight cars as they are being coupled in classification yards. The Japanese have developed and built LIM booster-retarders, in which a carriage with attached LIM primary windings is engaged by the underside of a freight car as it coasts over the carriage. [42,43] The LIM carriage regulates the speed of the car until the car reaches its destination.

Linear eddy current brakes utilizing the LIM have been tested in France, West Germany, Switzerland, and Japan. The condition of United States track, however, requires a larger nominal air gap, reducing achievable braking forces. Consequently, application of linear eddy current brakes to United States rail vehicles requires further investigation.

An analytical and experimental study of the use of LIM forces to improve rail vehicle dynamic performance is being conducted at Princeton University. [44,45,46] The LIMs will be mounted to the truck and will interact with a reaction rail placed between the conventional rails. Laterally oriented LIMs will be used to provide controllable lateral force, whereas a longitudinal LIM will supplement braking and propulsion.

Canada is conducting research with the LIM propulsion of the Intermediate Capacity Transit System (ICTS). The ability of the LIM to provide propulsion and braking forces independent of the weather-dependent wheel-rail adhesion limit is the primary interest.

There is interest in using the SLIM with an all-steel secondary rather than the conventional aluminum or copper secondary with steel used for "back iron." The intent is to reduce the guideway reaction rail cost. In 1975, the French Transportation Institute performed tests on such a SLIM as part of a larger study of various LIM reaction rails. [2] MITRE and the Canadian Institute of Guided Ground Transport (CIGGT) conducted tests with an all-steel secondary to supplement their earlier study concerning the integration of suspension and propulsion with the SLIM. [25] The test results indicated that an all-steel reaction rail is feasible. At the time no analysis of the all-steel secondary SLIM was performed.

TABLE 2.3: APPLICATIONS OF THE LIM TO RAIL VEHICLES

Application	Advantages	Disadvantages
Freight Car Booster-Retarder	Improved control of coupling speeds	Expense
	Reduced noise levels compared with clasp type booster-retarders	Not demonstrated for heavy U.S. freight cars
Linear Eddy-Current Brake	Reliable braking independent of adhesion conditions	Braking force diminishes as air gap increases
	Reduced maintenance	Generates an attraction force toward rail
	Uses existing rails	
		Temperature rise of rail
Rail Vehicle Propulsion	Not limited by wheel-rail adhesion	Inefficiency, low power factor
Rail vehicle actuator to improve dynamic performance	Forces directly between track and truck or carbody	Not yet demonstrated

2.3 TECHNOLOGY BASE ASSESSMENT AND IMPLEMENTATION POTENTIAL

The review of the worldwide development in tracked levitated systems has indicated that the technical feasibility of such a system has been demonstrated for both air cushion and magnetic suspensions. No fundamental technical barriers exist to prohibit their implementation. However, for each of the systems further engineering development is required before it is appropriate for revenue service. Both German and Japanese research programs are continuing the engineering required to develop revenue service high-speed intercity magnetically levitated and propelled systems. While the technical issues normally associated with the development of a new system remain to be solved, as cited above, the principal current issues concern economic and service aspects of high-speed tracked-levitated systems.

A study assessing the implementation of high-speed levitated systems in the Northeast Corridor of the United States has been conducted by Aerospace Corporation. [50] In this study, the significant capital costs associated with implementation of a new system were combined with anticipated operating costs to determine revenue levels required to support such a system in the year 2000. It found that if enough passengers were diverted from air and automobile travel, a high-speed TLV system operating at 360 km/hr. would break even at a lower fare than conventional rail systems operating at 215 km/hr, if after the year 2000 annual traffic growth was 5% per year. The study also reported anticipated reductions in total petroleum use on the Northeast Corridor if a sufficient number of passengers were diverted from air and automobile travel. These findings were subject to potential inaccuracies in the estimated performance of TLV in terms of capital and operating costs.

Similar implementation studies have been conducted regarding TLV in Canada, Japan, and West Germany. [1]

The application studies assessing the implementation of TLV systems indicate that the principal barriers to implementation are:

(1) The normal uncertainties associated with the development of projected performance and reliability of a new technology

(2) The need for large capital investment to establish new systems

These factors coupled with the development of advanced rail systems such as the British APT, the French TGV, and the Japanese Bullet Train have tended to decrease the research and development interest in high-speed TLV systems in many countries except of West Germany and Japan.

In North America, interest has refocused primarily on improving conventional rail systems, with some activity devoted to exploring hybrid systems that incorporate noncontacting propulsion with conventional railsystems. [44,51]

3. ANALYSIS OF NONCONTACTING PROPULSION SYSTEMS PERFORMANCE

3.1 INTRODUCTION

3.1.1 Purpose and Scope of Analysis

The review of those noncontacting suspension and propulsion systems that may be combined with conventional rail systems show that the linear induction motor is one of the most promising forms of propulsion that can be directly implemented into a conventional rail vehicle-steel rail system. The linear induction motor can produce thrust, lateral and normal forces when interacting with a passive steel track or a steel track clad with a conductor such as aluminum. The coupling of a LIM propulsion unit into a conventional rail vehicle and the utilization of the existing roadbed and track allow maximum use of existing track work in a transportation system. Such a hybrid system combining conventional rail with non-contacting propulsion combines the advantages of the LIM and the use of an existing roadbed.

The combination of a LIM with conventional rail vehicles has attracted interest in both the United States and Canada. [42,51] Studies explore the laying a continuous aluminum clad flat steel rail between conventional rails (which serves as the reaction rail for a single sided LIM while the vehicle is supported and guided on conventional rails). These studies have included a prototype vehicle/track evaluation in Canada [51] and small-scale experiments in the United States. [41]

In addition to interest in systems in which an aluminum clad steel track has been added to the roadbed for LIM propulsion, interest has developed in the technical feasibility of using existing conventional rail not only to support and guide the vehicle but also to serve as the LIM reaction rail.

In the current study the technical feasibility of utilizing conventional rail as LIM reaction rails, and the use of the LIM to both propel and levitate a vehicle are discussed. To investigate application of the LIM to the rail systems, two analytical models were used:

> (1) A model for the LIM employing an all-steel secondary (ASLIM), as shown in Figure 3.1

> (2) A model for the LIM employing an aluminum sheet-back iron secondary (ALLIM), as shown in Figure 3.2

Both models predict thrust, normal force, efficiency and power factor as a function of the LIM design parameters and operating conditions (slip, current, frequency, and air gap).

Although there have been some experimental studies with an all-steel secondary (ASLIM), little analytical work has been performed. A model for the ASLIM is utilized in this study, in order to consider application of the LIM to conventional rail vehicles. Use of the ASLIM is studied to provide or supplement thrust, braking
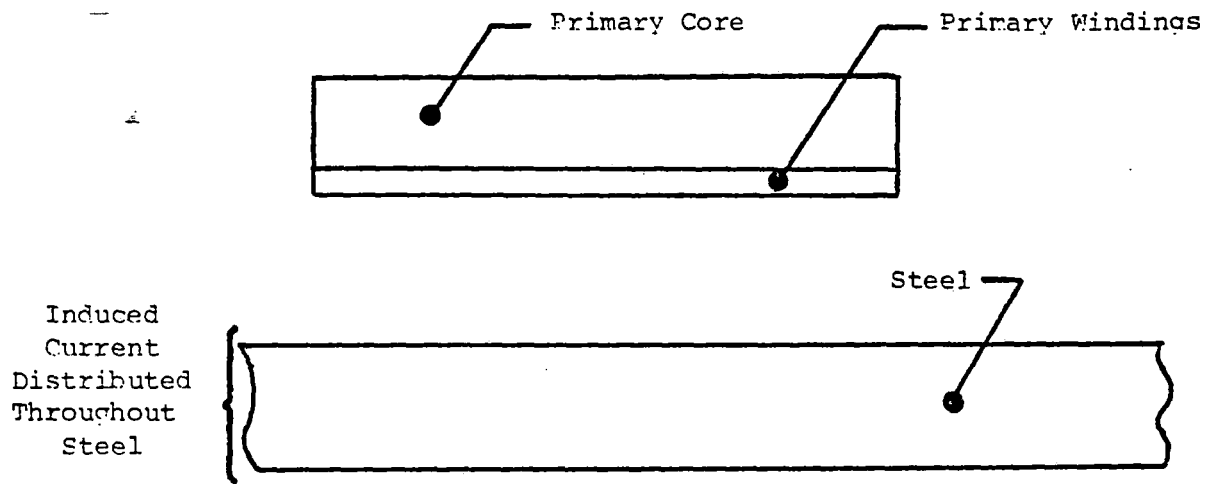
FIGURE 3.1: LIM WITH AN ALL-STEEL SECONDARY (ASLIM)
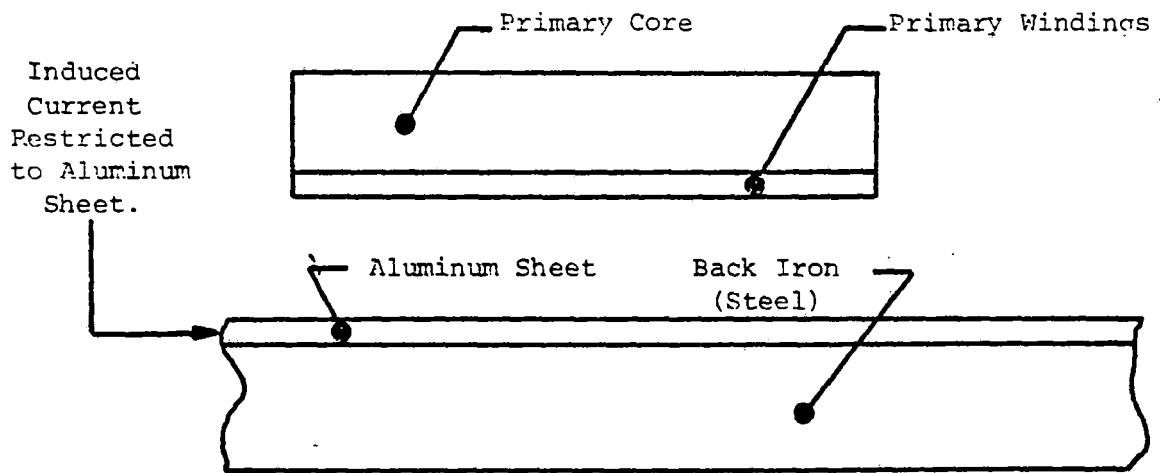
FIGURE 3.2: LIM WITH AN ALUMINUM SHEET-BACK IRON
SECONDARY (ALLIM)

and stabilizing forces. Specific applications could include
assisting propulsion or braking on wet rails, steep grades, or
during emergency braking. The use of existing conventional rails
rather than construction of reaction rails represents a substantial
savings in guideway costs.

The characteristics of the LIM with an aluminum sheet-back iron
secondary (ALLIM) have been studied by Poloujadoff [27],
Yamamura [22], and the General Electric Company [31]. The ALLIM
has provided propulsion for several experimental prototypes
such as the HSST systems [8,9,10], the ROMAG system [40], the TR04
vehicle, and theTU02 vehicle. It will be used with several pro-
posed systems including the ICTS system [2,18], the Telebus system
[2], and the C-Bahn system [2]. The ALLIM model is used to evalu-
ate the feasibility of utilizing the substantial normal force gen-
erated by the LIM to provide or supplement suspension forces while
providing thrust for a vehicle.

3.1.2 Qualitative Description of LIM Operation

The operation of the LIM may be understood by considering the LIM
as a rotary induction motor that has been unwound as shown in Figure
3.3. The torque in the rotary machine corresponds to a longitu-
dinal force (thrust) in the linear machine. However, there are
two features of the linear machine that make its performance dif-
ferent from the rotary machine:

    (1)   Forces normal to the secondary and primary surfaces
           cancel for the rotary machine. For linear machines,
           the normal forces do not cancel and can often exceed
           the thrust force.

    (2)   There are two ends to the primary in the linear
           machine that do not exist in the rotary machine.
           This feature gives rise to effects that can sub-
           stantially alter performance.

The LIM, like the rotary induction motor, requires only a passive
conductor for its secondary. The primary windings generate a
sinusoidal magnetic-traveling wave in the air gap, as shown in
Figure 3.4, when they are excited by a.c. current. As the flux
sweeps across the secondary, currents induced in the secondary
introduce an additional magnetic-traveling wave into the air gap.
The superposition of the primary- and secondary-generated waves
form the air gap traveling wave. The air gap traveling wave has
the same speed and wavelength as the primary and secondary travel-
ing waves but a different phase and amplitude, as shown in the
phasor diagram of Figure 3.4. The air gap traveling wave inter-
acts with the secondary and primary currents to generate a longi-
tudinal force (thrust) and a repulsive normal force. The repulsive
normal force competes with an attractive force generated by the
stator core interacting with the flux. The net normal force can
be either attractive or repulsive, depending on which force is
greater.

The relative motion between the air gap traveling wave and the

Primary

Secondary

Primary
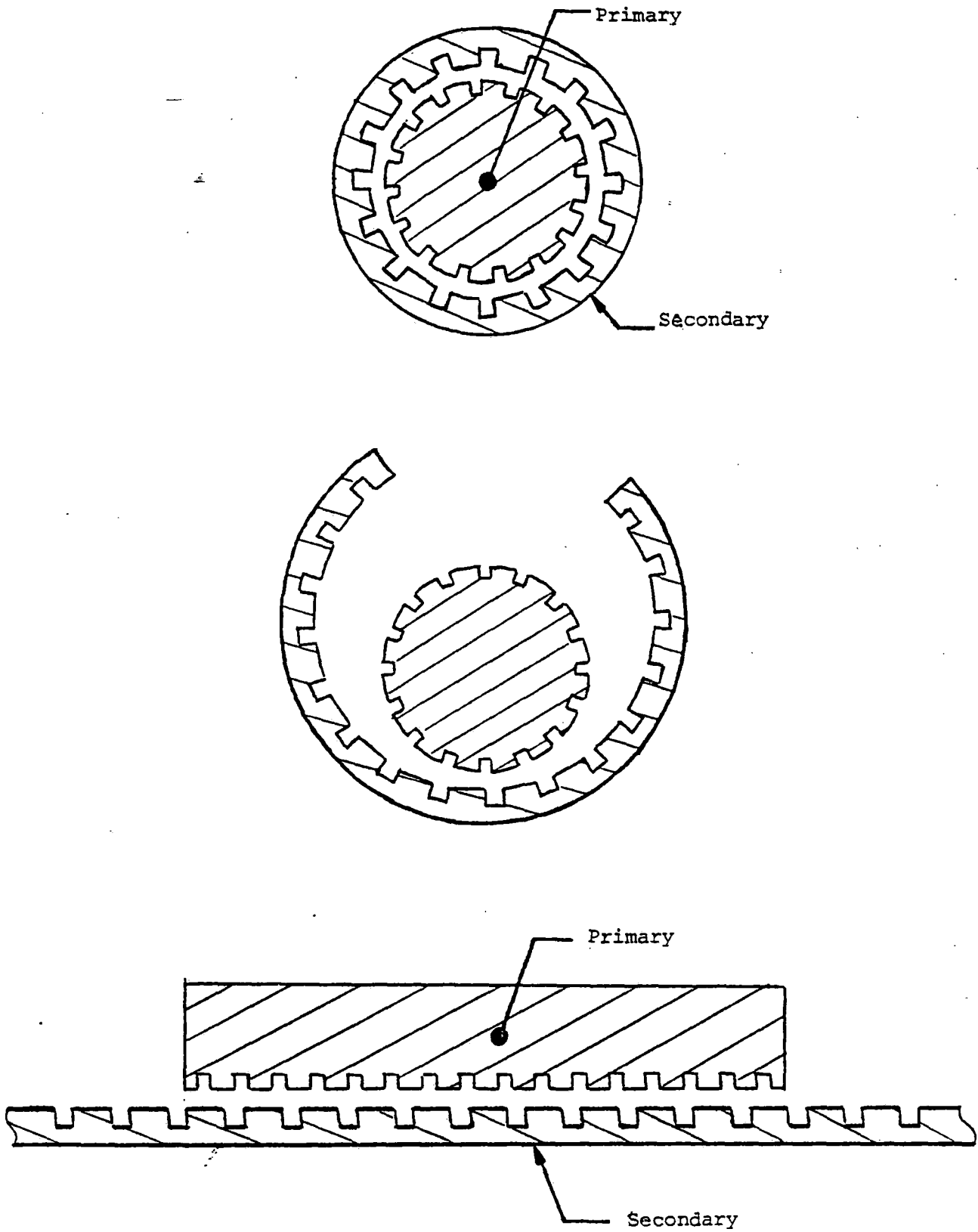
Secondary

FIGURE 3.3: RELATIONSHIP OF THE LIM TO THE ROTARY INDUCTION
MOTOR
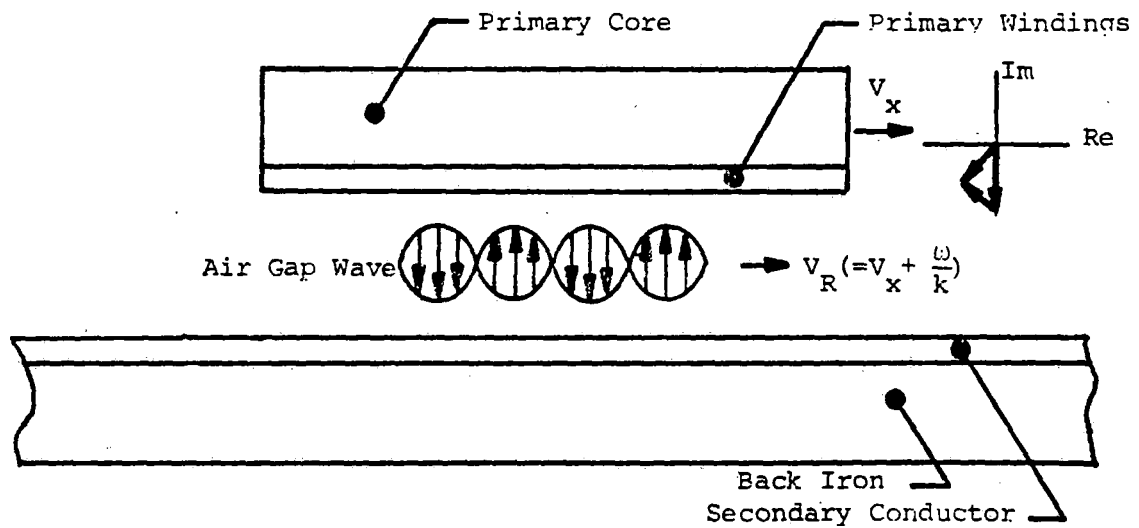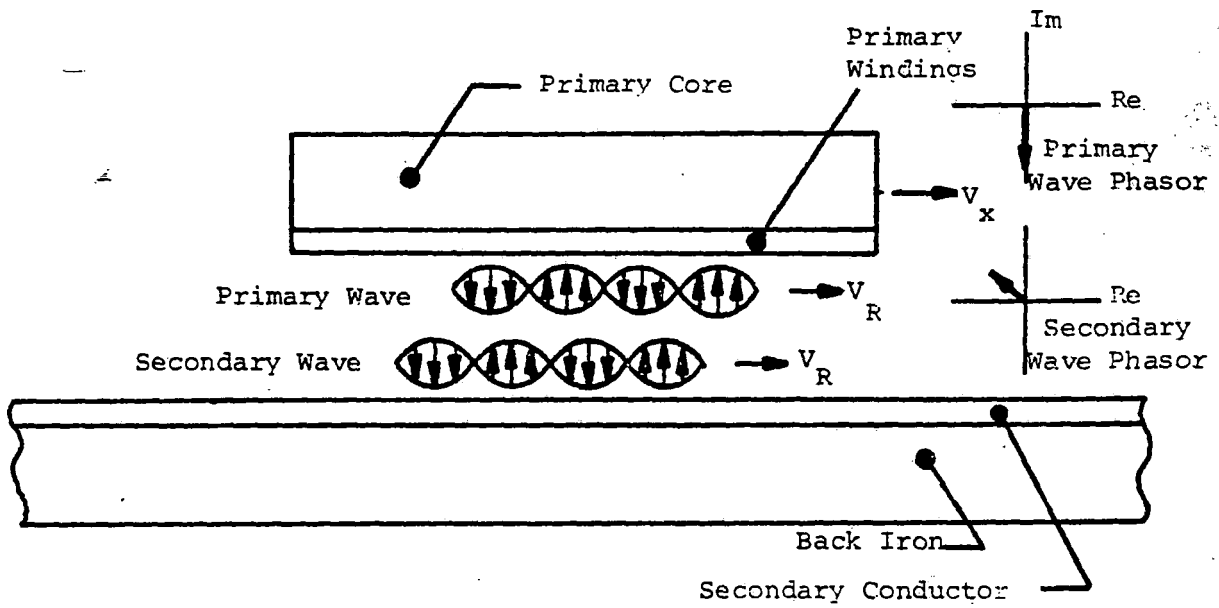
FIGURE 3.4: AIR GAP FLUX TRAVELING WAVE

a) Constituent Air Gap Waves

b) Total Air Gap Wave

secondary has an important influence on LIM performance. Slip is a measure of this relative motion. It is defined as the ratio of the relative speed between the traveling wave and the secondary, V_R, to the synchronous speed of the LIM, ω/k. Therefore, with ω, the wave radian frequency and k equal to π divided by the pole pitch:

$$S = 1 + \frac{k\ V_x}{\omega} \qquad (3\text{-}1)$$

and conversely:

$$V_x = (S-1)\frac{\omega}{k} \qquad (3\text{-}2)$$

A special case for LIM operation occurs when the slip is zero, i.e. $V_x = -\omega/k$. During synchronous operation, the air gap traveling wave appears stationary to the secondary. Consequently, for this condition no secondary currents are induced other than those arising from end effects.

Performance of the LIM may be strongly influenced by speed-dependent phenomena associated with its finite length, the end effects. As the primary moves, its leading and trailing edges induce currents in the secondary because of the discontinuity of flux at these points. The flux generated by these currents is superposed on the conventional induction motor air gap flux, and performance can be substantially altered. The phenomena of end effects increase with speed. The model used for the ALLIM in this study includes the end effects, whereas the model for the ASLIM does not. The end effects are less important for the ASLIM, as discussed in Chapter 4.

The LIM employing an aluminum sheet-back iron secondary (ALLIM) uses the back iron (made of steel) merely as a low-reluctance path for flux. The back iron may or may not be laminated. In either case, the useful induced currents are restricted to the aluminum sheet.

For the LIM employing an all-steel secondary (ASLIM), the steel serves as a conductor for induced currents as well as a low reluctance path for flux.

3.2 MODEL DESCRIPTION

This section describes models used for both the LIM with an aluminum sheet-back iron secondary (ALLIM) and the LIM with an all-steel secondary (ASLIM). Much of the development of the ALLIM model is based on work by Poloujadoff [27]. The models predict thrust, normal force, efficiency, and power factor--criteria required for the applicability of a LIM to vehicle propulsion and suspension, as a function of operating conditions (slip, current, frequency, air gap), and various LIM design parameters. Both models are analytical, allowing convenient application to LIM design.

The analytical models have been developed following standard LIM analysis techniques and are described in detail in reference [64]. The analysis considers steady-state operation of the LIM. The currents carried in the discrete primary windings are represented as an equivalent surface current density that varies sinusoidally in time and in space along the longitudinal axis of the LIM primary. The analysis assumes the LIM iron is not saturated. The thrust, and

normal force are calculated directly from the air gap flux density. The power and efficiency are computed, including both primary and secondary losses. These losses include primary winding losses and leakage flux losses, but do not include hysteresis.

The forces generated in the LIM depend directly on the air-gap flux density. This density is calculated for the case of an all steel secondary and for an aluminum clad secondary. The assumptions for the air-gap flux model for each case are summarized below.

All-Steel Secondary (ASLIM)

The ASLIM relies on the direct interaction of the LIM primary with the steel. In this case, LIM operation depends on induced currents in the steel. The field problem for the all-steel secondary is more complicated than for the aluminum sheet back iron secondary, because induced secondary currents cannot be assumed to flow uniformly in a thin conductive layer. Since the current density varies with the depth into the secondary, the problem is two-dimensional. To overcome this difficulty, this study assumes that end effects are insignificant for the operating conditions of interest, which include moderate and low speeds. Experimental work directed by MITRE at the Canadian Institute of Guided Ground Transport has shown that end effects are relatively insignificant for the all-steel secondary LIM [25]. When end effects are neglected only the particular solution is of interest, which varies sinusoidally in the longitudinal direction. Consequently, the problem reduces to one-dimension. The following additional assumptions have been made to perform the analysis on the ASLIM shown in Figure 3.5:

(1) The LIM is considered a slice of an infinitely wide motor, i.e., secondary current flows parallel to the y-axis only.

(2) There is no variation in field quantities laterally.

(3) The material constitutive relationship is assumed to be linear, i.e., saturation is neglected.

(4) The steel secondary is assumed to be infinitely thick for the field analysis.

The fourth assumption is justified if the steel thickness, T, is greater than the skin depth, as discussed in reference [64]. In general, this condition is satisfied for practical operating conditions.

The model accounts for return path current losses with an effective steel resistance which depends upon geometry and material properties, as described in reference [64].

FIGURE 3.5: FEATURES OF THE ASLIM

Aluminum Sheet-Back Iron Secondary (ALLIM)

In the aluminum sheet-back iron secondary (ALLIM), secondary currents are restricted primarily to the aluminum sheet placed on top of the back iron, as shown in Figure 3.6. The back iron (made of steel) serves as a low-reluctance path for the flux. Consequently, the secondary current is modeled as a surface current density, and the field quantities do not have to be determined as a function of depth into the secondary. The analysis for the ALLIM, however, includes end effects.

A one-dimensional analysis was used for the ALLIM because it provides analytical expressions for LIM performance that account for the influence of the end effects. Despite a large range in model complexity, Figure 3.8 [62] shows the close agreement in predicted thrusts of four different models. The Mosebach one-dimensional theory, similar to the model used in this study, yields nearly the same result as the three-dimensional Oberrettl Theory.

Several assumptions have been made in this study:

(1) Current flow in the secondary is restricted to the aluminum sheet.

(2) The secondary current flows in a rectangular fashion, as shown in Figure 3.6, parallel to the y-axis while under the primary ($|y| < \ell/2$) and parallel to the x-axis while not under the primary ($\ell/2 < |y| < \ell'/2$).

(3) There is no variation in field quantities along the y or z-axes in the air gap ($|y| < \ell/2$).

(4) The material constitutive relationship is assumed to be linear, i.e. saturation is neglected.

(5) The air gap is multiplied by the Carter coefficient [63], a correction factor relatively close to unity, which accounts for the slotting of the primary.

In a LIM, the current paths are similar to those shown in Figure 3.7 rather than perfectly rectangular. However, the rectangular paths of Figure 3.6 are an approximation that includes the substantial return path losses—those losses associated with the current flow parallel to the x-axis, in a one-dimensional analysis. [27]

The solution for the air-gap flux is determined in reference [64], based upon these assumptions.

3.3 MODEL IMPLEMENTATION

The models described in Section 3.2 have been implemented with two computer programs, SLIMRAIL.FOR (ASLIM model) and LIM.FOR (ALLIM model), as described in reference [64]. The programs produce tables and plots of LIM performance as a function of slip for a given set of design parameters and operating conditions. The operating conditions include the input peak phase current I.
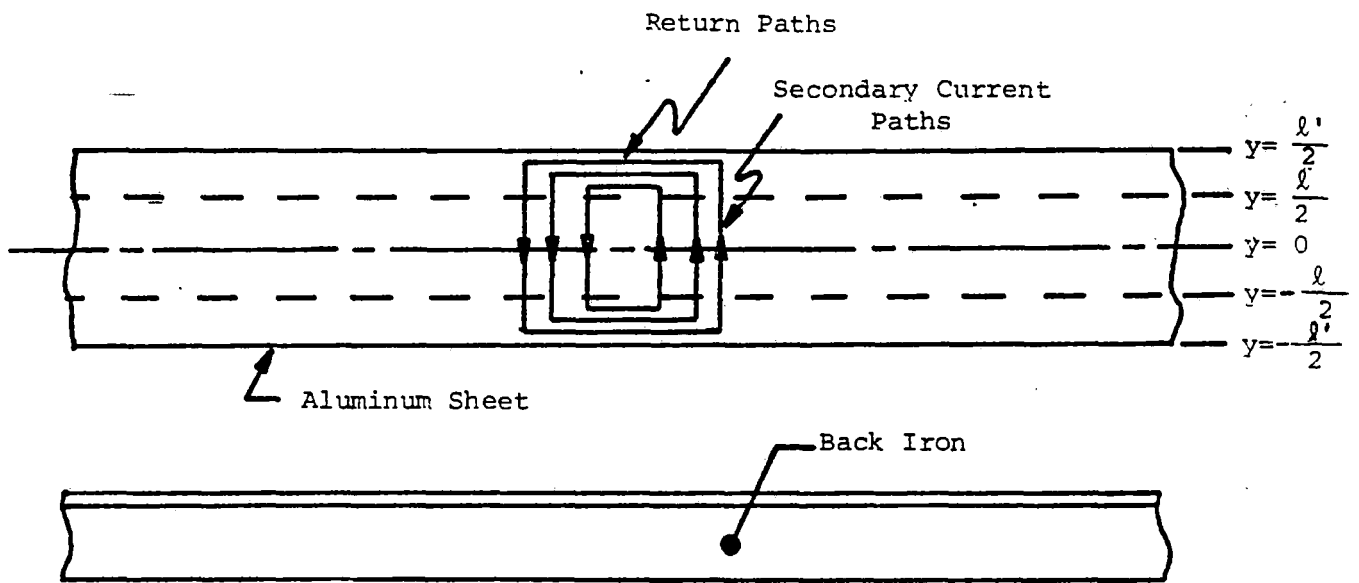
FIGURE 3.6: ALLIM SECONDARY WITH IDEALIZED SECONDARY CURRENT PATHS
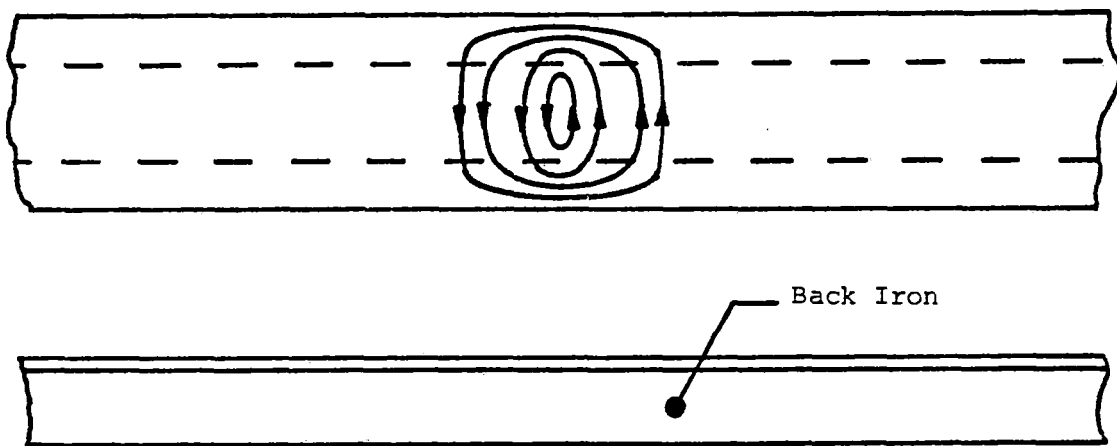
FIGURE 3.7: ALLIM SECONDARY WITH ACTUAL SECONDARY CURRENT PATHS
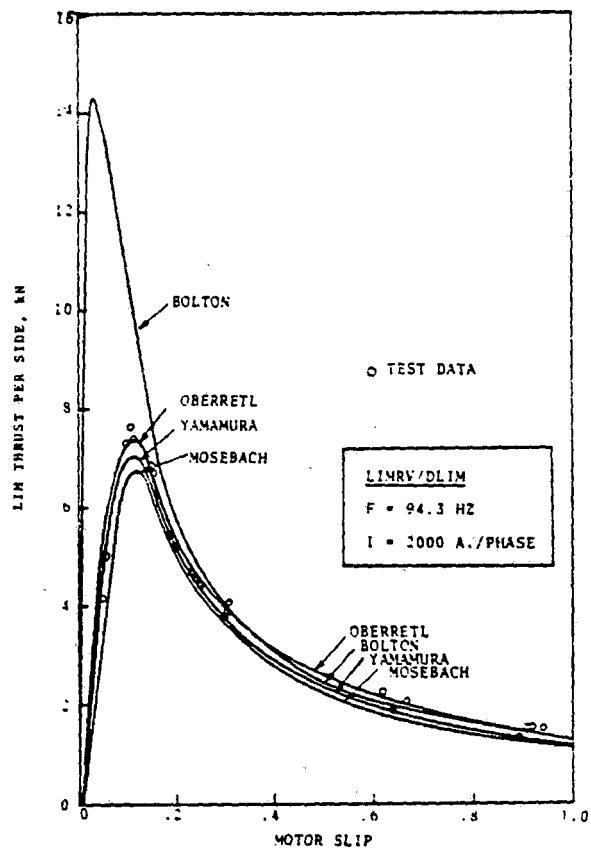
FIGURE 3.8: COMPARISON OF VARIOUS LIM
ANALYSES [62]

3.4 PRINCIPAL LIM PERFORMANCE CHARACTERISTICS

The analyses described were applied to two different LIM configurations (both with aluminum sheet-back iron secondaries) and operating conditions to compute performance in terms of thrust, normal force, efficiency and power factor as a function of slip. First, the configuration that was tested experimentally in this study is considered, and second, a configuration defined in the literature [23] and tested by General Electric has been selected.

The important design parameters for the G.E. test LIM and the LIM used in this study (ALLIM) are listed in Table 3.1. The G.E. test LIM is wider and has two fewer poles. The operating conditions chosen for the two cases are listed in Table 3.2. The difference in input current for the two cases results in substantially larger thrust and normal force values for the G.E. test LIM. The trends of the thrust and normal force curves, however, are similar, since forces scale with the square of the input current at all slips. The higher excitation frequency of the G.E. test LIM enhances the end effects and tends to make the important features of the performance curves occur at lower slips, e.g. peak thrust, peak efficiency, peak power factor and the changeover to repulsion normal force.

Figures 3.9-3.12 are plots of LIM performance as a function of slip for the test LIM used in this study. The design parameters are summarized in Chapter 4, and the operating conditions are listed in Table 3.2. The ALLIM model (LIM.FOR) was used to generate the plots.

For thrust and normal force, curves are included in each plot for the following cases:

(1)   End effects neglected (only particular solution used)

(2)   End effects included for boundary conditions where flux vanishes instantly at the ends of the air gap (no fringing)

(3)   End effects included for boundary conditions where primary core extends to $\pm\,\infty$ (fringing included)

For efficiency and power factor only the latter two cases are plotted.

Figure 3.10 illustrates the substantial decrease in normal force with increasing slip. At low slips, the attraction force exerted on the primary core and secondary back iron by the flux is dominant: whereas at high slips, the repulsion force has become comparable to the attraction force because the increase of induced secondary current. Consequently, the net normal force is only slightly attractive at S=1.0. It is possible for the normal force to be repulsive at high slips for different operating conditions or design parameters, as is demonstrated below.

TABLE 3.1: MAJOR DESIGN PARAMETERS FOR TEST LIM AND G.E. LIM

PARAMETER	TEST LIM	G.E. LIM
Primary length (m)	1.0	0.965
Primary width (m)	0.0668	0.1715
Secondary conductor width (m)	0.1175	0.2985
Secondary conductor thickness (m)	3.175×10^{-3}	3.175×10^{-3}
No. of poles	6	4
Pole pitch	0.17	0.20

TABLE 3.2: OPERATING CONDITIONS FOR TEST LIM AND G.E. LIM

QUANTITY	TEST LIM	G.E. LIM
g (m)	1.0×10^{-2}	2.14×10^{-2}
ω (radians/s)	376.99	1885.0
I(A) (peak phase current)	30.0	424.26
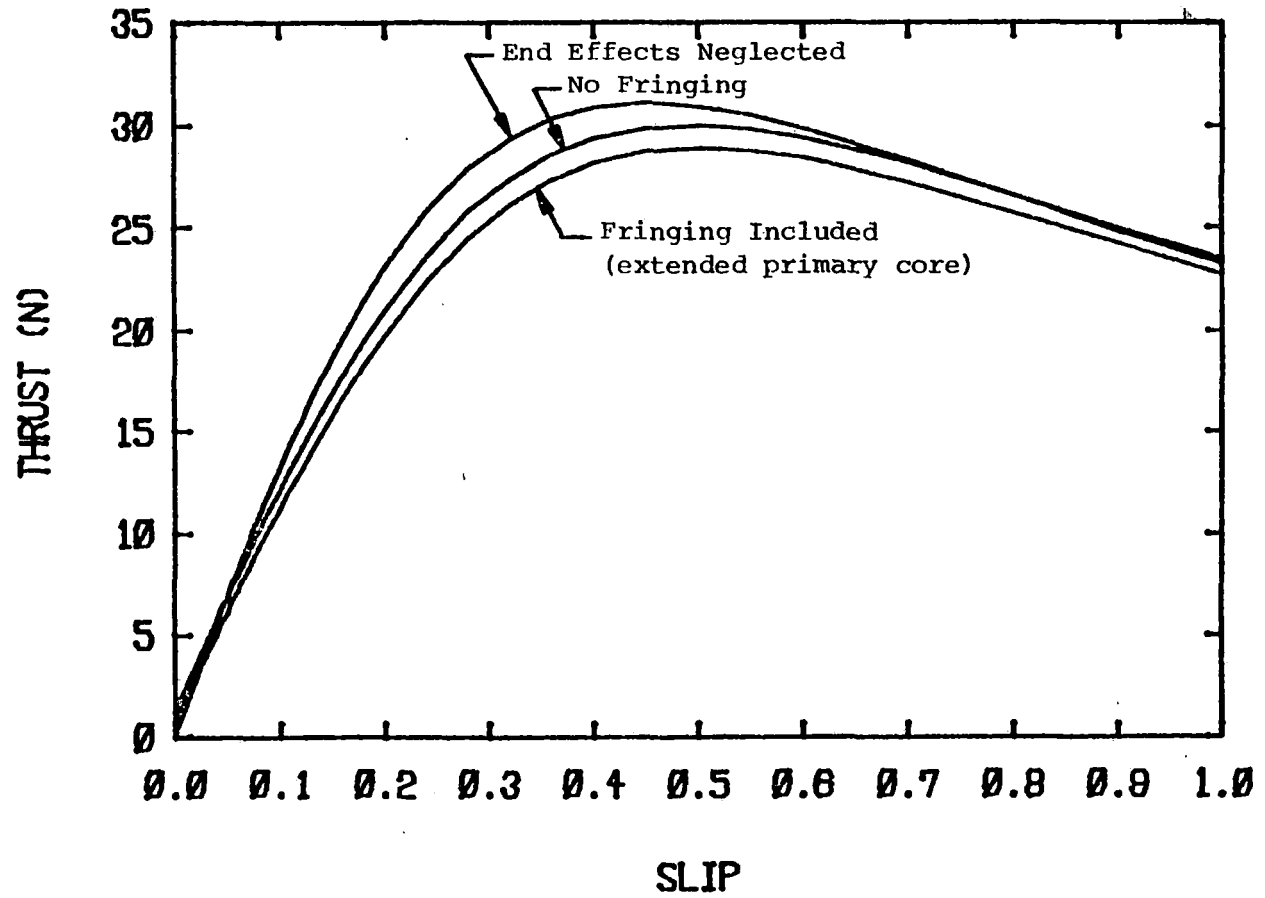
FIGURE 3.9: THRUST VS. SLIP FOR TEST LIM
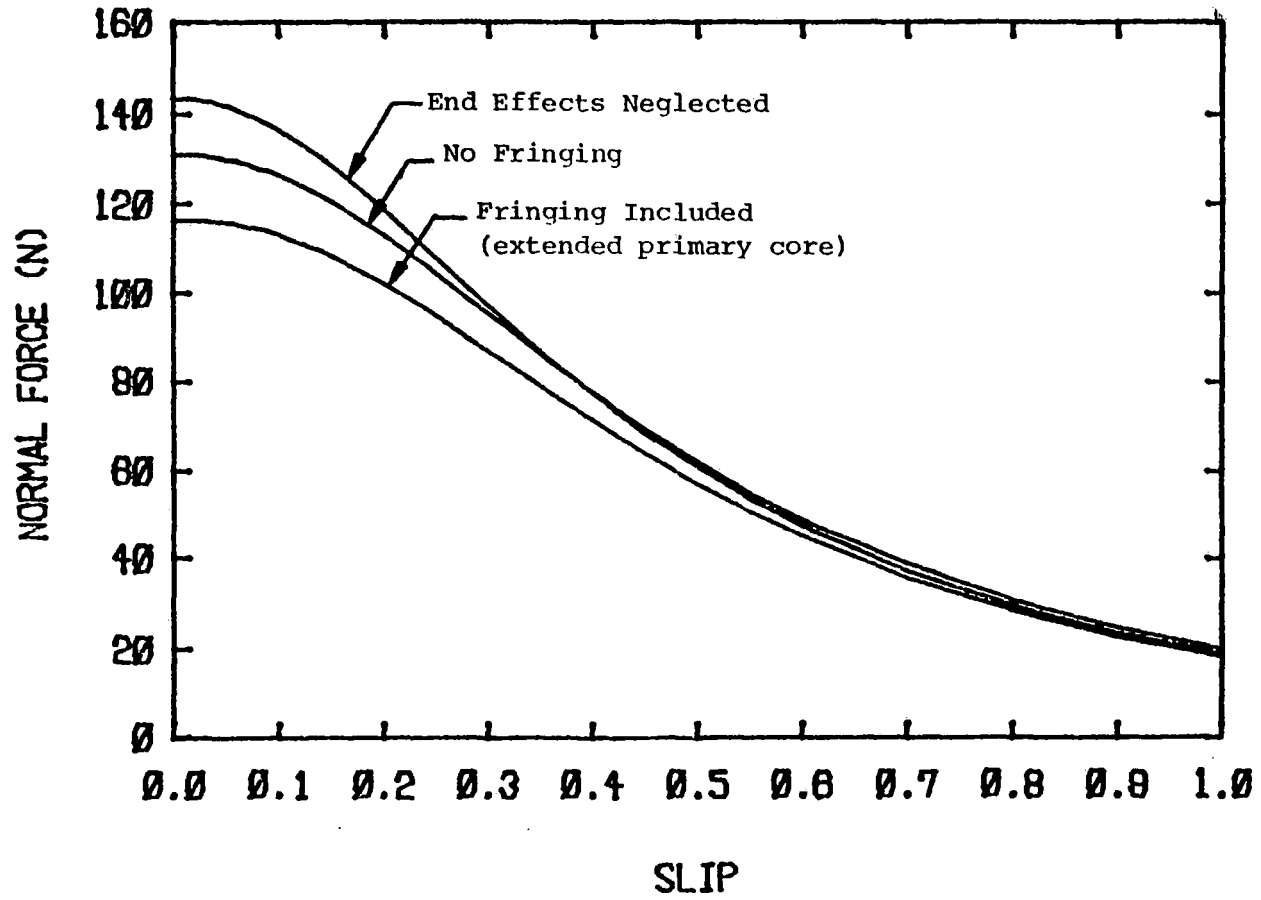
FIGURE 3.10: NORMAL FORCE VS. SLIP FOR TEST LIM
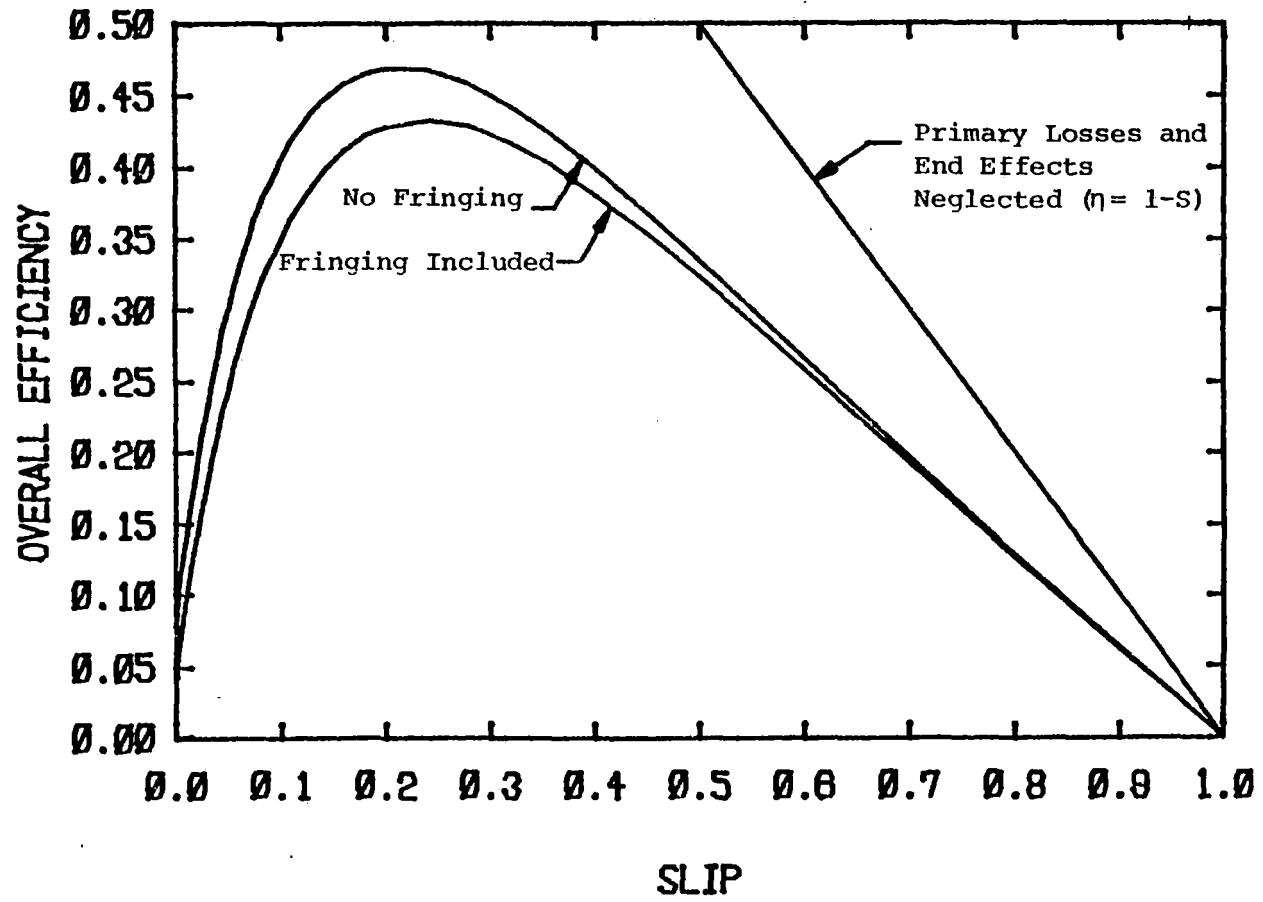
FIGURE 3.11: EFFICIENCY VS. SLIP FOR TEST LIM
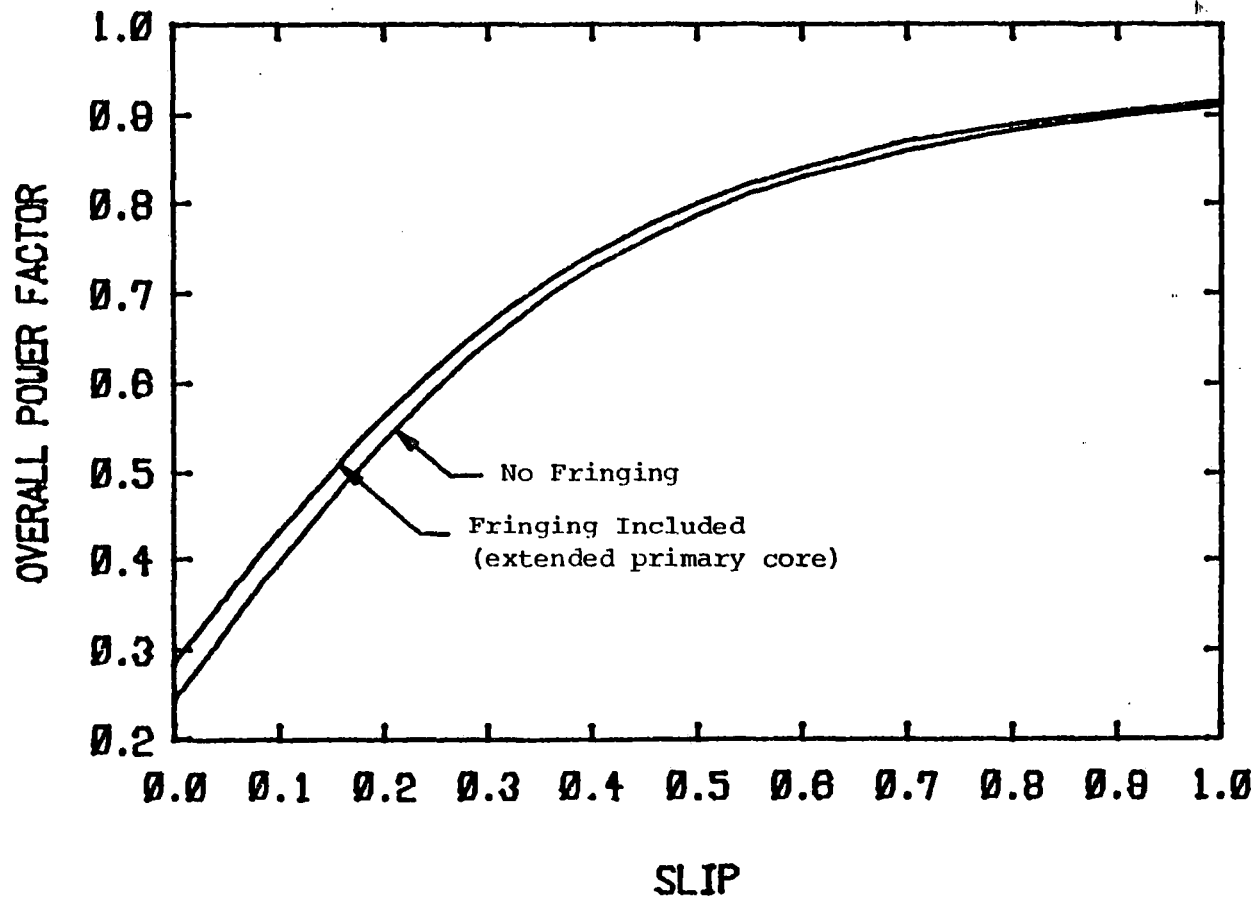
FIGURE 3.12: POWER FACTOR VS. SLIP FOR TEST LIM

The efficiency curves of Figure 3.11 start at relatively low values at zero slip because of the primary winding losses. The primary winding losses do not change with slip for constant current operation. Consequently, they influence efficiency substantially at low slips, where the LIM output power (thrust power), and secondary losses due to induced currents are relatively insignificant. As slip increases, the efficiency approaches a peak at S ≃ 0.22 because of the increasing thrust output. As slip increases above 0.25, however, the resistive losses in the secondary become dominant and efficiency drops off. The efficiency curves approach the η=1-S curve, which neglects primary losses and end effects, both insignificant at high slips.

Figure 3.12 illustrates the generally low power factor exhibited by the LIM at low slips, a fundamental problem with its application to vehicles. The reason for this is the relatively small amount of induction present at low slips. Consequently, the air gap wave is predominantly a primary-generated wave which produces an inductive impedance at the LIM input terminals.

To demonstrate the LIM performance characteristics for a significantly different set of design parameters and operating conditions, the ALLIM model was also applied to the G.E. test LIM. [23] The operating conditions for this LIM are listed in Table 3.2. Figures 3.13-3.16 are plots of thrust, normal force, efficiency and power factor vs. slip respectively. In each plot, except Figure 3.16, the G.E. mesh matrix analysis result is also included. [23] The G.E. model is based on a detailed mesh matrix analysis, whereas the analysis in this study is based on a one-dimensional, analytical analysis. The G.E. power factor curve is not given in its report. [23]

There are two major aspects of the LIM performance shown in Figures 3.13-3.16 that are substantially different from the performance curves of Figures 3.9-3.12:

(1) The end effects have a substantially greater influence on LIM thrust and normal force.

(2) The plots of thrust, normal force, efficiency and power factor are more compressed horizontally; the peak thrust and efficiency occurs at a lower slip: the normal force diminishes more rapidly with slip and turns repulsive: the power factor peaks and then diminishes with slip.

The substantial reduction of thrust and normal force by the end effects at low slips is due to the relatively high speed necessary to approach synchronous speed at an excitation frequency of 1885.0 radians/s and a pole pitch of 0.2 in. The high speed enhances the induction at the ends of the LIM and also draws the front end effect further into the air gap. The end effect waves reduce thrust and normal force by cancelling useful flux.
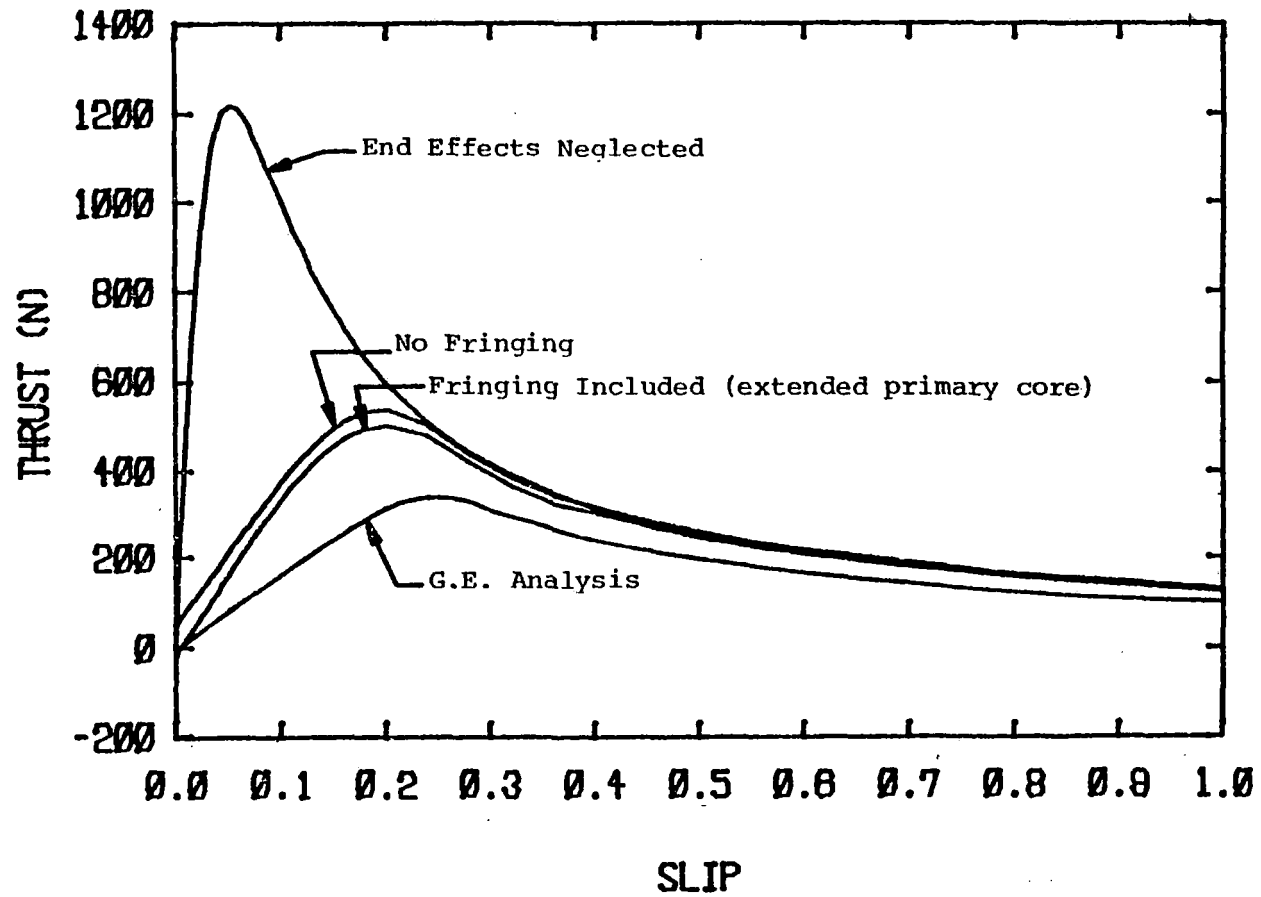
FIGURE 3.13: THRUST VS. SLIP FOR G.E. TEST LIM
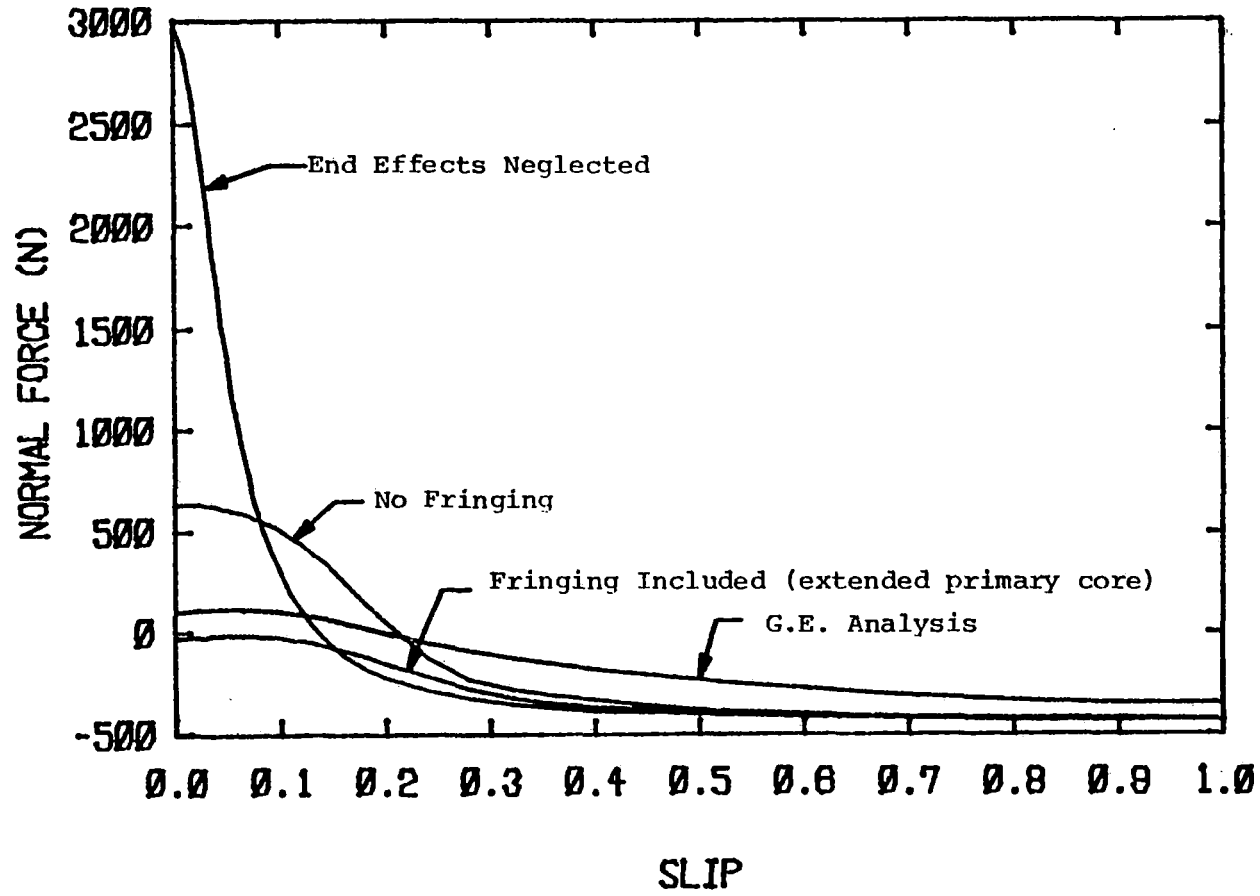
FIGURE 3.14: NORMAL FORCE VS. SLIP FOR G.E. TEST LIM
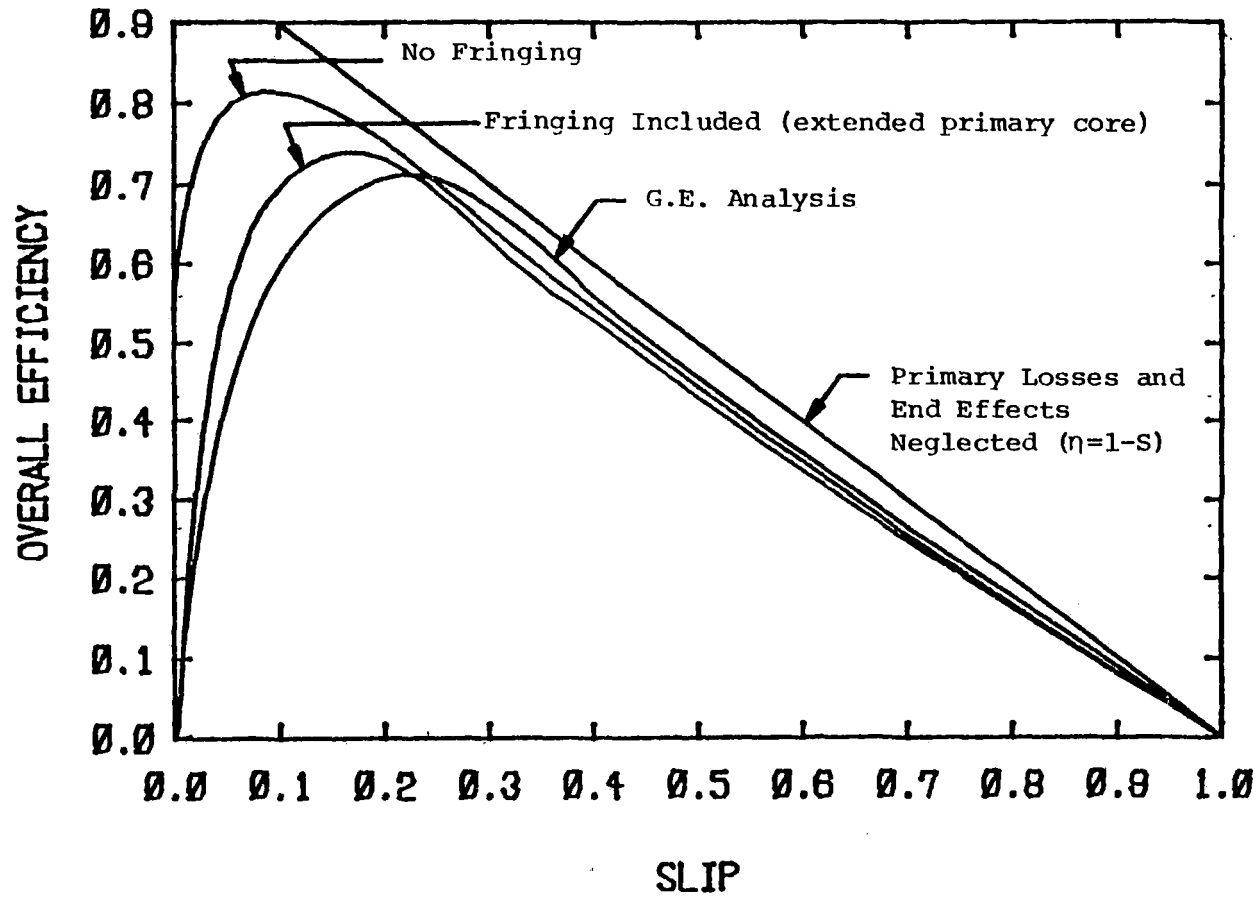
FIGURE 3.15: EFFICIENCY VS. SLIP FOR G.E. TEST LIM
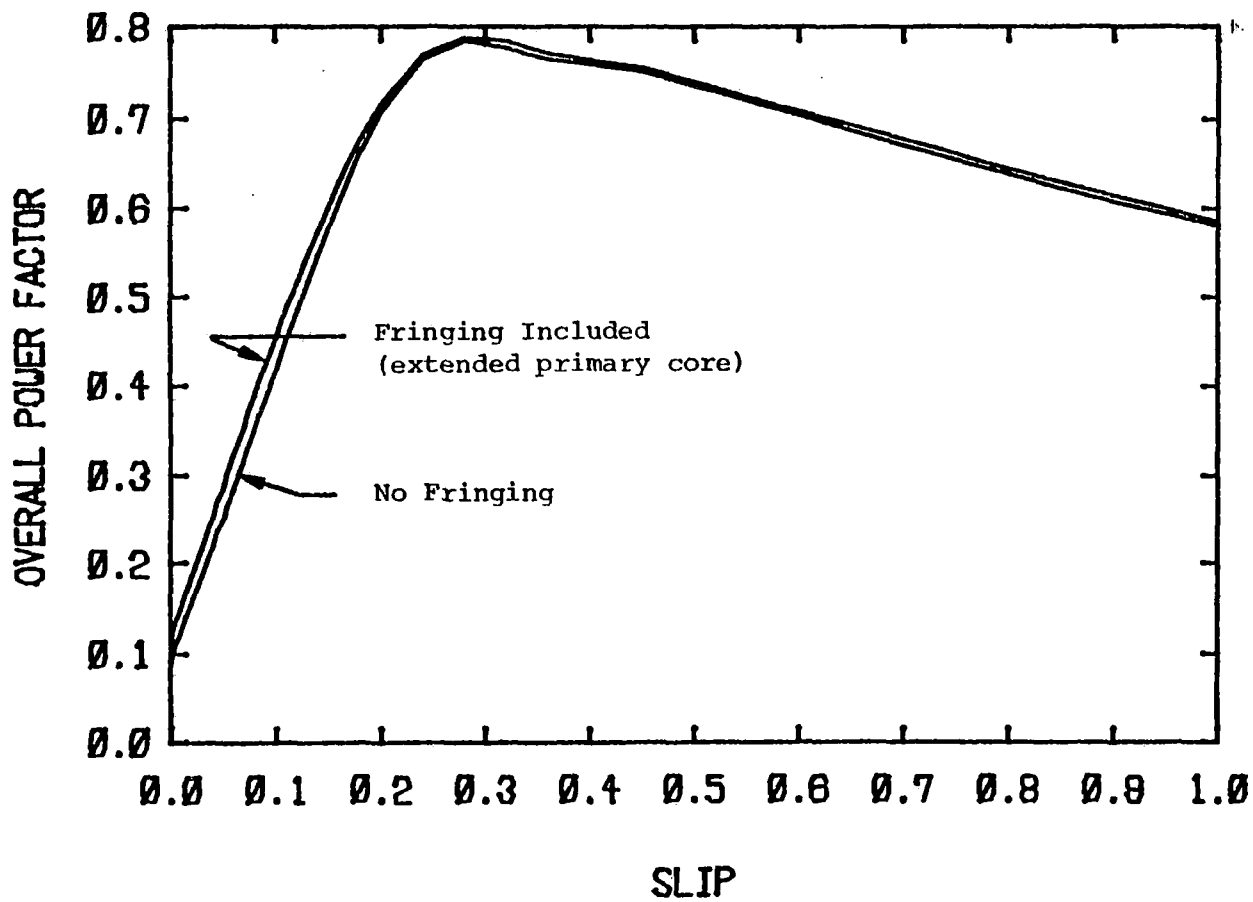
FIGURE 3.16: POWER FACTOR VS. SLIP FOR G.E. TEST LIM (G.E. analysis not available)

The relatively high excitation frequency, ω, implies that the air gap wave frequency that the secondary "sees," $S\omega$, increases rapidly with slip. Consequently, the phase lag angle, ψ, increases proportionately faster with slip. As a result, thrust, normal force, and power factor also change more rapidly. Specific manifestations include:

(1) Peak thrust occurs at a relatively low slip.

(2) The attractive force diminishes more rapidly with slip and becomes a repulsion force at a relatively low slip.

(3) The power factor peaks and then diminishes.

The final point occurs because the air gap flux tends to vanish as slip increases. Consequently, the slip-independent leakage flux becomes dominant and the LIM impedance becomes more inductive, reducing the power factor.

4. LINEAR INDUCTION MOTOR EXPERIMENTAL AND ANALYTICAL CHARACTERISTICS

4.1 TEST FACILITY

To provide experimental verification of the analyses described in Chapter 3, experimental measurement of the performance characteristics of a prototype LIM has been performed. An experimental facility, shown in Figures 4.1 and 4.2, has been utilized (developed, as described in reference [65]).

The facility uses a one-inch-thick steel ring as the LIM secondary. The secondary is epoxy-bonded to a turntable fabricated from 6061-T6 aluminum 3/8 inch thick. The LIM primary is rigidly mounted to the stationary frame, with provisions for adjustment of the air gap and offset with respect to the secondary.

Relative motion between the primary and secondary is achieved by rotating the turntable. The speed of the secondary and, hence, the slip is controlled by adjustment of the input voltage to a 25 hp d.c. motor. The motor drives the axle of the turntable through a toothed rubber belt with teeth. The angular speed of the turntable is continually monitored by the output voltage of a proximity sensor.

Two strain-gauge transducers, through which the primary is mounted to the frame, measure the thrust, normal force, and lateral force generated by the LIM. The output signals of the transducers are amplified by a factor of 2,000 and recorded on tape with an FM data recorder.

4.2 SCALE MODEL LIM DESCRIPTION

The scale model LIM was designed to generate the same distribution of flux in the air gap as the full-scale MITRE-CIGGT LIM [24], to insure that the phenomena present in a full-scale machine are observable in the experimental LIM. The scaling laws are derived in the literature [63,64] and have been used to design the test LIM as described in reference [65]. The specifications for the test LIM are listed in Table 4.1

The LIM primary core was fabricated from steel laminations. After construction of the primary core, the primary was wound with a double layer winding. To fill the end slots, extra windings were added.

The coils were fabricated using 12 gauge copper wire.

4.3 EXPERIMENTAL PERFORMANCE DATA

Two sets of experiments were performed in this study:

(1) Performance of the LIM with an all-steel secondary (ASLIM) was measured.

Turntable

Secondary

Axle

Turntable Mounting
Frame (lower
member)

drive belt

Drive Motor Mounting Frame

Drive Motor

Gear Box

Coupler

Sprocket (for
RPM measurement)

LIM Mounting Frame

Force Transducer

LIM

Turntable Mounting Frame (upper member)
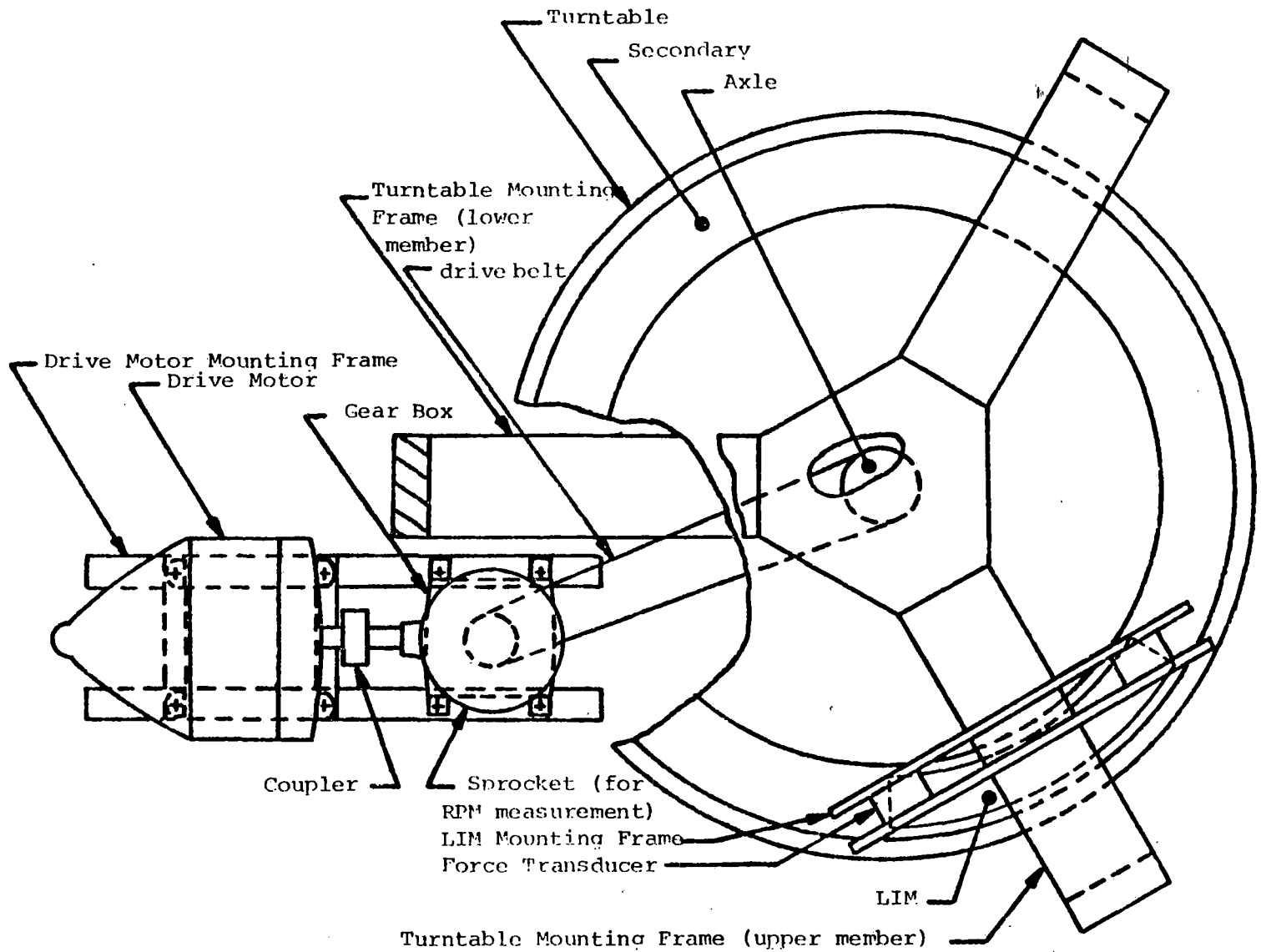
FIGURE 4.1:   TOP VIEW OF TEST FACILITY   (Not to Scale)
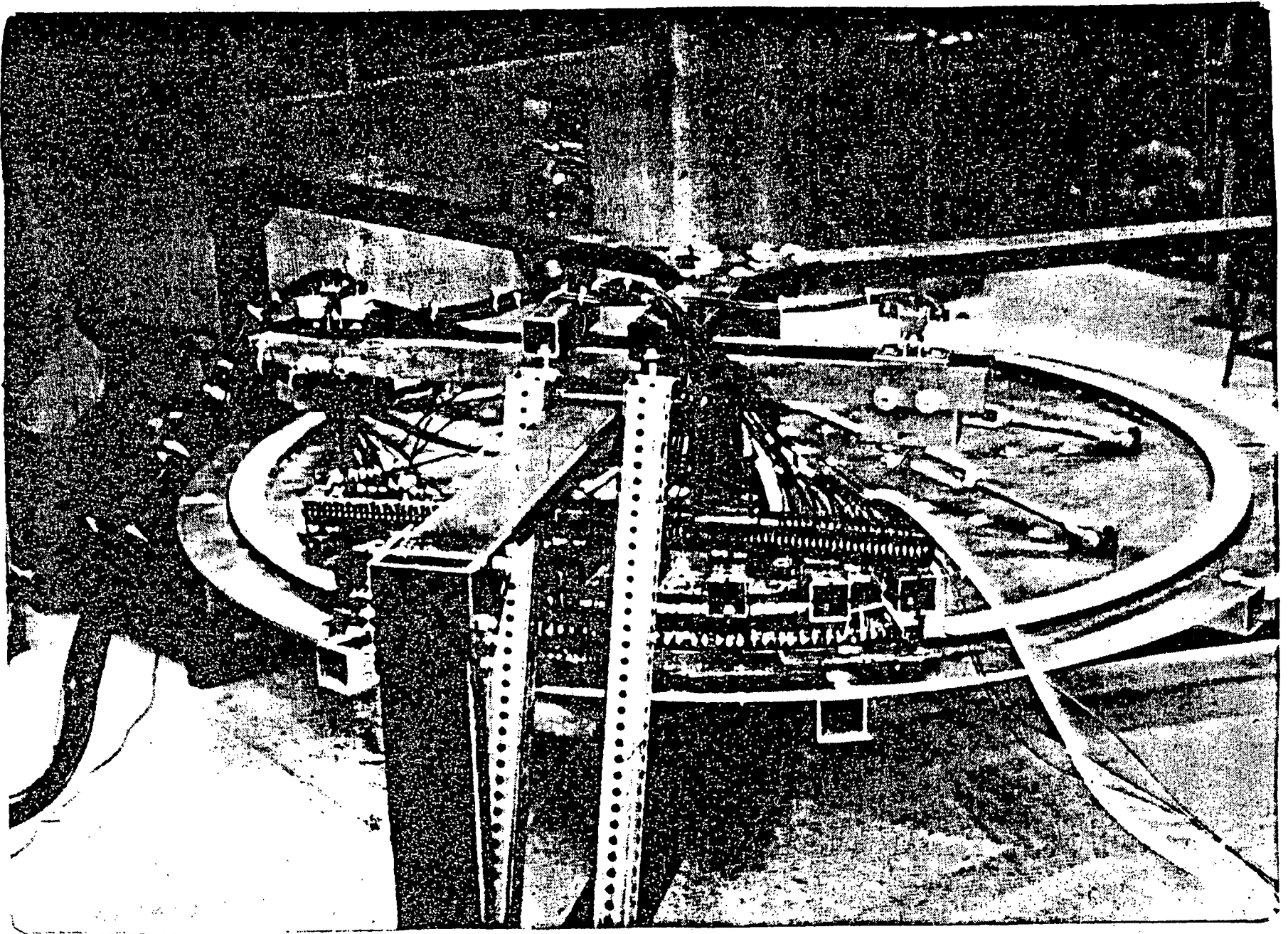
FIGURE 4.2: TEST FACILITY

TABLE 4.1

TEST LIM SPECIFICATIONS

CATEGORY	NUMBER
Primary	
lamination thickness	29 awg.
material	M-19 nonoriented steel
length	1.0 m
width	6.6675×10^{-2} m
centerline radius	1.0 m
slots per pole	9
pole pitch	0.167 m
slot width	1.0×10^{-2} m
slot depth	2.0×10^{-2} m
no. of slots	54
no. of poles	6
no. of phases	3
connection	wye
coil pitch	7/9
turns per coil	6
wire size	12 awg. copper
Secondary	
Back iron:	
centerline radius	1.0 m
width	6.6675×10^{-2} m
material	M-1020 steel
conductivity*	4.464×10^{6} mhos/m
permittivity**	6.283×10^{-4} H/m ($=500\mu_o$)
thickness	2.54×10^{-2} m

TABLE 4.1 (Cont.)

Conducting Sheet (ALLIM only)

centerline radius	1.0 m
width	11.748×10^{-2} m
material	6061-T6 aluminum
conductivity	2.5×10^{7} mhos/m
thickness	3.175×10^{-3} m

---

* Measured experimentally,

** An estimate.

(2) Performance of the LIM with an aluminum sheet-back
     iron secondary (ALLIM) was measured.

The first set of experiments, the ASLIM tests, were used to veri-
fy the analysis of the ASLIM. In addition measurements of lateral
force, not included in the analysis, were made. An aluminum sheet
was bonded to the steel, in order to adapt the facility for the
ALLIM tests. The ALLIM tests were used to verify the ALLIM
analysis. During the experiment the air gap and slip were varied,
while the LIM current and excitation frequency were held constant.

4.3.1 Instrumentation and Calibration

The LIM-generated forces were measured by the strain gauge trans-
ducers, and their output signals were recorded on tape with a
Racal FM recorder. Later these values were fed into a strip
chart recorder, to provide a hard copy record of the results.

The Phase A current was measured with a Tektronix TM503 current
probe and AM503 current probe amplifier and displayed on a dual
trace oscilloscope along with the phase A line-to-neutral voltage.
The oscilloscope display monitored the input current to the LIM
and the phase lag of the current with respect to the voltage for
calculation of the power factor.

The transducers were originally constructed at M.I.T. to measure
the forces exerted on cutting tools during machining operations.
Each transducer has three channels, one for each orthogonal direc-
tion of force. The transducers were calibrated, as described in
reference [64], with a distribution of point loads applied simul-
taneously at 11 equally spaced intervals along the length of the
primary.

4.3.2 Description of Tests

The tests conducted with the all-steel secondary and the aluminum
sheet-back iron secondary are listed in Tables 4.2 and 4.3,
respectively. All tests were performed with an input peak cur-
rent of 30A and a 60-Hz excitation frequency. The general format
set the air gap and offset of the primary with respect to the
secondary. Then slip was varied and the measurements made.

When all the desired slips had been achieved for a particular air
gap and offset, the primary was adjusted to a new air gap and off-
set.

4.3.3 All-Steel Secondary Results (ASLIM)

The measured thrust, normal force, lateral force and power factor
are plotted as a function of slip at various air gaps and offsets
in Figures 4.3-4.16. The results predicted by the ASLIM analysis
of Chapter 3 are included with a solid line in these plots for the
zero offset cases. In this study no analysis was performed for
the offset condition. The offset data, however, are useful for
comparison with the data for the centered LIM. There is no plot
of thrust for a 1.5 cm airgap, because the magnitude of the thrust

TABLE 4.2:   ALL-STEEL SECONDARY TESTS

Offset ───►│   │◄─

PRIMARY   ┌── air gap

SECONDARY   ──turntable
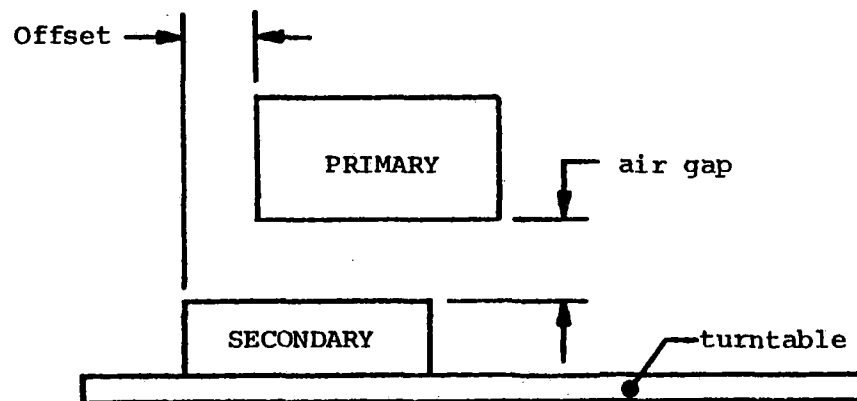
TESTS 1-7: Air Gap = 0.5 cm Offset = 0.0 cm		Tests 8-14: Air Gap = 1.5 cm Offset = 0.0 cm		Tests 15-21: Air Gap = 1.0 cm Offset = 0.0 cm	
Test No.	Slip	Test No.	Slip	Test No.	Slip
1	1.0	8	1.0	15	1.0
2	0.7	9	0.7	16	0.7
3	0.5	10	0.5	17	0.5
4	0.2	11	0.2	18	0.2
5	0.1	12	0.1	19	0.1
6	0.05	13	0.05	20	0.05
7	0.0	14	0.0	21	0.0

TABLE 4.2:   (Cont.)

Tests 22-28:	Air Gap = 0.5 cm Offset = 1.0 cm	Tests 29-35:	Air Gap = 0.5 cm Offset = 2.0 cm	Tests 36-45:	Air Gap = 0.5 cm Offsets = 0.0 cm
Test No.	Slip	Test No.	Slip	Test No.	Slip
22	1.0	29	1.0	36	1.0
23	0.7	30	0.7	37	0.7
24	0.5	31	0.5	38	0.6
25	0.2	32	0.2	39	0.5
26	0.1	33	0.1	40	0.4
27	0.05	34	0.05	41	0.3
28	0.0	35	0.0	42	0.2
				43	0.1
				44	0.05
				45	0.1

Tests 46-55:	Air Gap = 1.0 cm Offset = 0.0 cm
Test No.	Slip
46	1.0
47	0.7
48	0.6
49	0.5
50	0.4
51	0.3
52	0.2
53	0.1
54	0.05
55	0.0

Tests 1-10: Air Gap = 1.0 cm Offset = 0.0 cm		Tests 11-20: Air Gap = 1.5 cm Offset = 0.0 cm		Tests 21-30: Air Gap = 0.75 cm Offset = 0.0 cm	
Tests No.	Slip	Test No.	Slip	Test No.	Slip
1	1.0	11	1.0	21	1.0
2	0.7	12	0.7	22	0.7
3	0.6	13	0.6	23	0.6
4	0.5	14	0.5	24	0.5
5	0.4	15	0.4	25	0.4
6	0.3	16	0.3	26	0.3
7	0.2	17	0.2	27	0.2
8	0.1	18	0.1	28	0.1
9	0.05	19	0.05	29	0.05
10	0.0	20	0.0	30	0.0

TABLE 4.3 (Cont.)

Tests 31-40: Air Gap = 1.0 cm Offset = 0.0 cm		Test 41-50: Air Gap = 1.0 cm Offset = 1.0 cm		Tests 51-61: Air Gap = 1.0 cm Offset = 2.0 cm	
Test No.	Slip	Test No.	Slip	Test No.	Slip
31	1.0	41	1.0	51	1.0
32	0.7	42	0.7	52	0.7
33	0.6	43	0.6	53	0.6
34	0.5	44	0.5	54	0.5
35	0.4	45	0.4	55	0.4
36	0.3	46	0.3	56	0.3
37	0.2	47	0.2	57	0.2
38	0.1	48	0.1	58	0.1
39	0.05	49	0.05	59	0.05
40	0.0	50	0.0	60	0.0
				61	-0.05
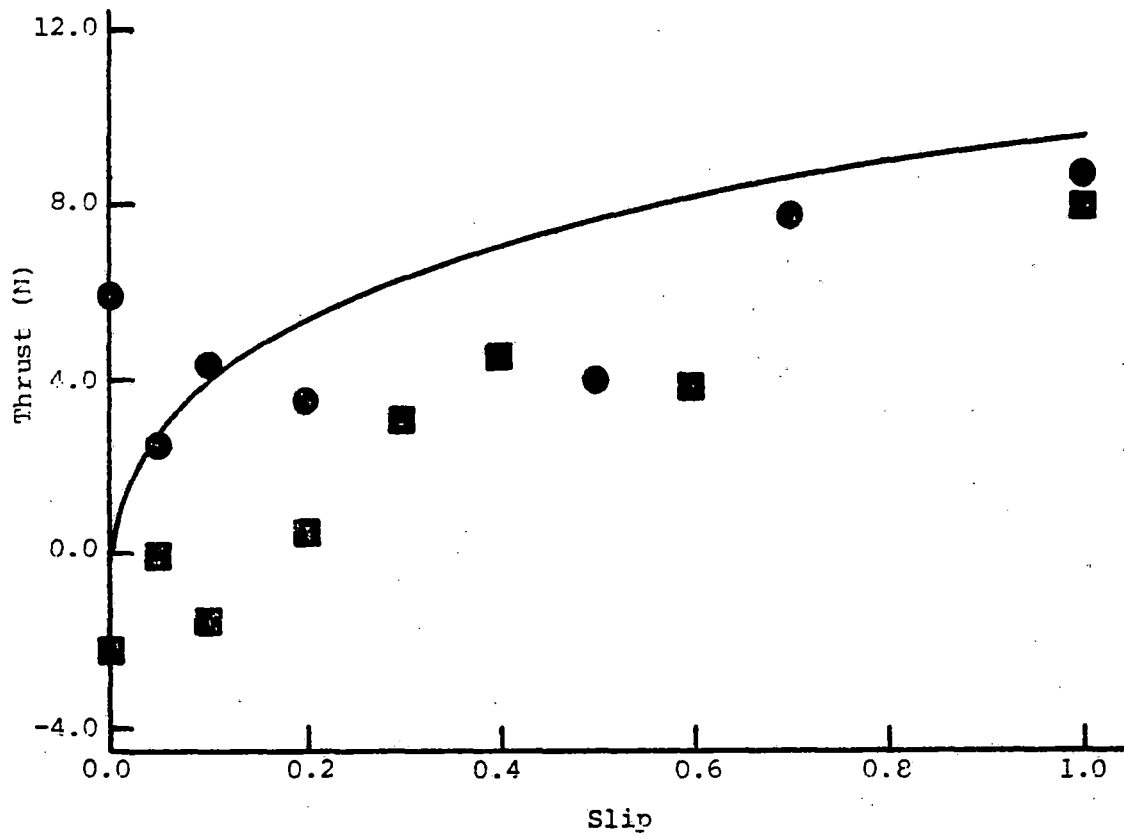
FIGURE 4.3: THRUST VS. SLIP FOR ASLIM (Gap=1.0 cm, Offset=0)
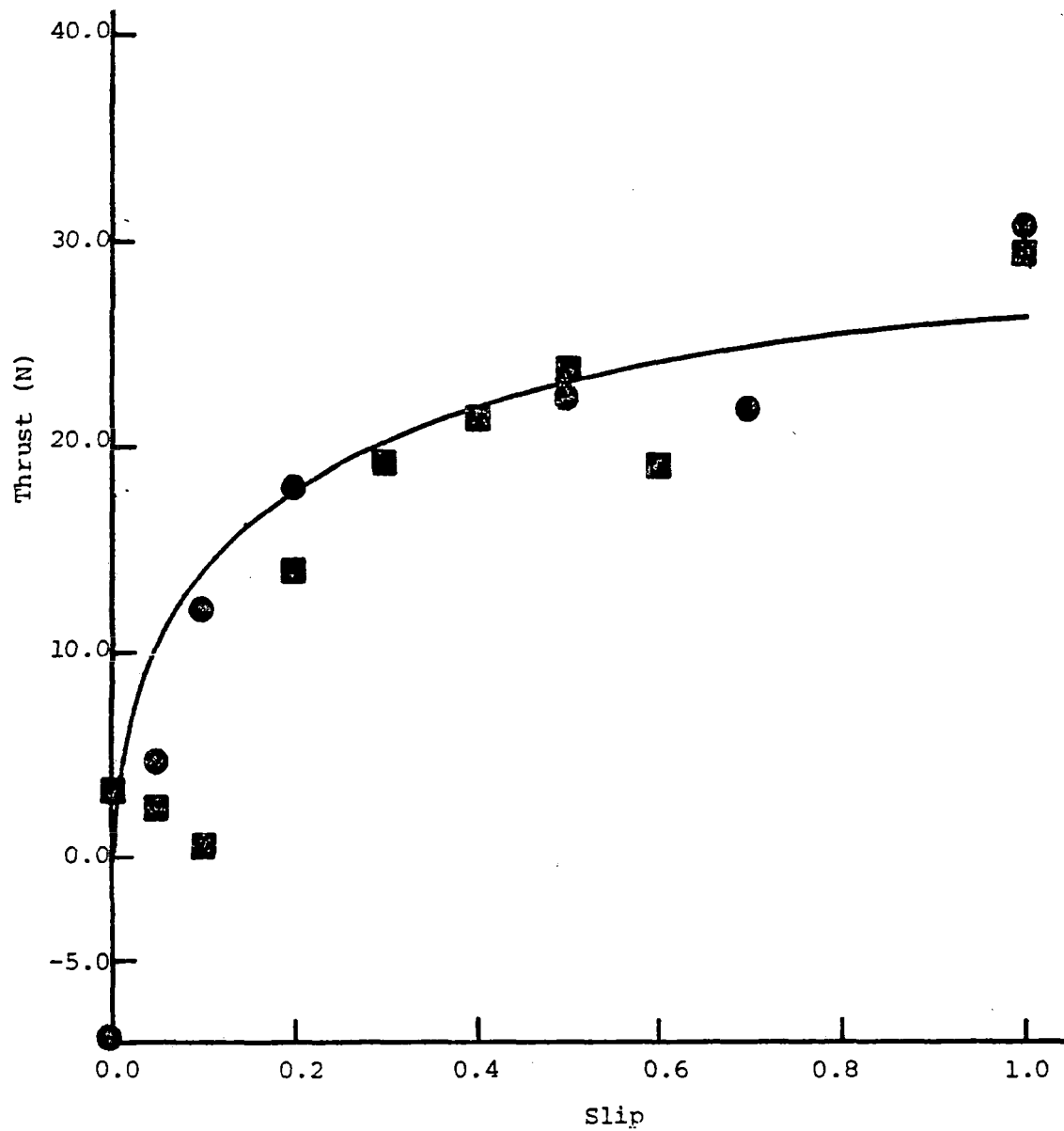
FIGURE 4.4: THRUST VS. SLIP FOR ASLIM (Gap=0.5 cm, Offset=0)
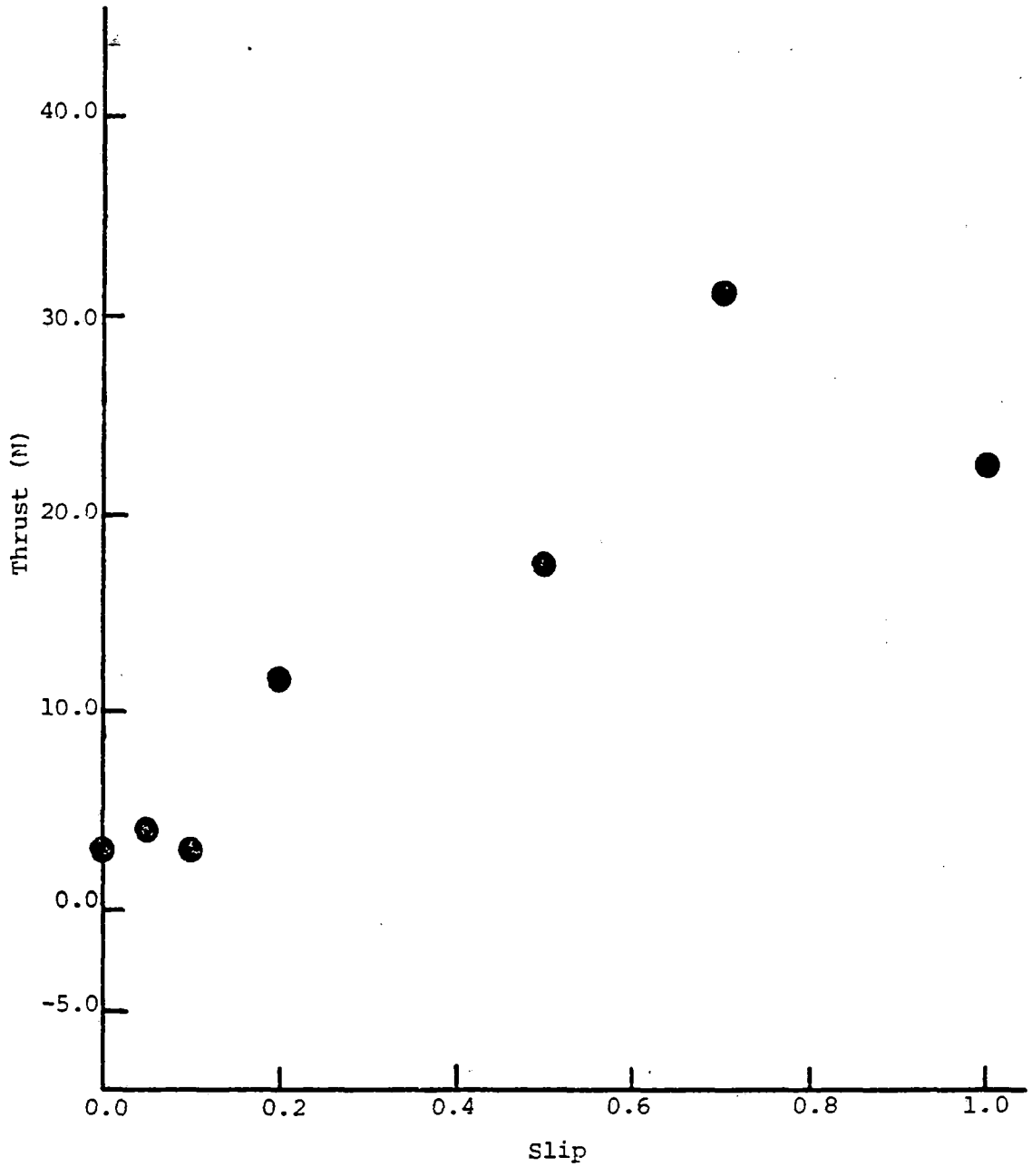
FIGURE 4.5: THRUST VS. SLIP FOR ASLIM (Gap=0.5 cm, Offset=1.0 cm)
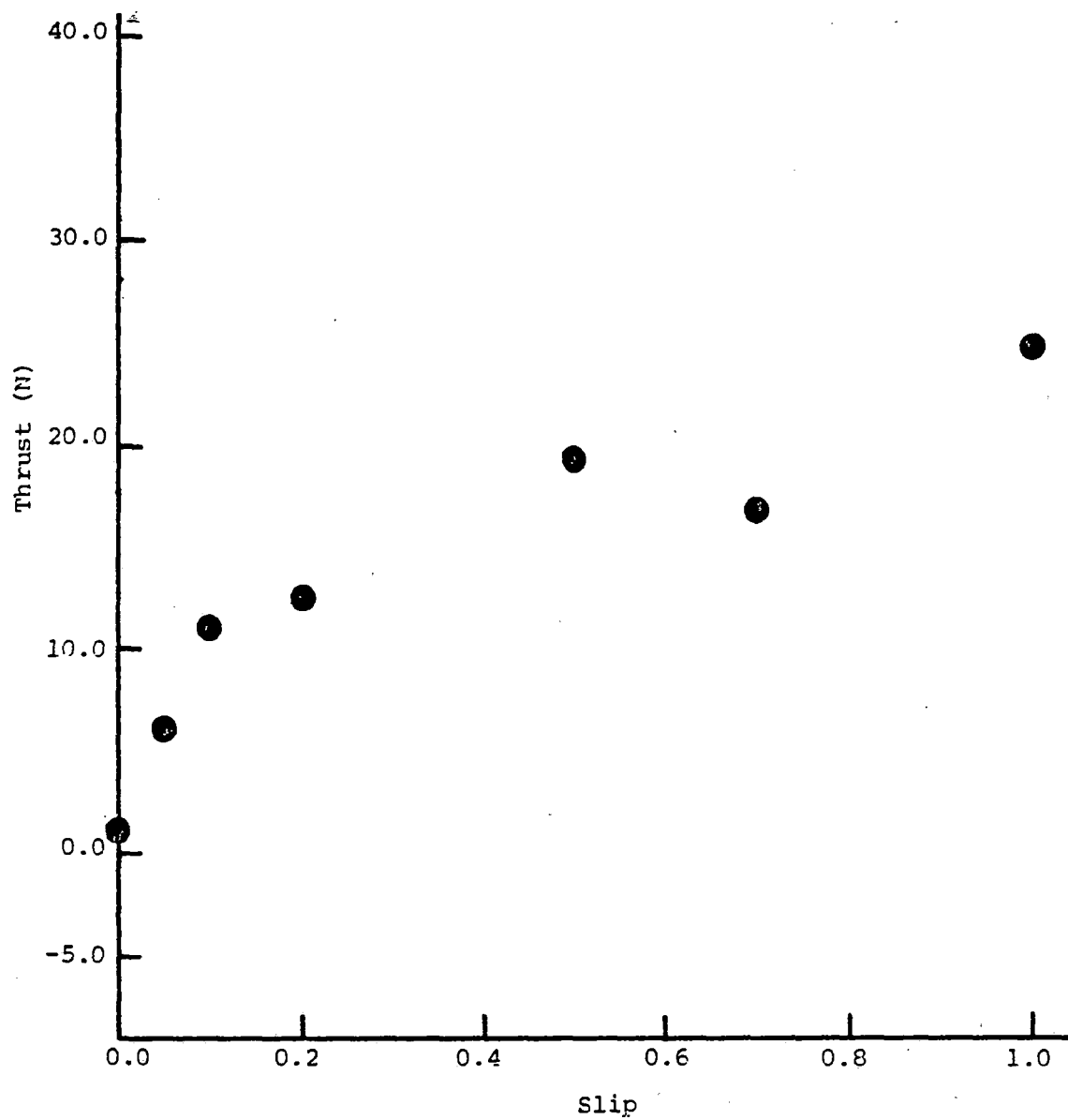
FIGURE 4.6:   THRUST VS. SLIP FOR ASLIM (Gap=0.5 cm, Offset=2.0 cm)
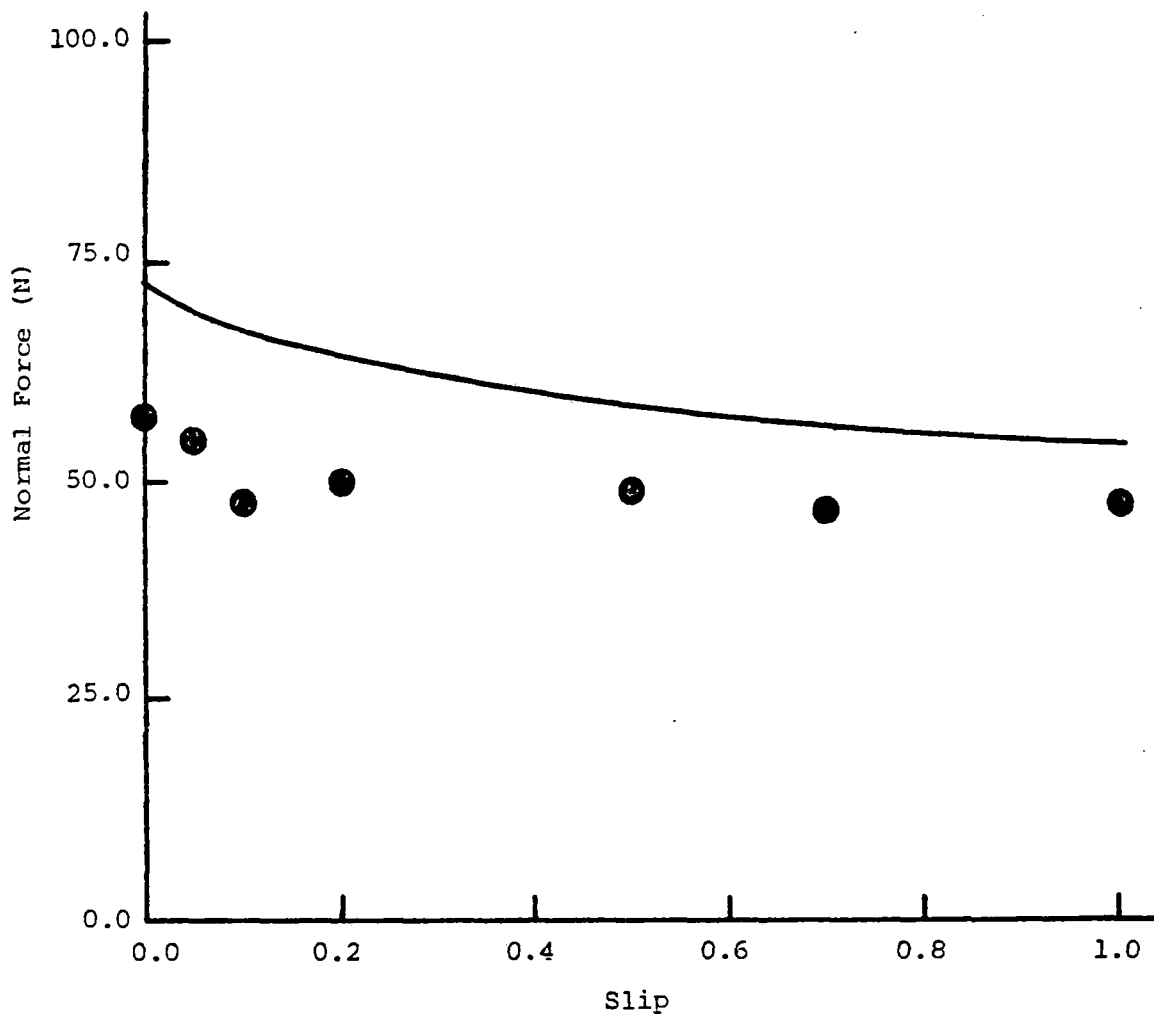
FIGURE 4.7:   NORMAL FORCE VS. SLIP FOR ASLIM (Gap=1.5 cm, Offset=0)
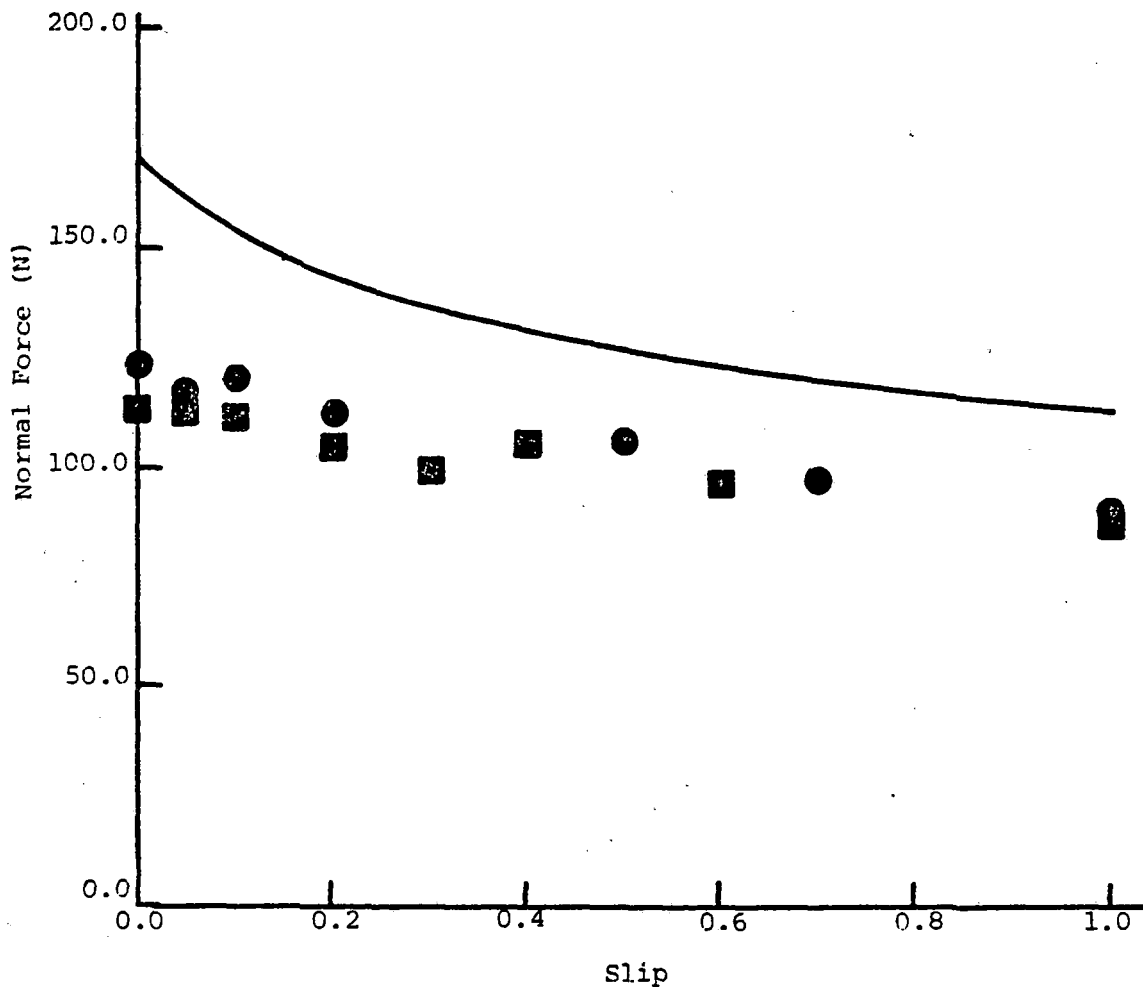
FIGURE 4.8:   NORMAL FORCE VS. SLIP FOR ASLIM (Gap=1.0 cm, Offset=0)
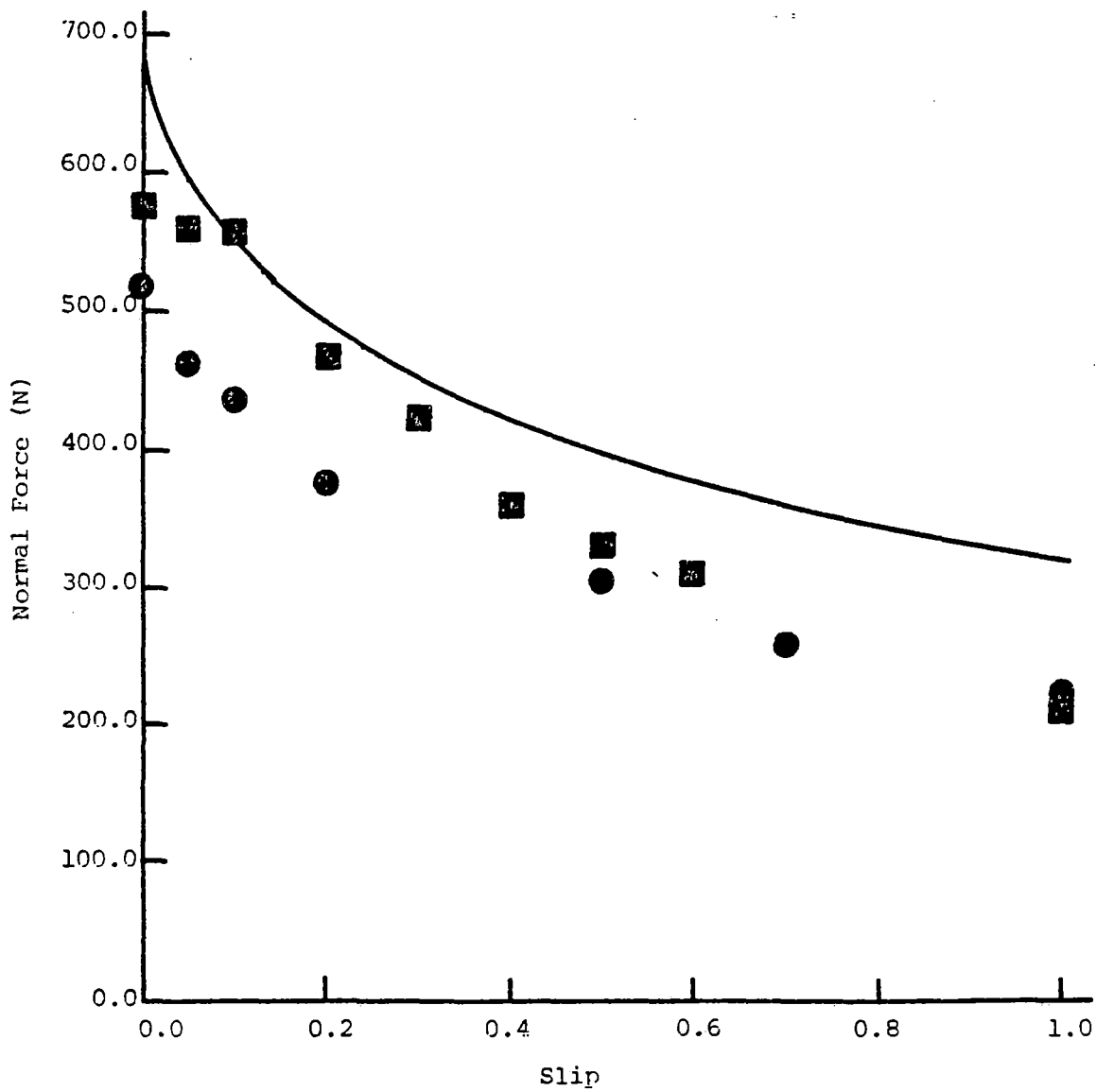
FIGURE 4.9:   NORMAL FORCE VS. SLIP FOR ASLIM
(Gap = 0.5 cm, Offset = 0)
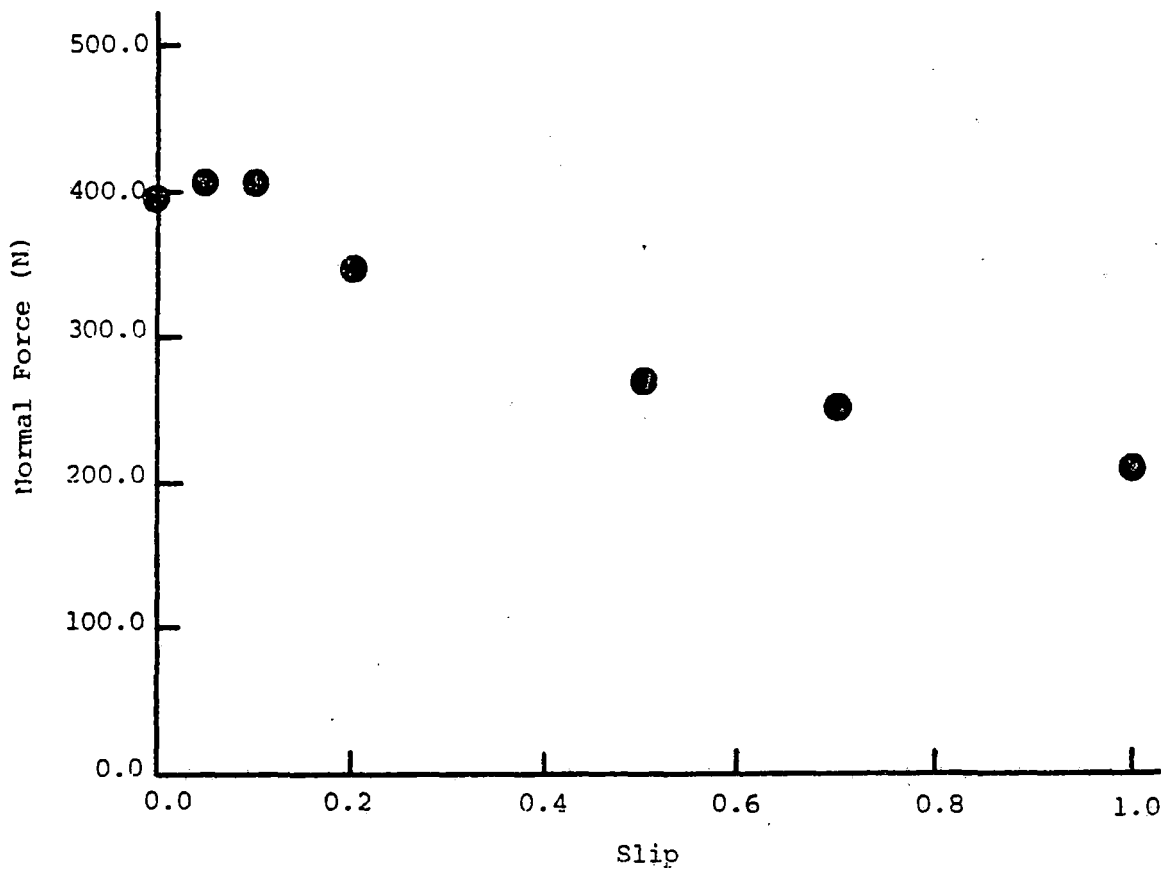
FIGURE 4.10: NORMAL FORCE VS. SLIP FOR ASLIM
(Gap = 0.5, Offset = 1.0 cr)
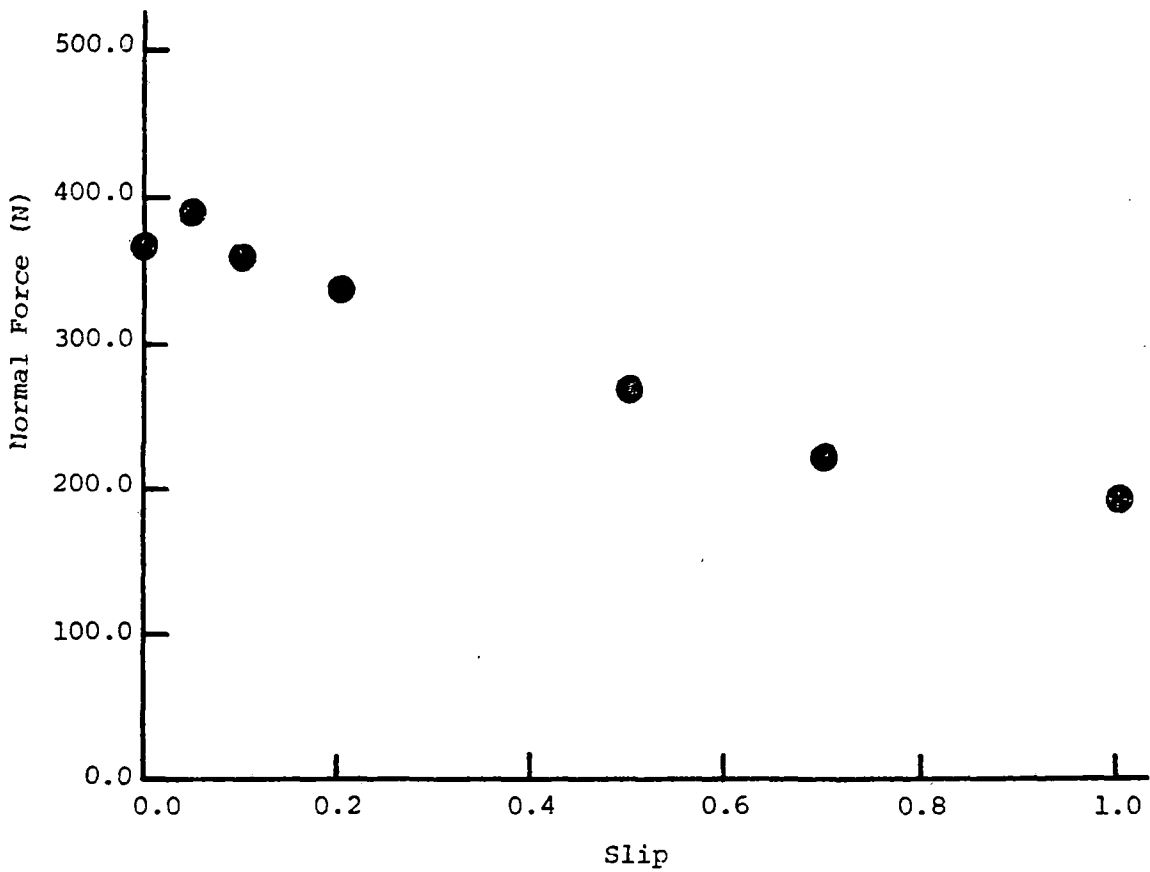
FIGURE 4.11: NORMAL FORCE VS. SLIP FOR ASLIM
(Gap = 0.5 cm, Offset = 2.0 cm)
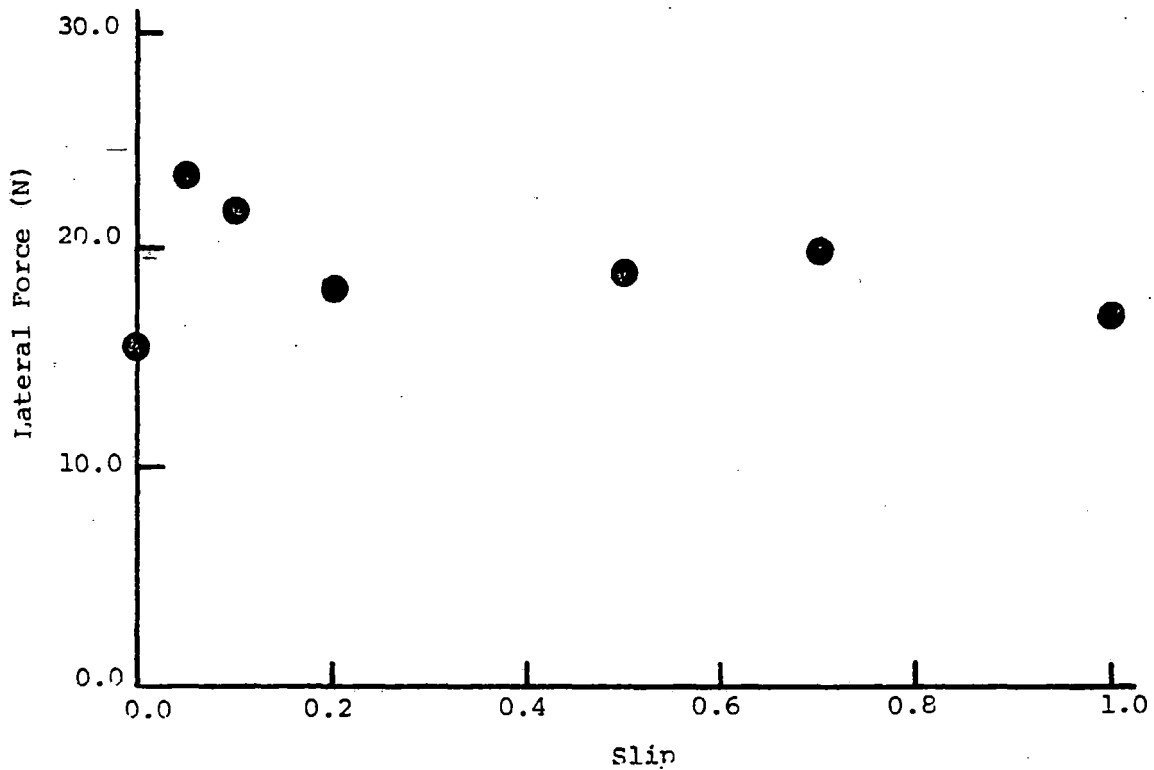
FIGURE 4.12: LATERAL FORCE VS. SLIP FOR ASLIM
(Gap = 0.5 cm, Offset = 1.0 cm)
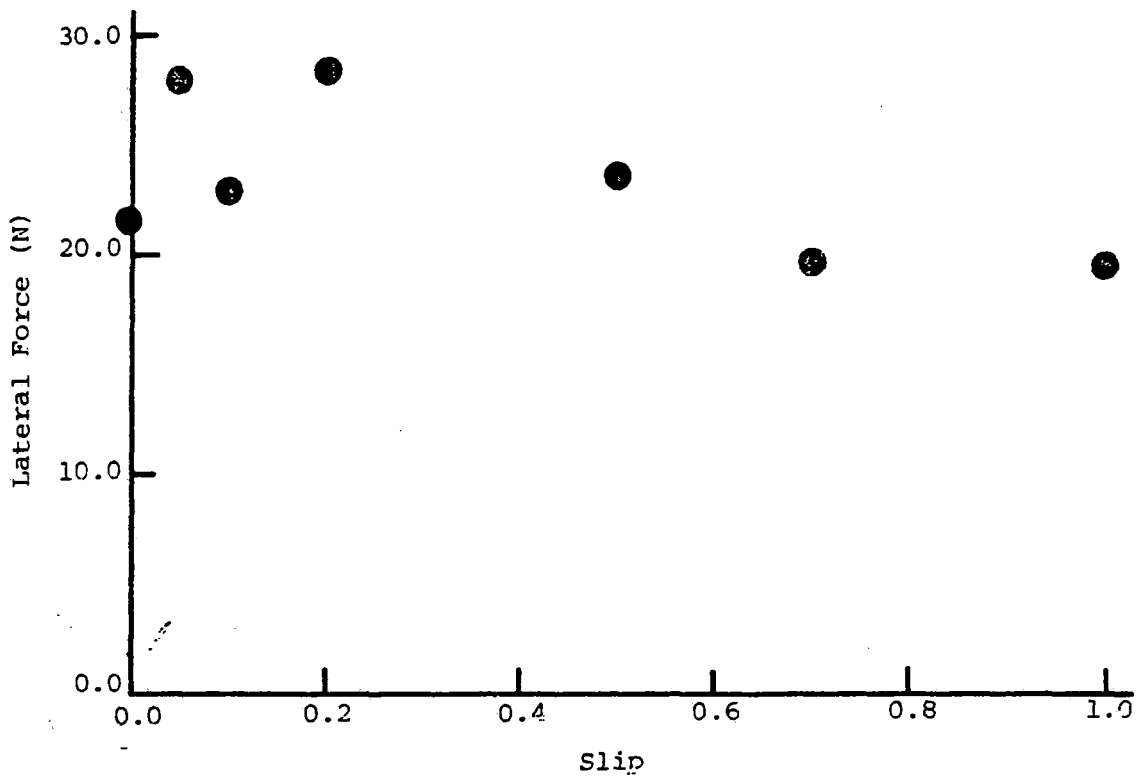
FIGURE 4.13: LATERAL FORCE VS. SLIP FOR ASLIM
(Gap = 0.5 cm, Offset = 2.0 cm)
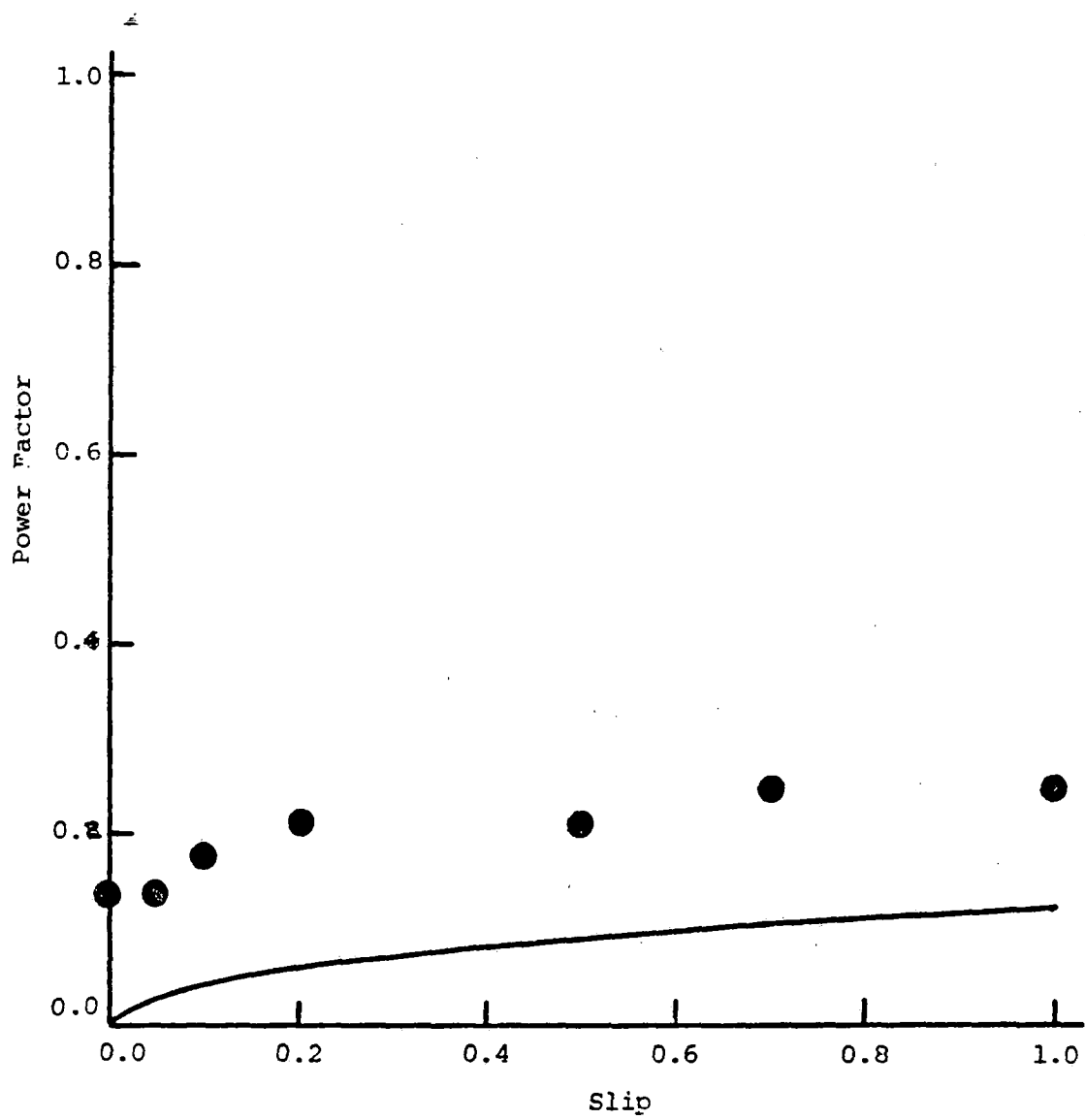
FIGURE 4.14: POWER FACTOR VS. SLIP FOR ASLIM
(Gap = 1.5 cm, Offset = 0)
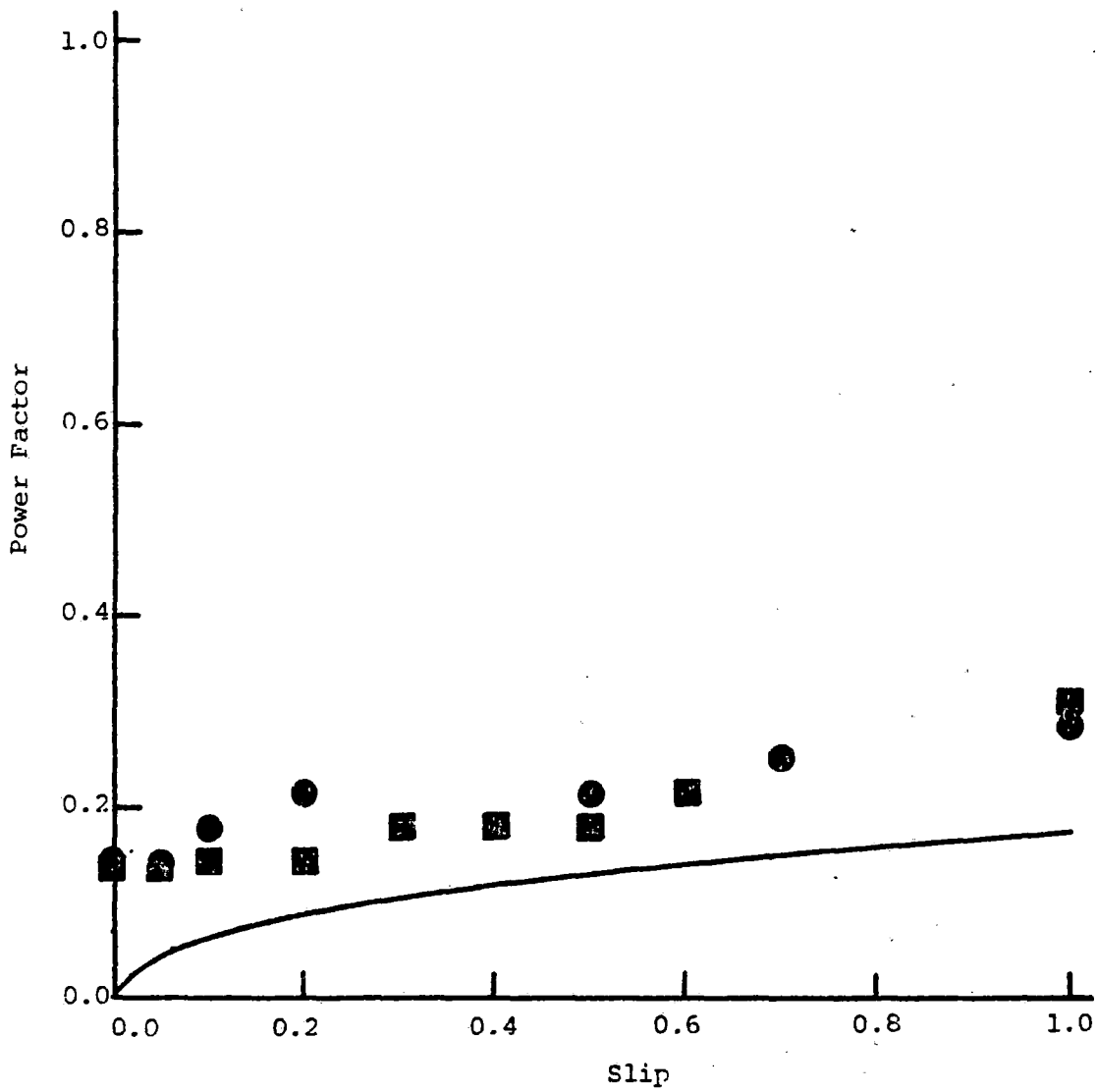
FIGURE 4.15: POWER FACTOR VS. SLIP FOR ASLIM
(Gap = 1.0 cm, Offset = 0)
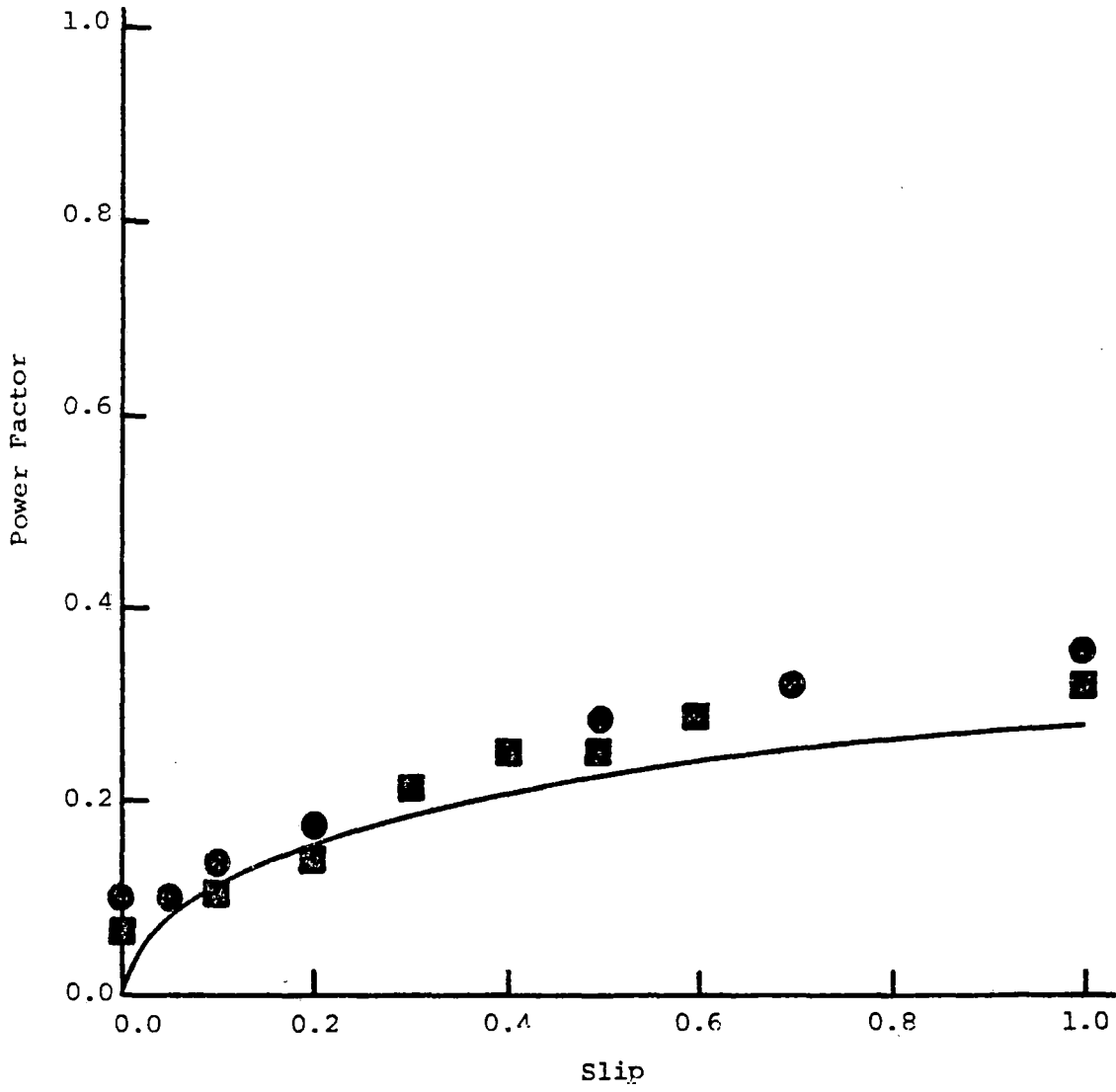
FIGUPE 4.16:   POWER FACTOR VS. SLIP FOR ASLIM
(Gap = 0.5 cm, Offset = 0)

was so small that only scattered data around zero were observed. Tests 36-55 included repeat tests and some additional tests at air gaps of 0.5 and 1.0 cm and no offset. These tests confirm the reliability of the experiment results. These results are plotted with squares rather than with circles.

The plots indicate that the SLIM analysis correctly predicts the trends of the data and in most cases is in good agreement numerically. The discrepancy between the predicted and measured thrust and normal force is due to several factors including:

(1) The simplicity of the model

(2) A phase imbalance, resulting in approximately 3% more current in Phase A than in Phases B and C

(3) Measurement error

The discrepancy between the predicted and measured power factor is discussed below. The agreement between measured and predicted results is satisfactory, considering the simplicity of the ASLIM model.

The fact that the analysis underestimates the measured power factor for large air gaps is a consequence of neglecting the primary winding resistance. As the air gap is increased, the air gap flux and its influence on the input impedance diminishes. Consequently, at large air gaps the primary resistance substantially increases the proportion of the input impedance which is resistive. As a result, the power factor exceeds the predicted values at large air gaps. For full-scale LIMs, the dominant contribution to the input impedance of the LIM is from the air gap flux. For this reason and the desire to maintain model simplicity for application in Chapter 5, the elimination of the primary resistance from the ASLIM power factor calculation is justified.

Several additional observations can be made concerning the data:

(1) The thrust has not reached a peak and is increasing at S=1.0.

(2) The normal force substantially exceeds the other LIM forces at all slips, is always attractive, and gradually diminishes as slips proceed from zero to one.

(3) The power factor is low at all slips and increases gradually, as slip proceeds from zero to one.

(4) The lateral force present at non-zero offsets is always restoring and gradually diminishes as slip proceeds from zero to one.

(5) Offsets of 1.0 and 2.0 cm do not substantially alter the thrust and normal force.

The first three observations are considered in Section 4.3.5,

-72-

since they may be contrasted with the behavior of the ALLIM thrust, normal force, and power factor.

The fourth observation is that the lateral and normal forces are orthogonal components of a force that originates predominantly from the flux interaction with the ferromagnetic primary core and secondary back iron. Consequently, the normal and lateral force exhibit similar behavior, as slip is varied. The final observation suggests that the LIM primary could be offset with respect to the secondary without substantially degrading performance.

4.3.4 Aluminum Sheet-Back Iron Secondary Results (ALLIM)

An aluminum sheet was bonded to the upper surface of the steel, in order to conduct tests on an aluminum sheet-back iron secondary. Initial testing indicated that the entry end (left) transducer measured fewer normal and lateral forces than the exit end (right) transducer, but there was no consistent discrepancy in thrust. In order to determine the reason for this, the LIM phase sequence and the turntable direction were reversed so that the right transducer became the entry end transducer. Under these conditions, the right transducer measured fewer normal and lateral forces, indicating that end effects were responsible for the difference in measurements. Although end effects do not significantly influence overall LIM performance for the operating conditions and LIM design parameters of the tests conducted in this study, they do substantially reduce the air gap flux locally in the vicinity of the entry end transducer, reducing the measured normal and lateral forces. Since thrust acts along the longitudinal axis of the LIM, the thrust measurement is not significantly influenced by local variation of air gap flux in the vicinity of the transducer.

The plots of measured thrust, normal force, lateral force and power factor as a function of slip are shown in Figures 4.17-4.33. For the zero offset cases, three analysis curves are included in the force plots: the curve neglecting end effects, the curve including end effects with no fringing, and the curve including end effects with fringing. In the plots of power factor as a function of slip only, the latter two curves are included.

For all plots of LIM forces as a function of slip, the analysis including end effects and fringing agrees most closely with the measured forces. This is also the case for Figures 3.20 and 3.21. There is little difference between the predicted power factors for the analyses with and without fringing.

The analysis correctly predicts the trends of the data in all the plots. The numerical agreement between the predicted and measured normal force is close. The numerical discrepancy between analysis and data for thrust may be due to the factors cited in Section 4.3.3 and, in addition, the increased influence of end effects for the ALLIM. The overestimation of the power factor by the analysis, especially at high slips may be due to an underestimation of leakage inductance, which is influential at high

-73-
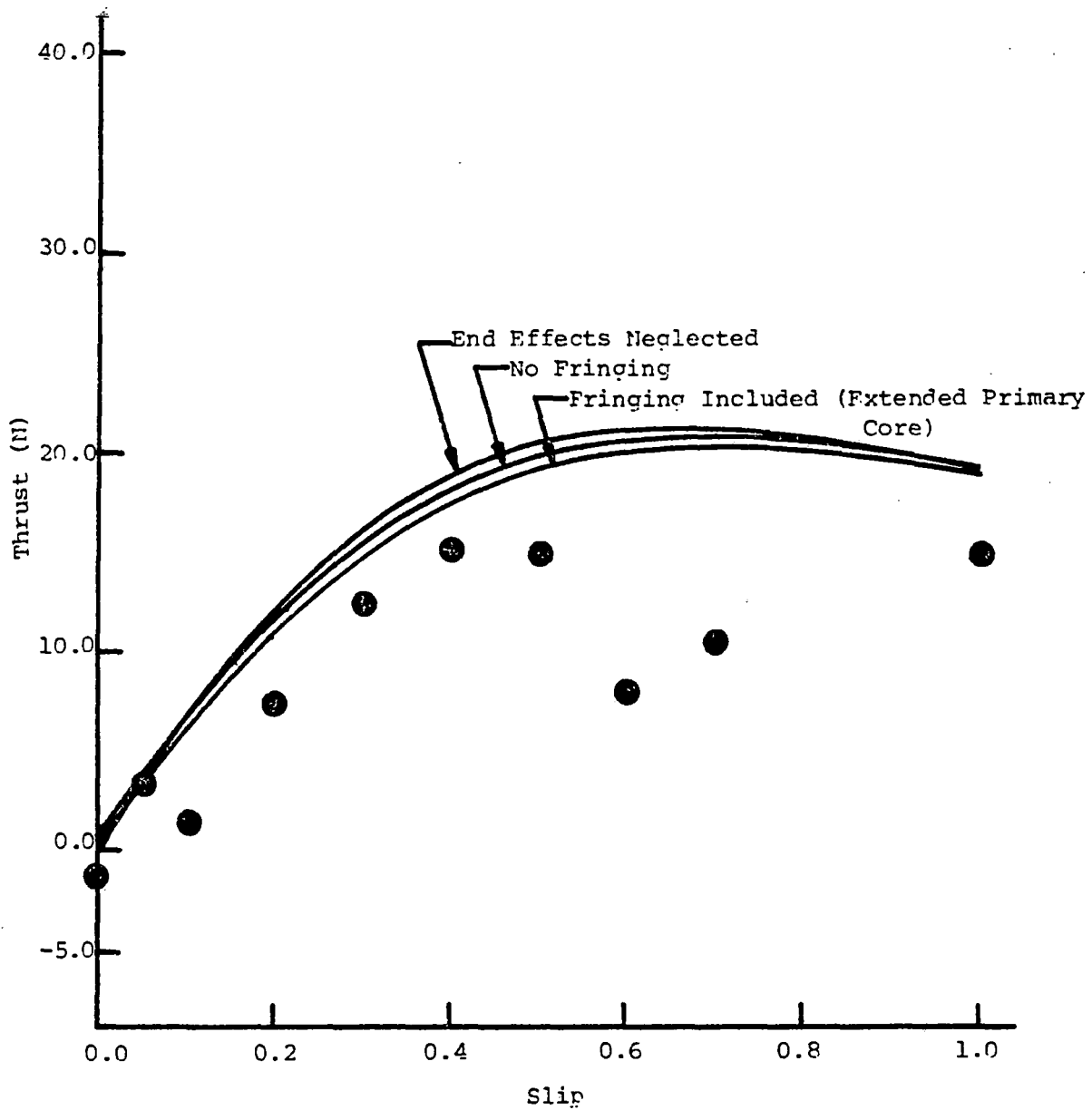
FIGURE 4.17: THRUST VS. SLIP FOR ALLIM
(Gap = 1.5 cm, Offset = 0)
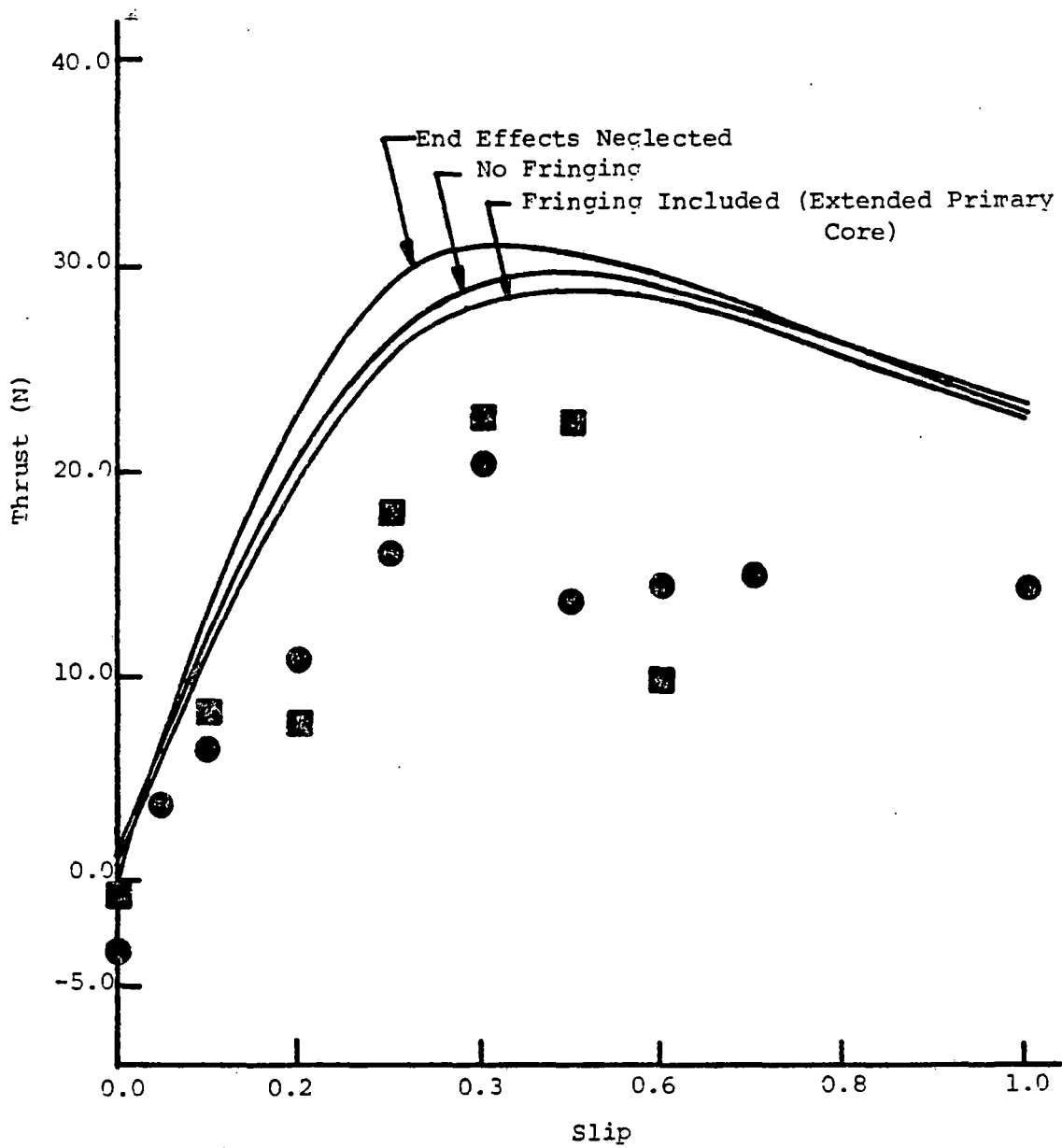
FIGURE 4.18: THRUST VS. SLIP FOR ALLIM
(Gap = 1.0 cm, Offset = 0.0 cm)
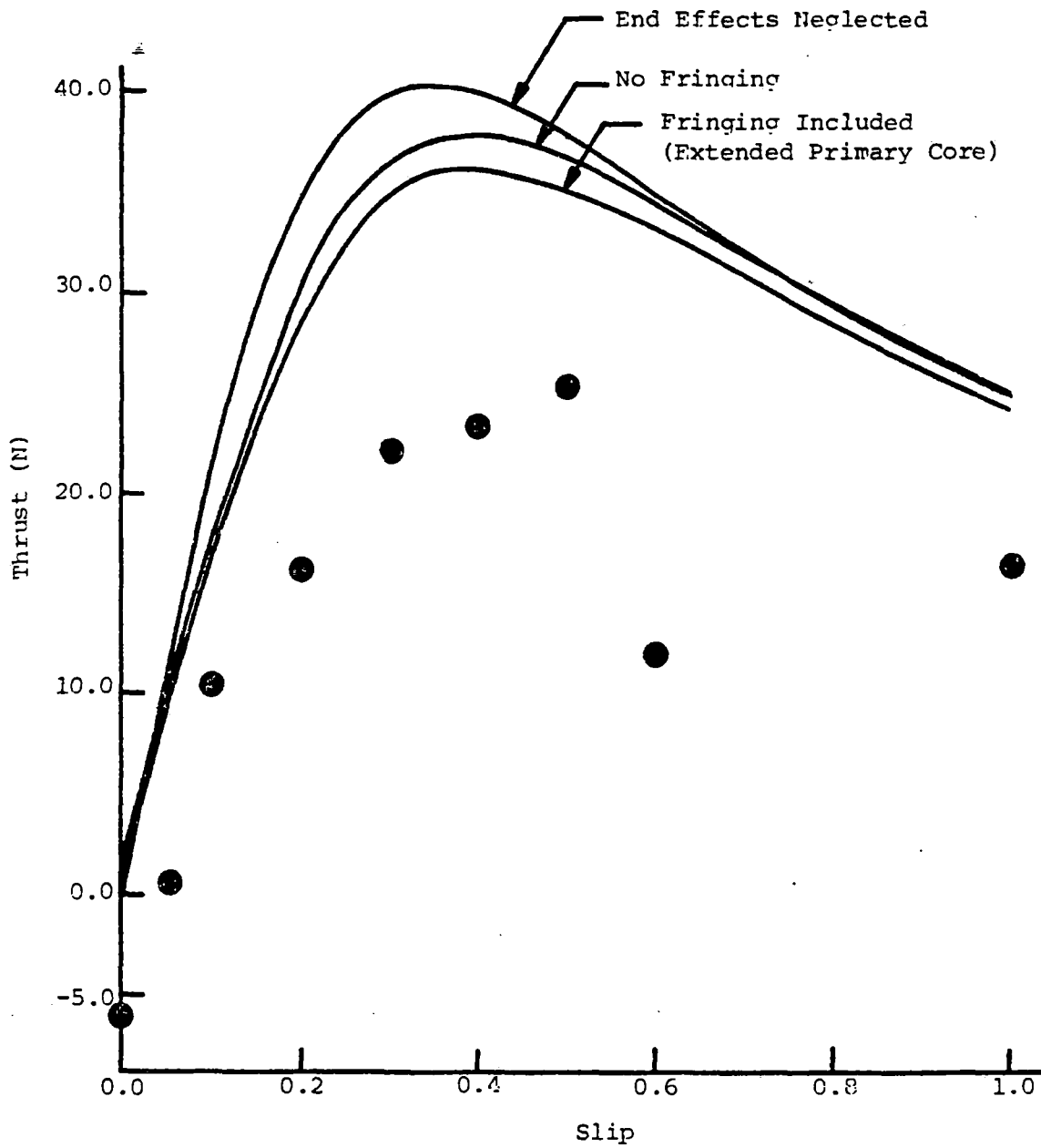
FIGURE 4.19: THRUST VS. SLIP FOR ALLIM
(Gap = 0.75 cm, Offset = 0)
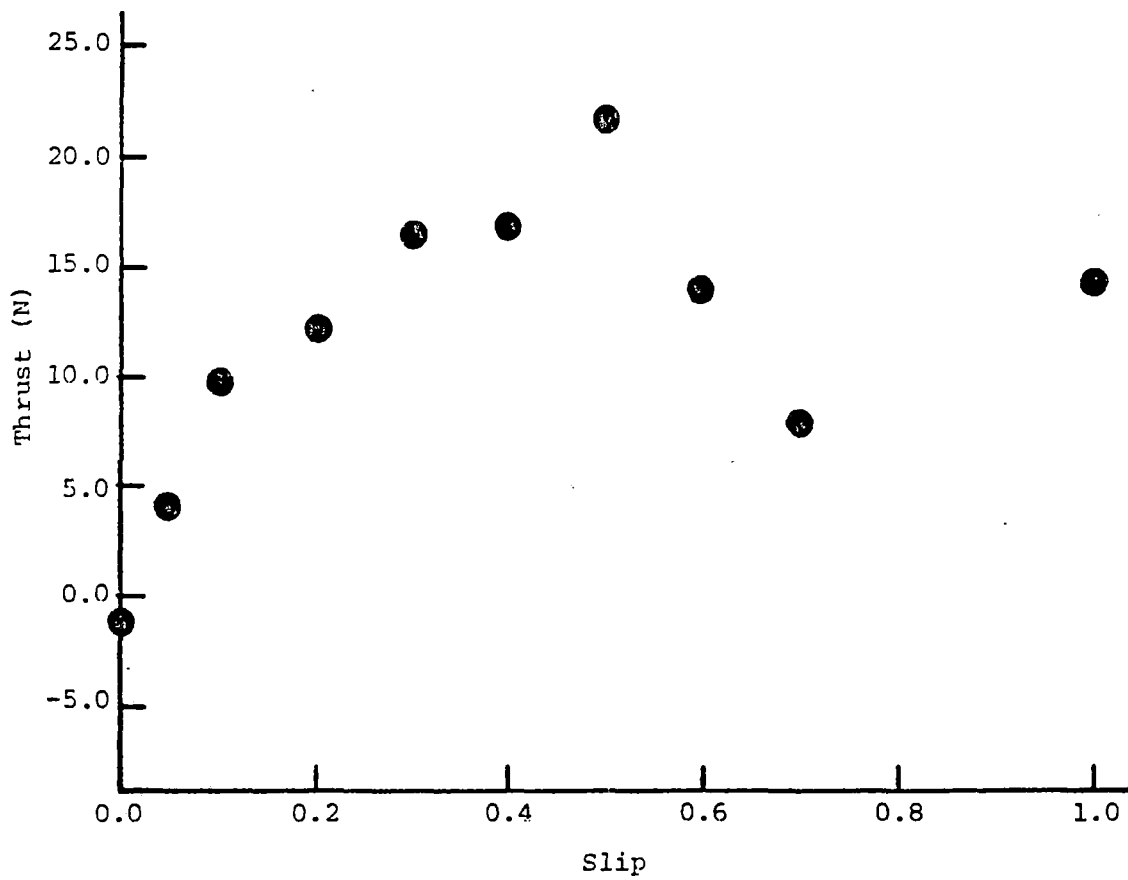
FIGURE 4.20: THRUST VS. SLIP FOR ALLIM
(Gap = 1.0 cm, Offset = 1.0 cm)
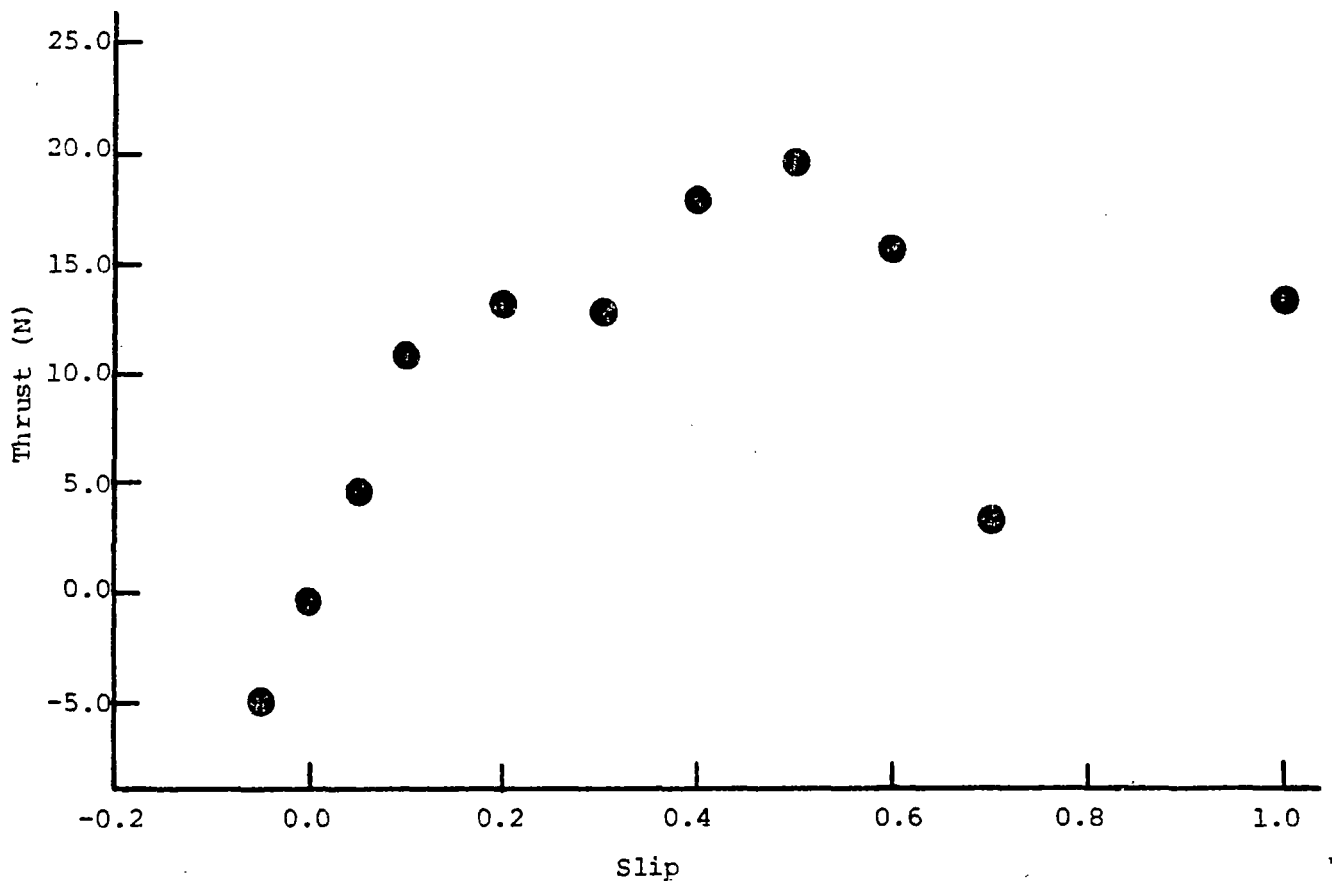
FIGURE 4.21:   THRUST VS. SLIP FOR ALLIM
(Gap = 1.0 cm, Offset = 2.0 cm)
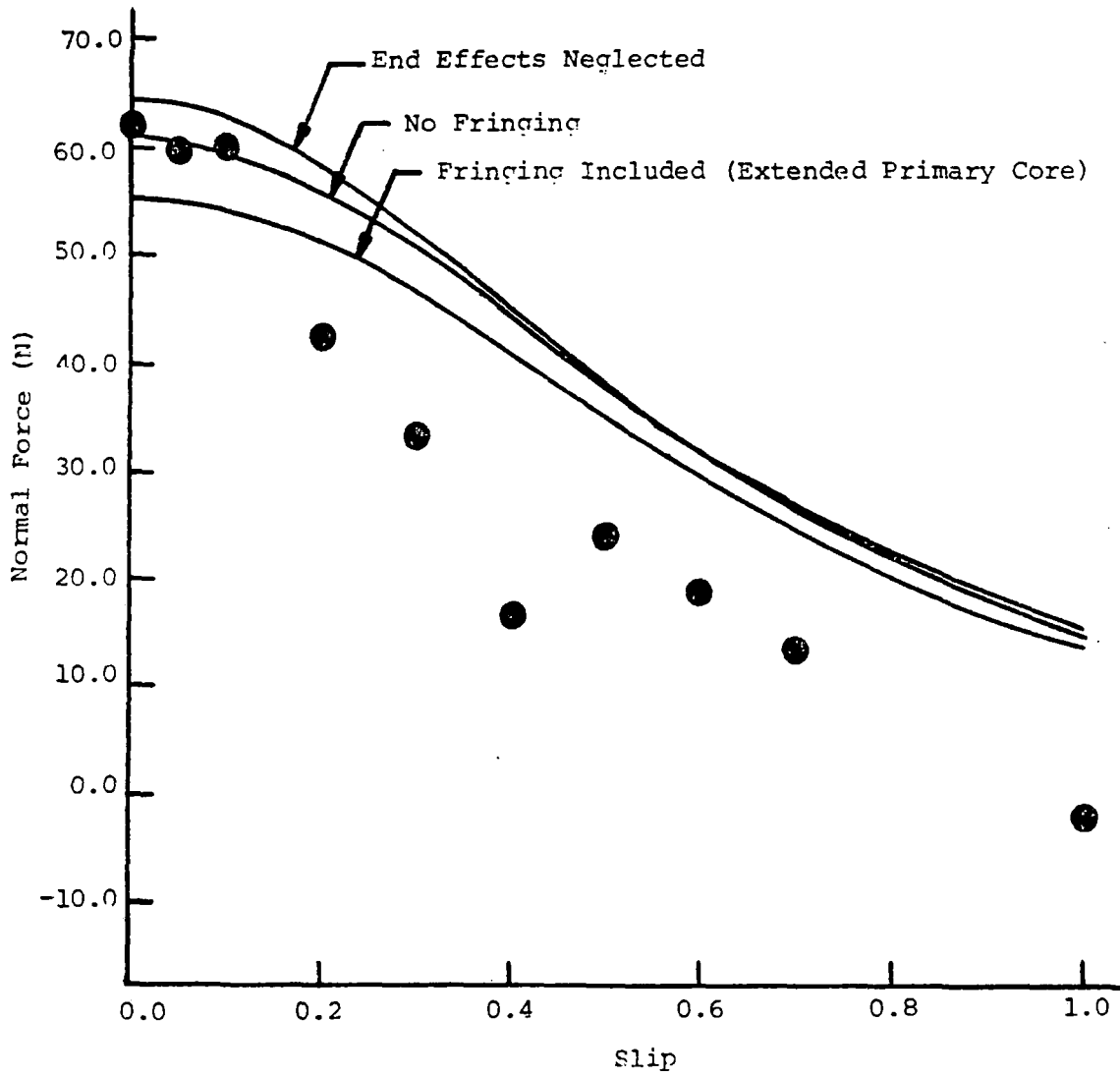
FIGURE 4.22: NORMAL FORCE VS. SLIP FOR ALLIM
(Gap = 1.5 cm, Offset = 0)
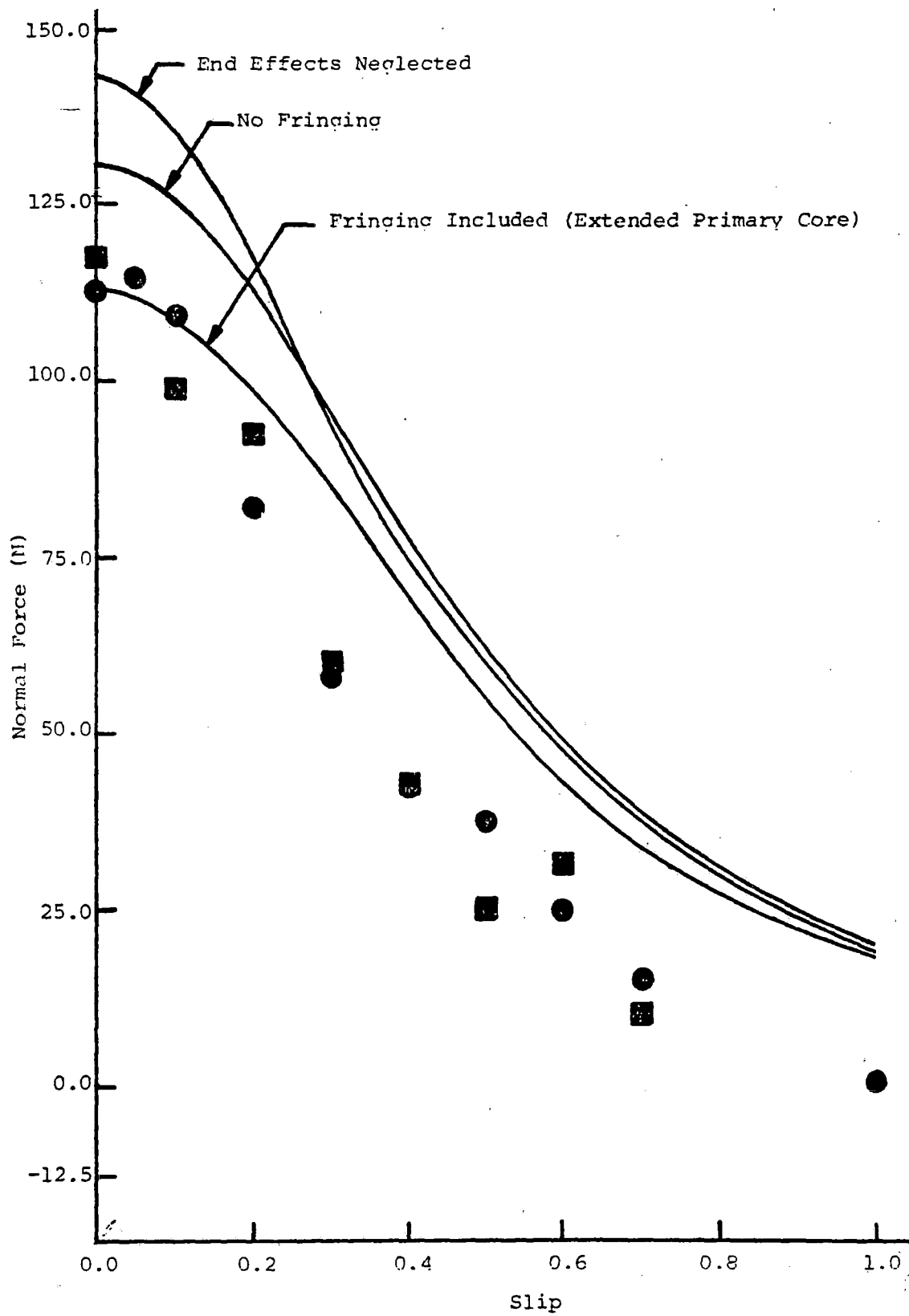
FIGURE 4.23: NORMAL FORCE VS. SLIP FOR ALLIM
(Gap = 1.0 cm, Offset = 0)
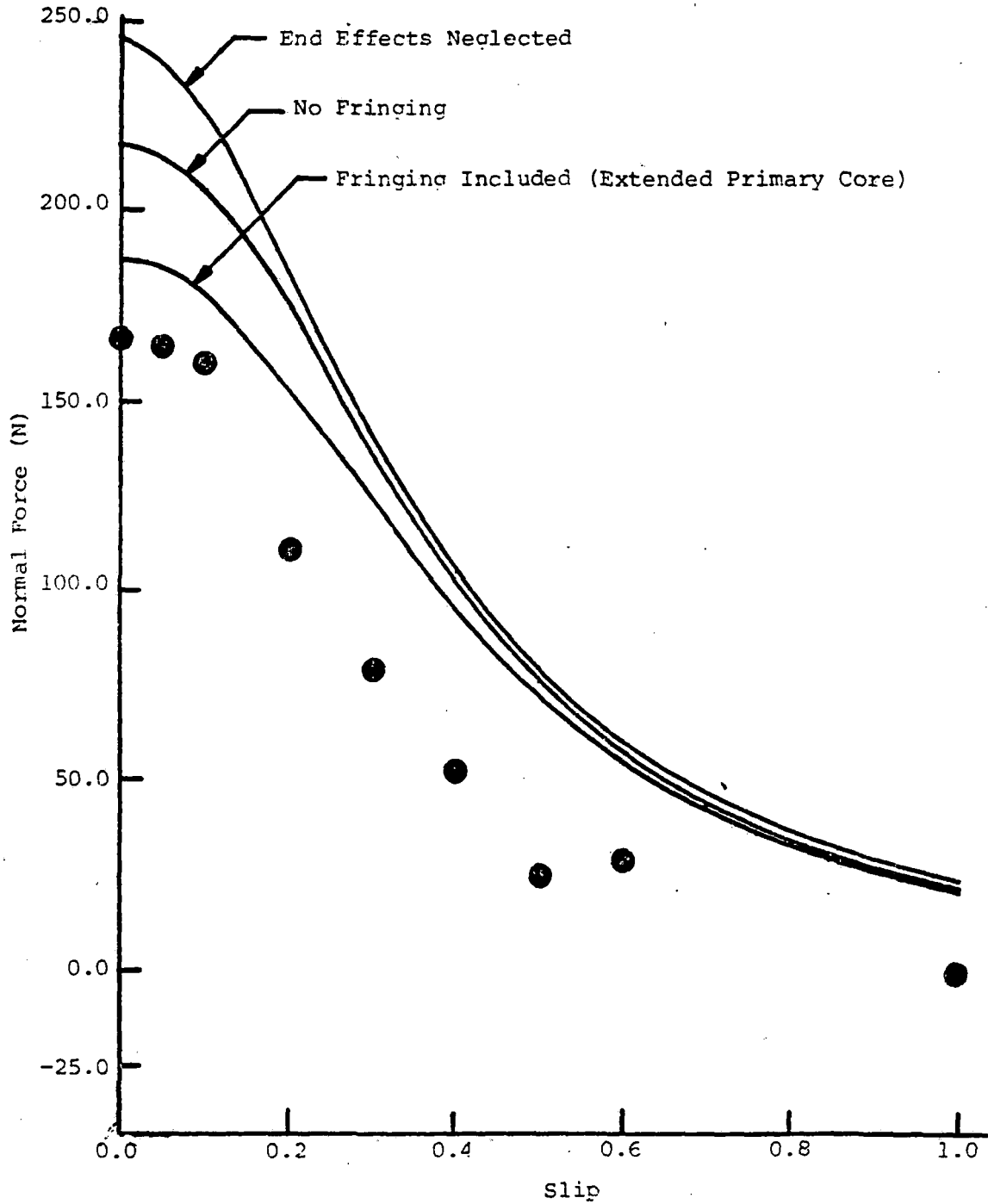
FIGURE 4.24: NORMAL FORCE VS. SLIP FOR ALLIM
(Gap = 0.75 cm, Offset = 0)
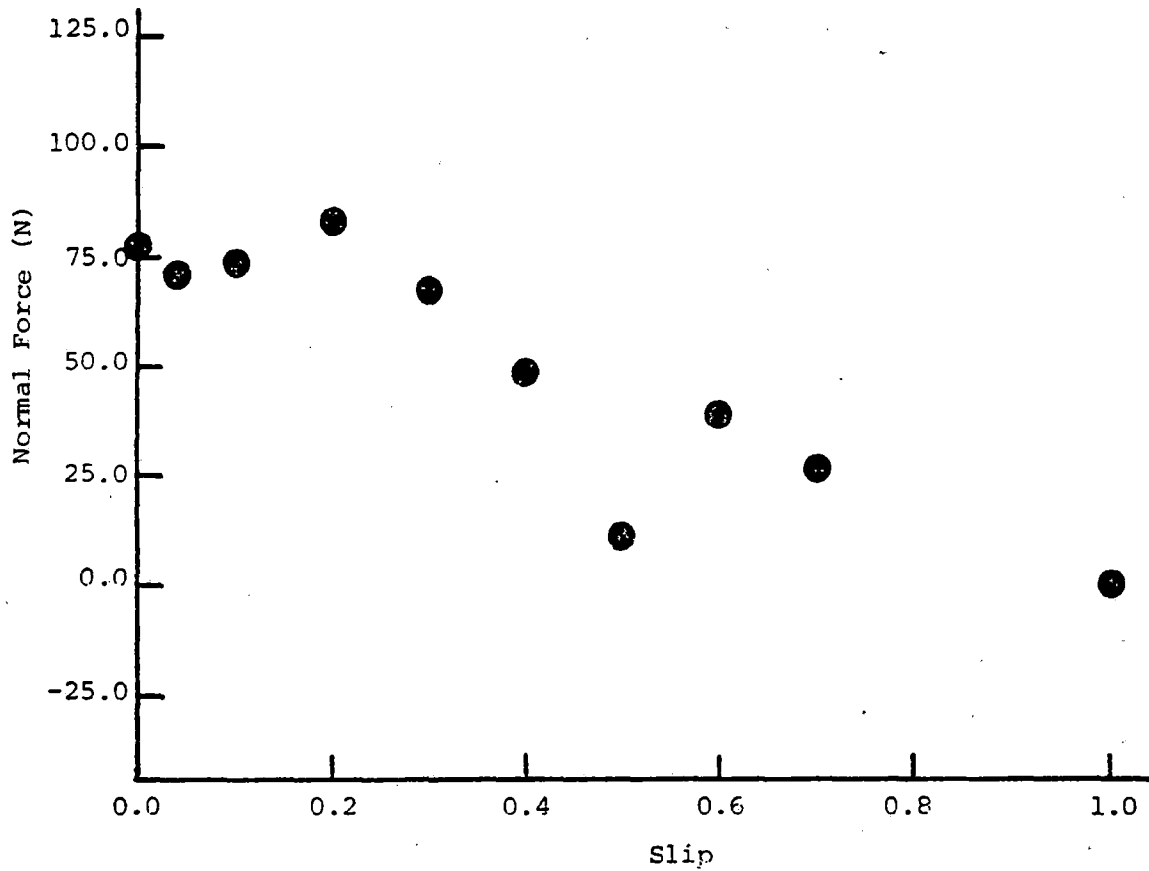
FIGURE 4.25: NORMAL FORCE VS. SLIP FOR ALLIM
(Gap = 1.0 cm, Offset = 1.0 cm)
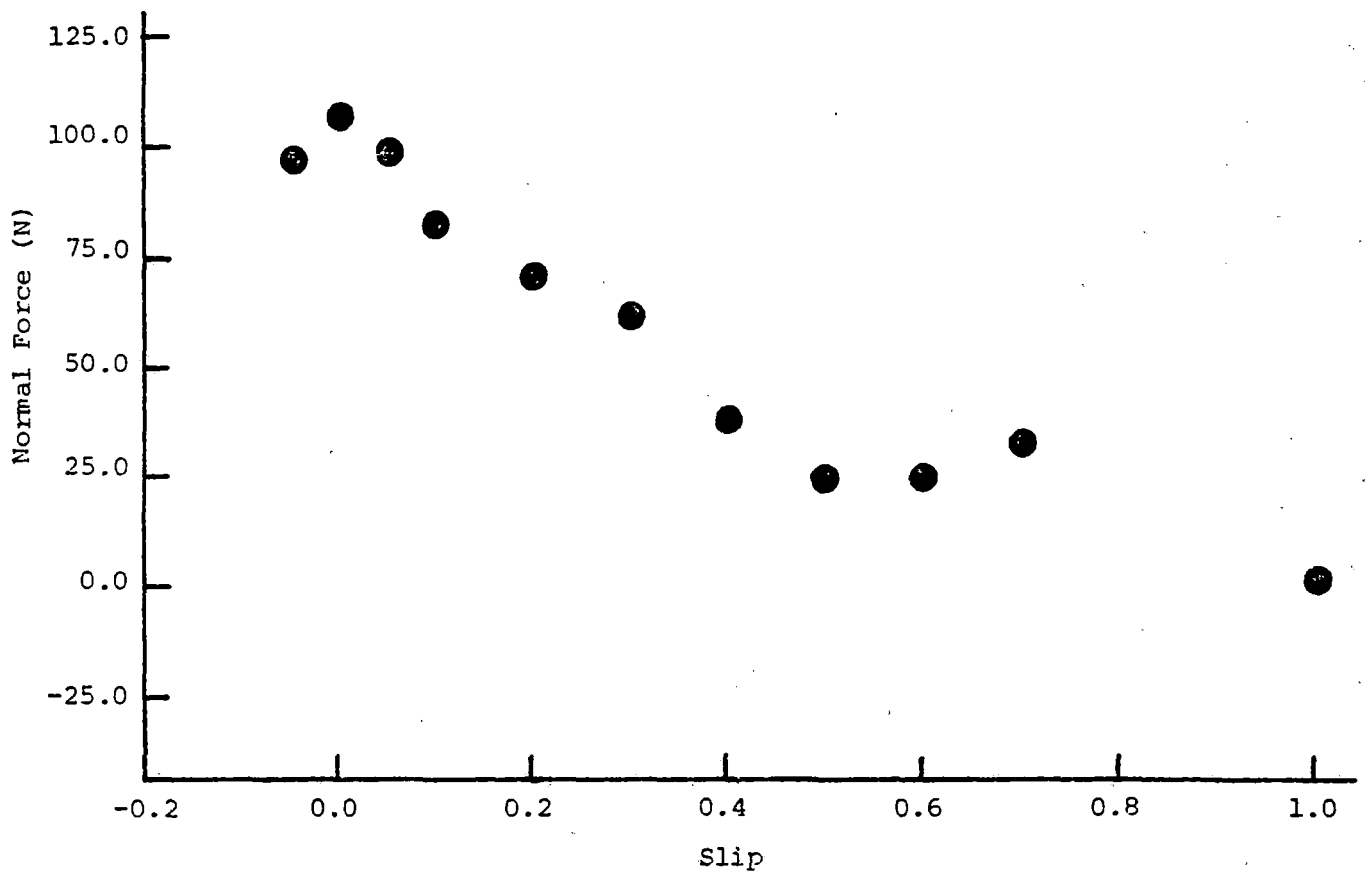
FIGURE 4.26: NORMAL FORCE VS. SLIP FOR ALLIM
(Gap = 1.0 cm, Offset = 2.0 cm)
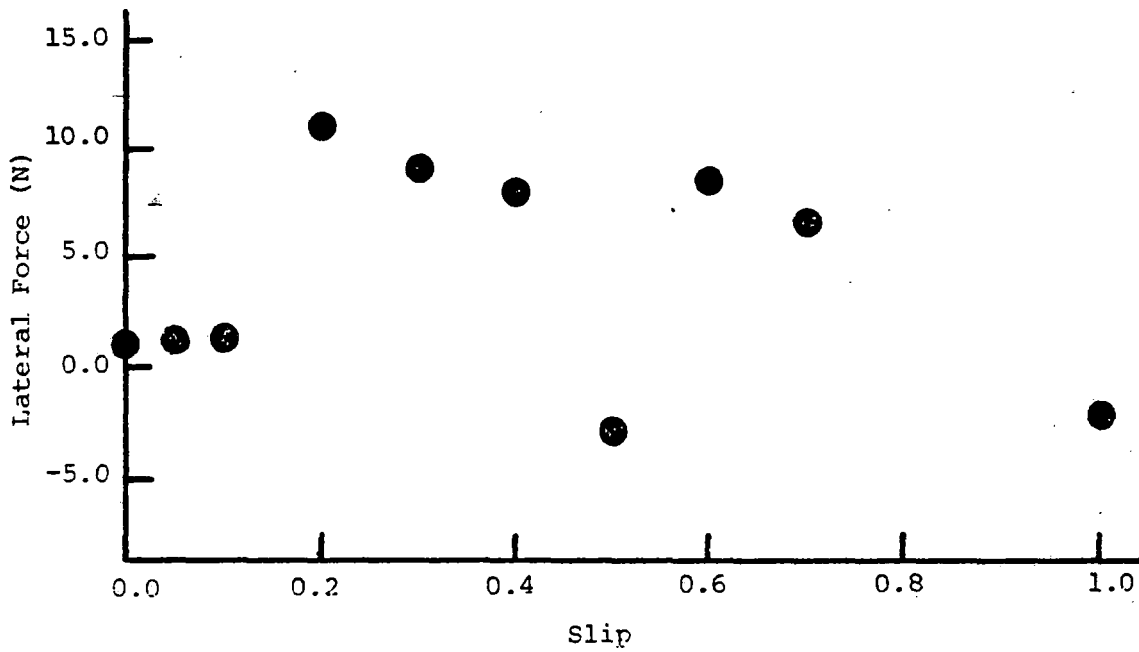
FIGURE 4.27: LATERAL FORCE VS. SLIP FOR ALLIM
(Gap = 1.0 cm, Offset = 1.0 cm)
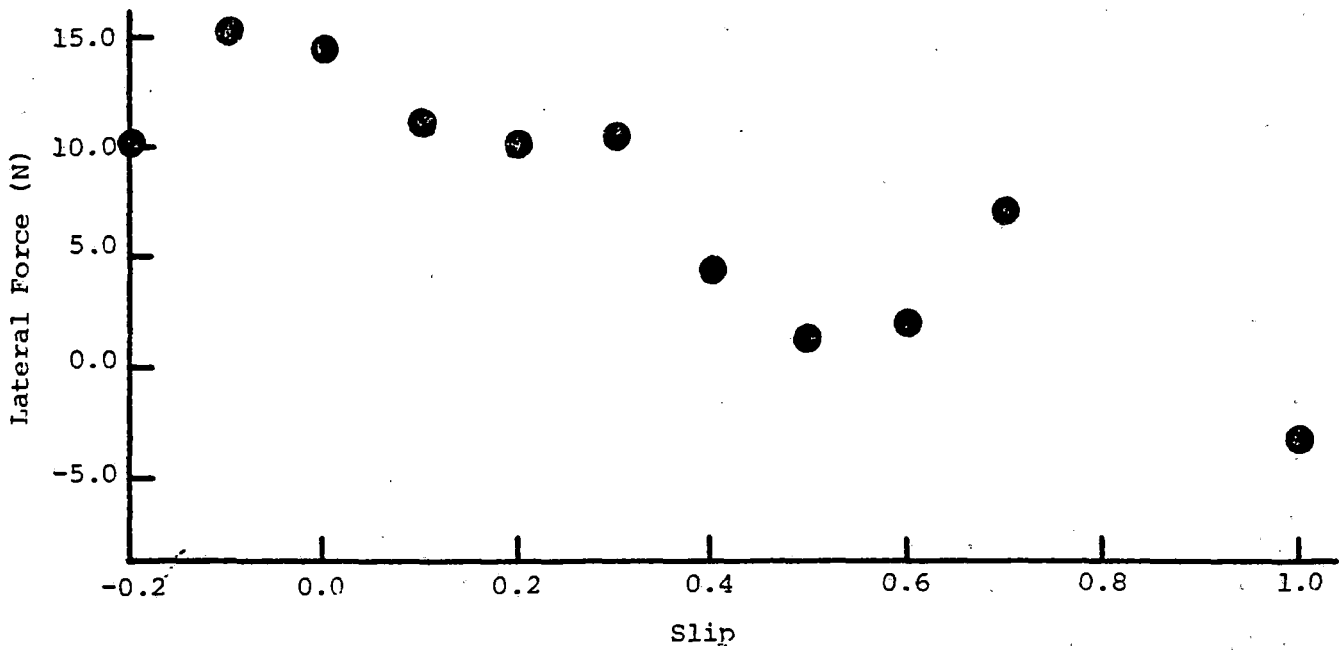
FIGURE 4.28: LATERAL FORCE VS. SLIP FOR ALLIM
(Gap = 1.0 cm, Offset = 2.0 cm)
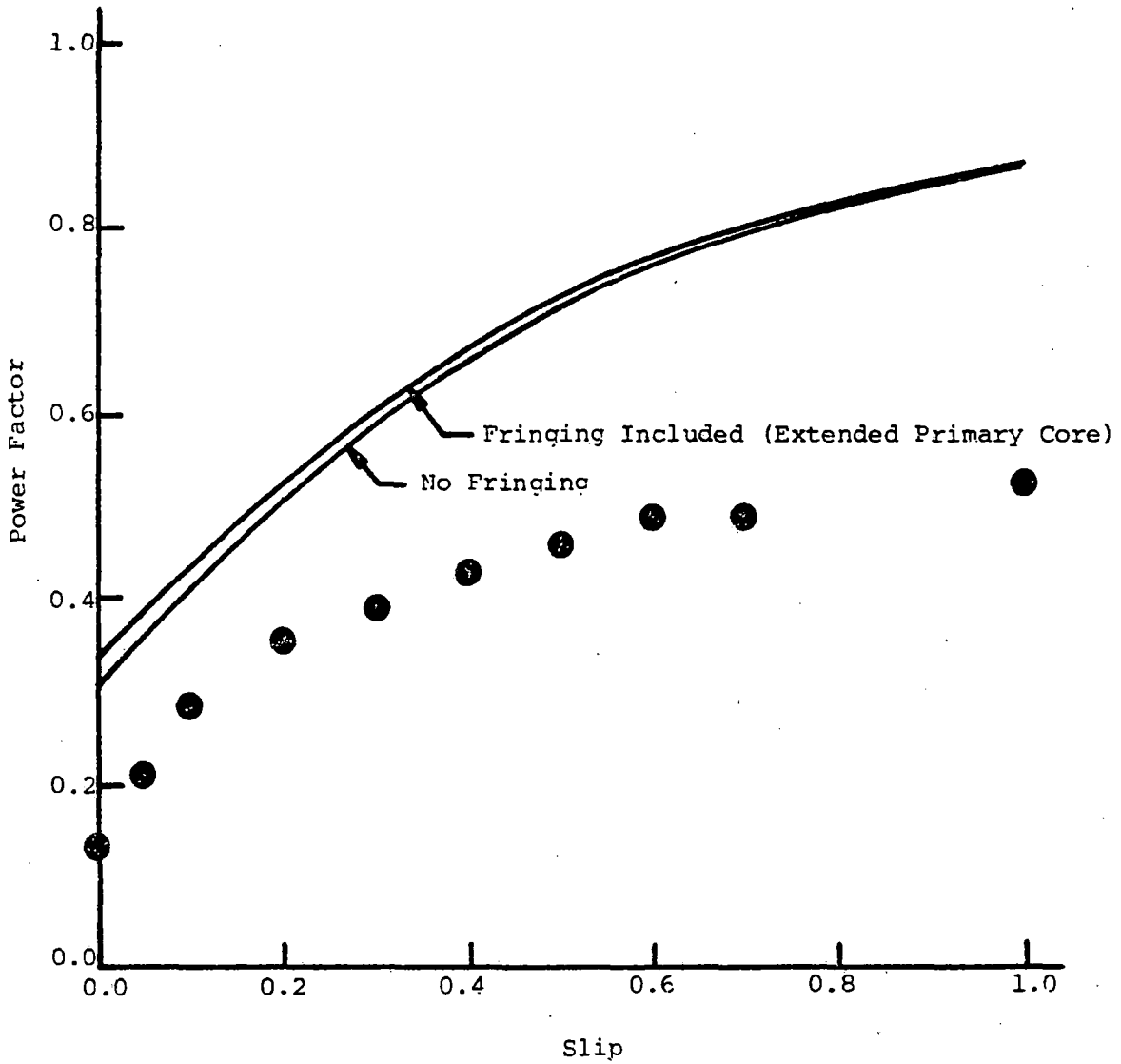
FIGURE 4.29: POWER FACTOR VS. SLIP FOR ALLIM
(Gap = 1.5 cm, Offset = 0)
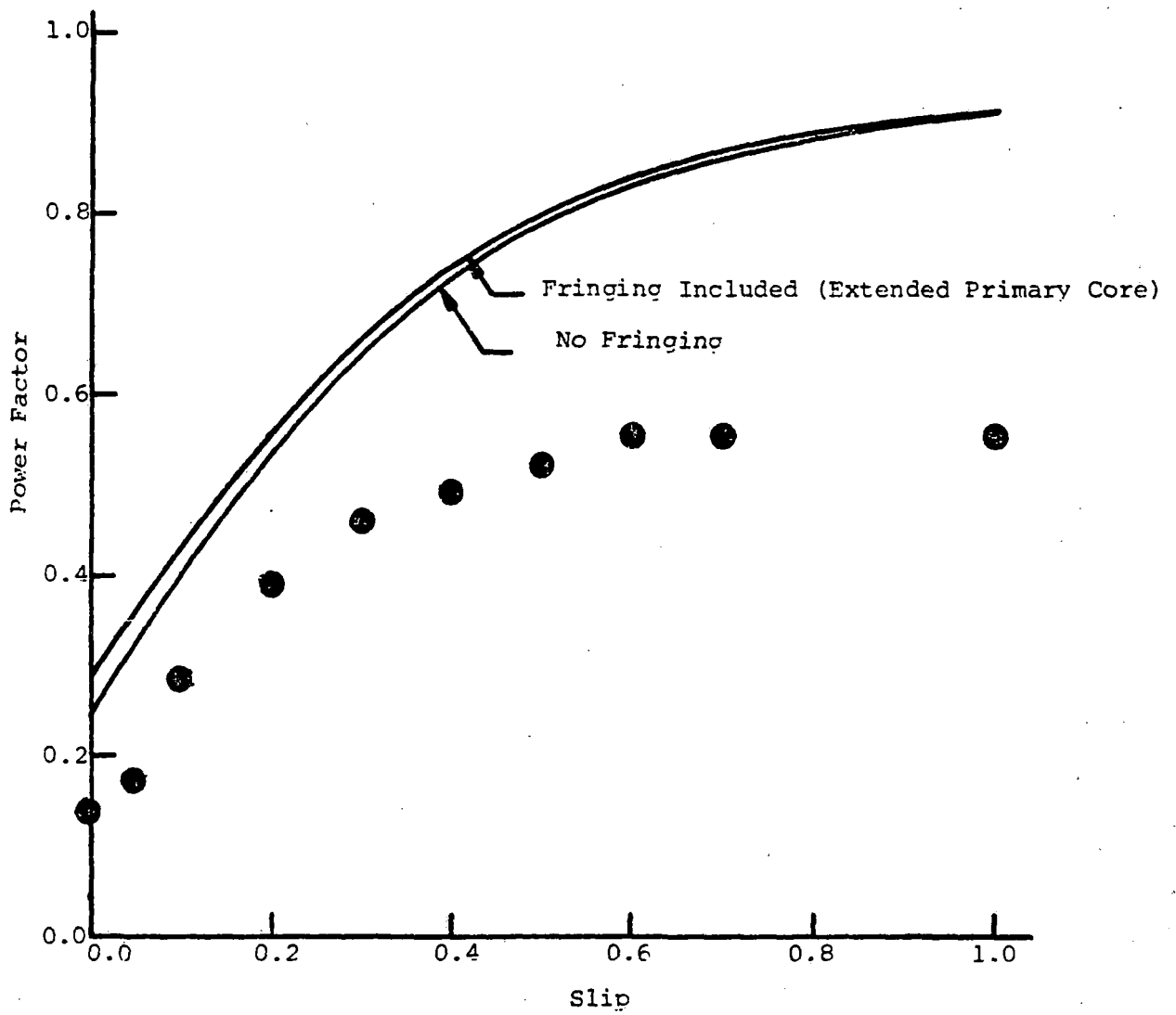
FIGURE 4.30: POWER FACTOR VS. SLIP FOR ALLIM
(Gap = 1.0 cm, Offset = 0)
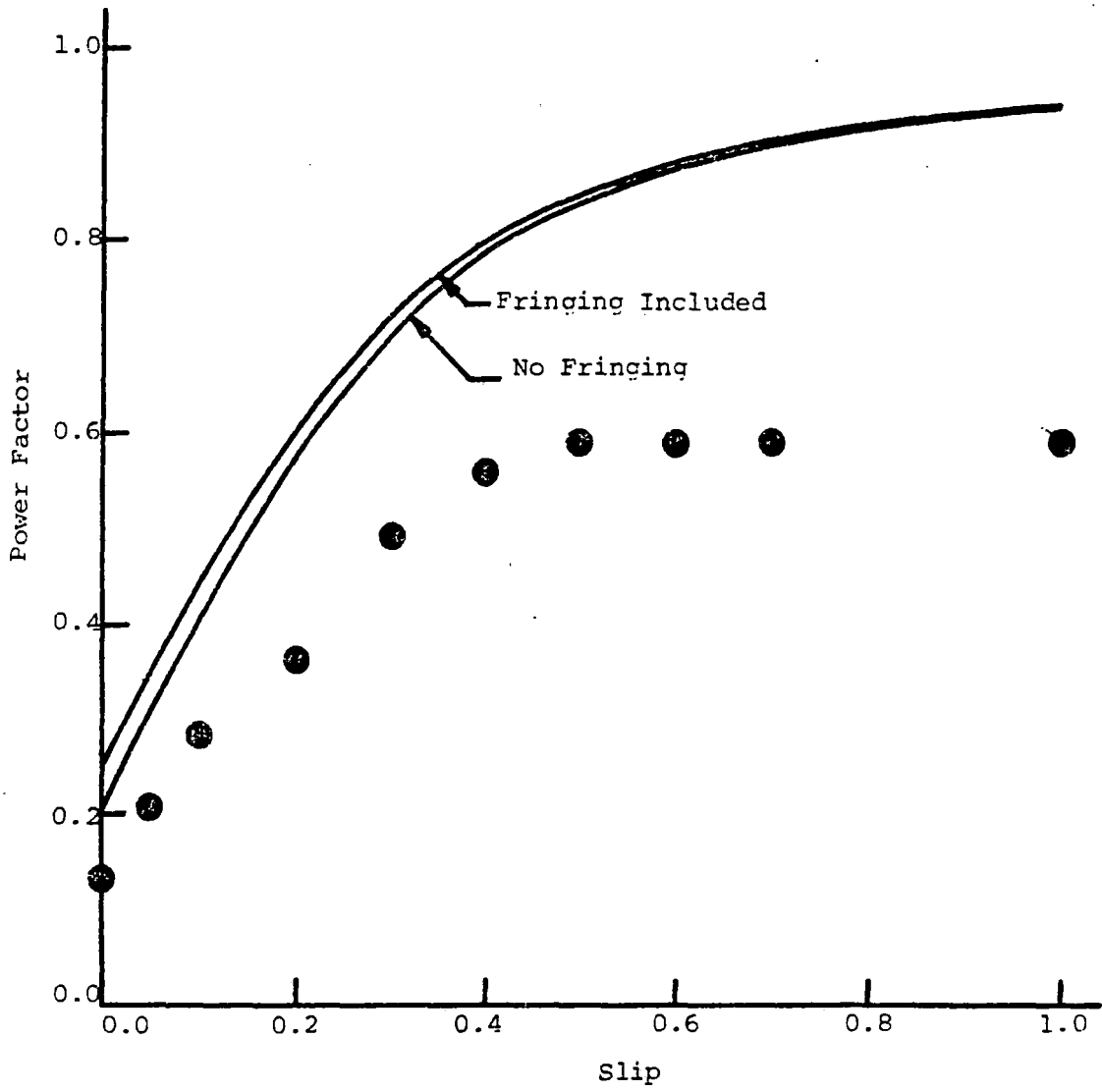
FIGURE 4.31: POWER FACTOR VS. SLIP FOR ALLIM
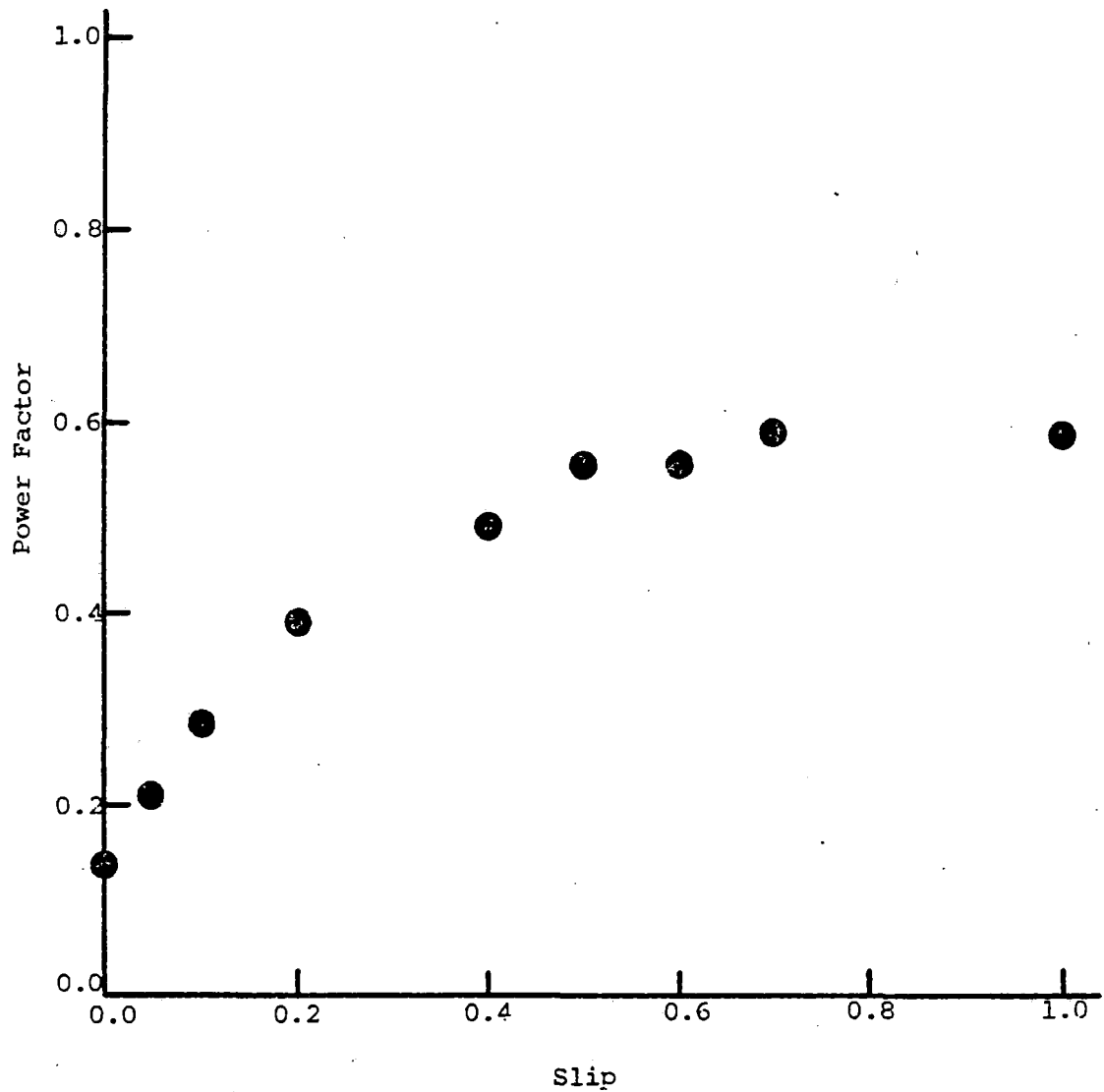
FIGURE 4.32: POWER FACTOR VS. SLIP FOR ALLIM
(Gap = 1.0 cm, Offset = 1.0 cm)
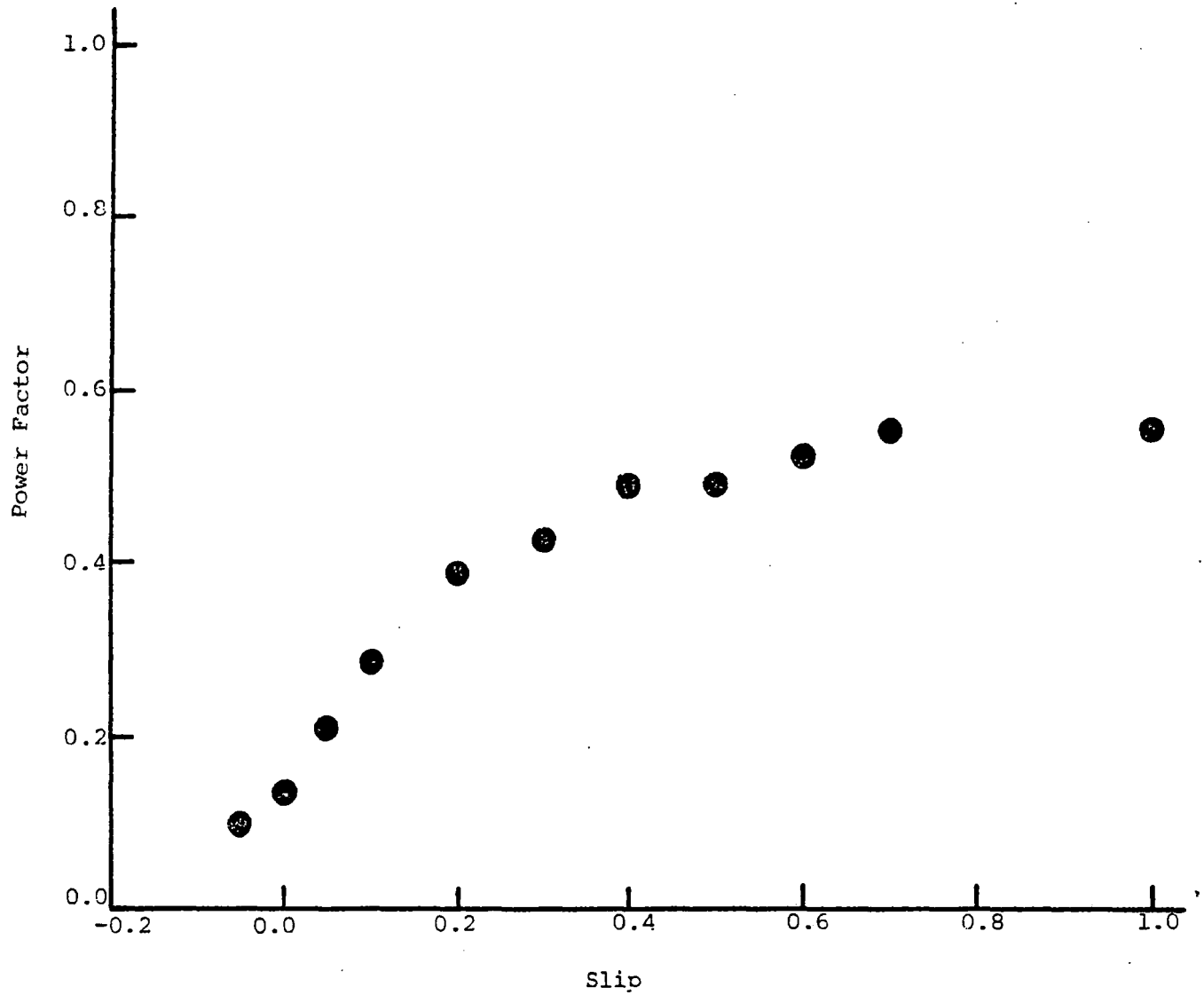
FIGURE 4.33: POWER FACTOR VS. SLIP FOR ALLIM
(Gap = 1.0 cm, Offset = 2.0 cm)

slips, as pointed out in Section 3.4.

Several observations can be made concerning the data.

(1)   The thrust reaches a peak at a slip less than 1
      and is declining at S=1.0.

(2)   The thrust reaches a peak at lower slips, as the
      air gap is decreased.

(3)   The normal force substantially exceeds the other
      LIM force at low slips and is always attractive,
      although it is nearly zero at a slip of 2.

(4)   The power factor increases rapidly at low slips
      and levels off at 0.5-0.6 at S=0.5.

(5)   The lateral force is generally a restoring force,
      although significant data scatter occur.

(6)   Offsets of 1.0 and 2.0 cm do not substantially alter
      thrust and normal force.

These observations are discussed in Section 4.3.5.

4.3.5   Comparison of the ASLIM and the ALLIM

Performance Results

Direct comparison between the ASLIM and ALLIM results at air gaps
of 1.0 and 1.5 cm are given below.

(1)   The thrust reaches a peak between slips of zero
      and 1 for the ALLIM, whereas thrust is still
      increasing at a slip of 1 for the ASLIM.

(2)   The normal force for the ALLIM is equal to the
      ASLIM normal force at zero slip. However, as
      slip increases, the ALLIM attractive normal force
      diminishes rapidly, nearly becoming repulsive at
      a slip of 1. The ASLIM normal force decreases more
      slowly with slip.

(3)   The power factor increases rapidly at low slips
      and then levels off for the ALLIM, whereas the
      power factor increases slowly and steadily for
      the ASLIM. The ASLIM never achieves a power
      factor comparable with the high value for the
      ALLIM at slips between zero and 1.

These differences may be explained by the phasor diagram of
Figure 4.34. The angle, ψ, represents the lag in the response
of the secondary to incoming primary flux. If the secondary
were reviewed as having an effective inductance and resistance,
a time constant could be associated with the secondary,
(L/R) sec.
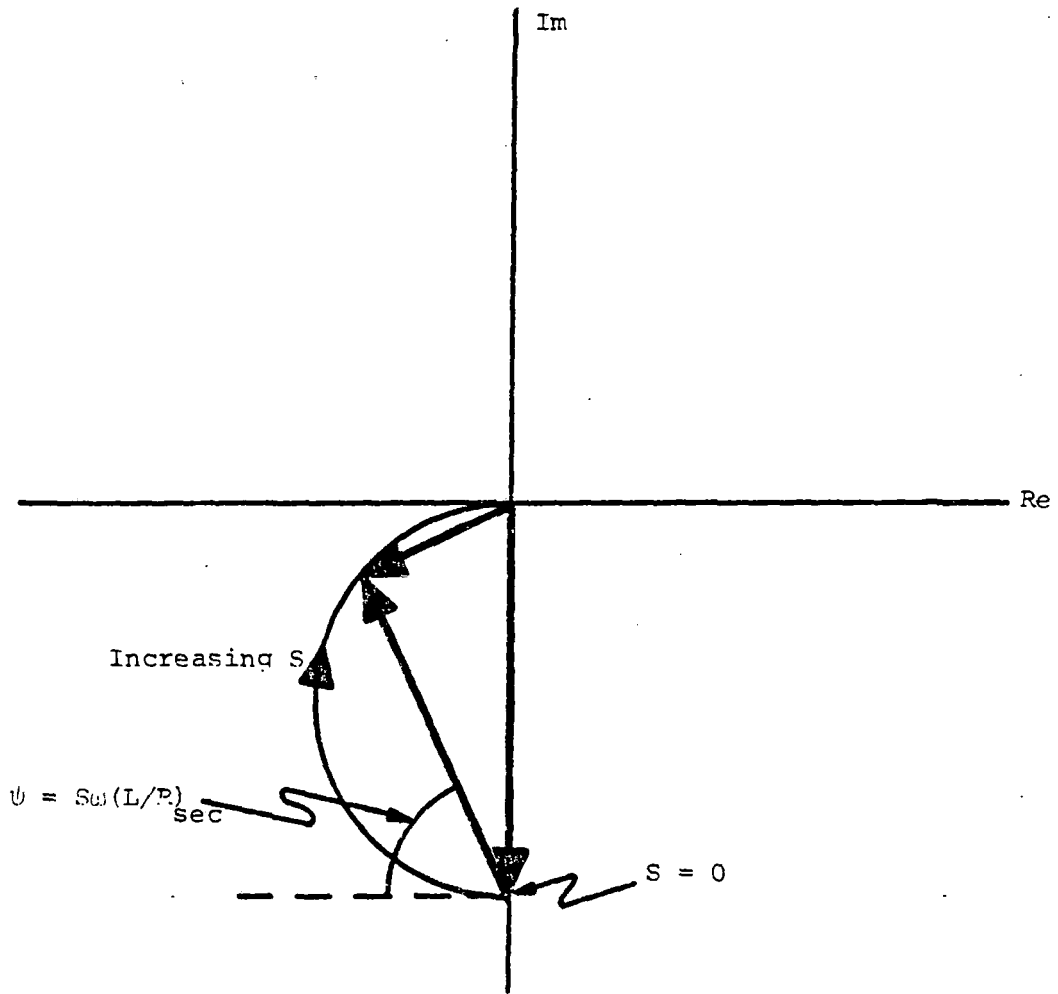
FIGURE 4.34: AIR GAP FLUX PHASOR DIAGRAM

$$\psi = S\omega (L/R)_{sec} \qquad\qquad (4\text{-}1)$$

The behavior of the ASLIM thrust, normal force, and power factor curves in comparison with the corresponding ALLIM curves can be attributed to the greater effective resistance of the all-steel secondary.

The greater effective resistance for the ASLIM secondary reduces the lag angle, ψ, for a particular slip and excitation frequency. Consequently, the thrust peaks more gradually with slip; and the power factor increases more gradually with slip for the ASLIM. The normal force for the ASLIM and ALLIM is equal at zero slip. As the phasor diagram indicates, this is because the secondary does not contribute to the airgap flux at synchronous operation (S=0).

The effective resistance of the ASLIM or ALLIM secondary depends on several factors

(1) The effective resistance of the ALLIM secondary diminishes, as the thickness of the secondary conducting sheet is increased.

(2) The effective resistance of the ASLIM secondary diminishes, as the skin depth increases.

(3) The effective resistance of the ALLIM or ASLIM secondary increases, as the resistivity of the secondary conductor increases.

(4) The effective resistance of the ALLIM or ASLIM secondary diminishes, as the width of the secondary conductor is increased, since the return path losses are reduced.

All these factors contribute to the difference in the effective resistance of the ASLIM and ALLIM secondaries tested in this study. In order to isolate the influence of secondary width, the ASLIM thrust and normal force analysis is repeated for an air gap of 1.0 cm and no offset without the resistivity correction factor, which accounts for return path losses. Although these curves, shown in Figures 4.35 and 4.36, are more similar to the ALLIM curves of Figures 4.19 and 4.23, they still exhibit a greater effective secondary resistance than the ALLIM curves. Consequently, for the operating conditions and design parameters of this study, the ASLIM secondary has a greater effective resistance than the ALLIM secondary, regardless of the secondary width. If frequency were increased above 60 Hz, then the difference in effective secondary resistance would be greater, since the skin depth of the all-steel boundary would decrease.

The secondary time constant, $(L/R)_{sec}$, illustrates that the thrust generated by the ALLIM reaches a peak at lower slips, as the air gap is reduced. Reducing the air gap increases the effective inductance of the secondary and, hence, the time constant and lag
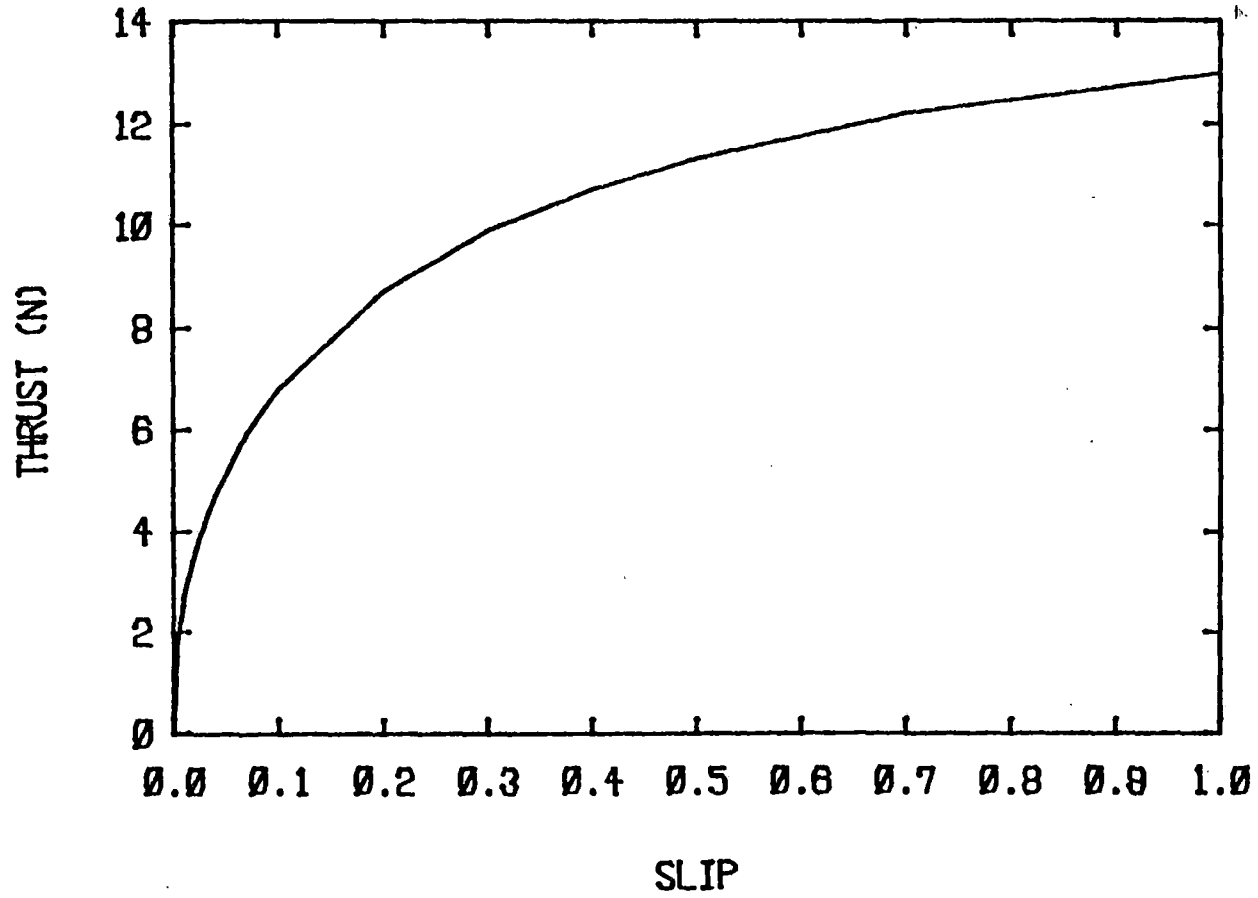
FIGURE 4.35: THRUST VS. SLIP PREDICTED BY ASLIM ANALYSIS NEGLECTING
RETURN PATH LOSSES
(Gap = 1.0 cm, Offset = 0)
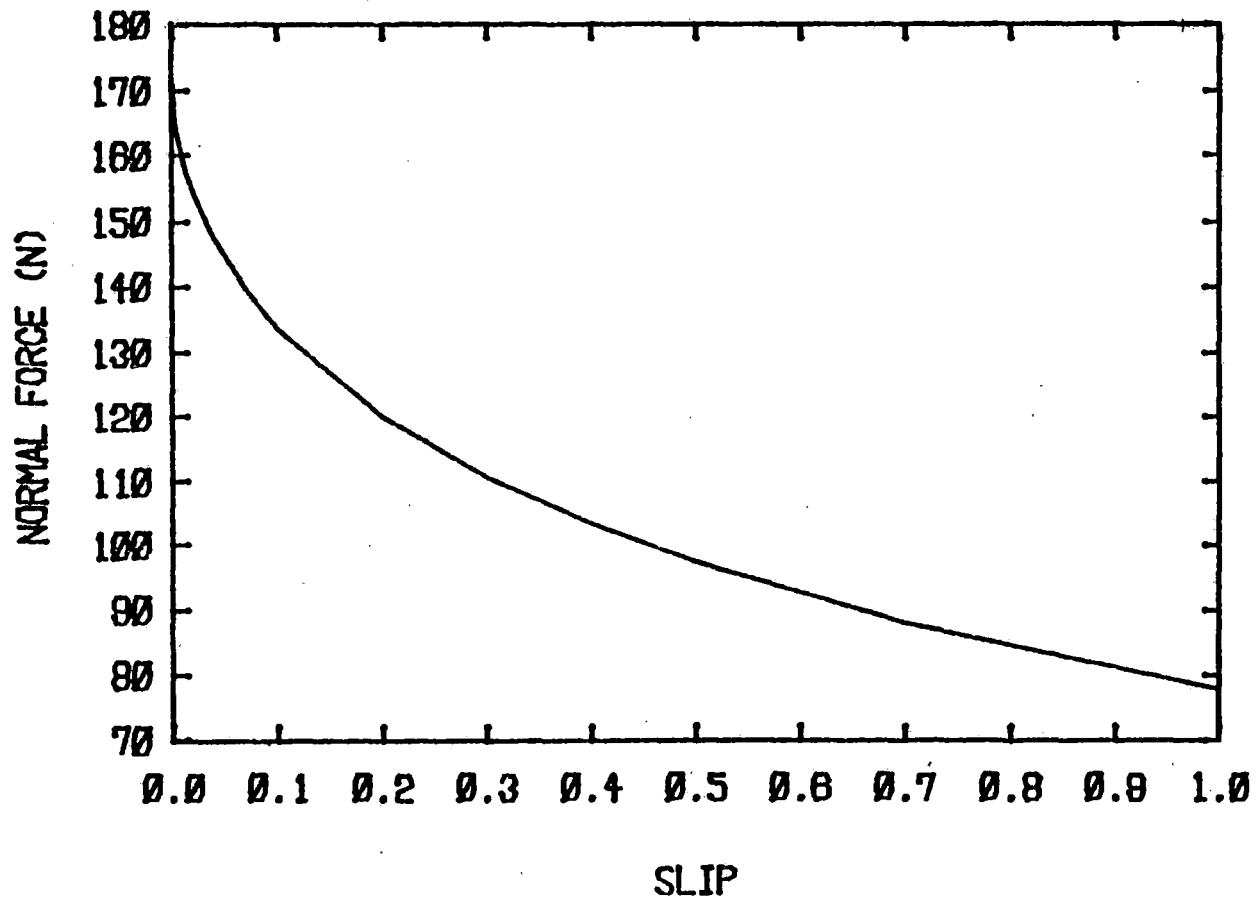
FIGURE 4.36: NORMAL FORCE VS. SLIP PREDICTED BY ASLIM ANALYSIS
NEGLECTING RETURN PATH LOSSES
(Gap = 1.0 cm, Offset = 0)

angle, ψ, for a particular slip and excitation frequency. The effective secondary inductance is increased by reducing the air gap, since the air gap flux generated by secondary current is increased.

The fact that end effects are more pronounced for the ALLIM than the ASLIM, cited as justification for neglecting end effects in the ASLIM analysis, is a consequence of the greater time constant associated with the ALLIM secondary. End effects are caused by secondary current induced by the air gap flux discontinuity at the ends of the LIM. The end effect-induced currents, decay at a rate specified by the secondary time constant, $(L/R)_{sec}$. The penetration depth of the entry end effect-induced currents is related to the product of the secondary speed relative to the primary and the secondary time constant. Since the ASLIM secondary time constant is smaller, the end effect decays faster and does not significantly alter overall LIM performance.

5. APPLICATION OF THE LINEAR INDUCTION MOTOR TO VEHICLE SYSTEMS

5.1 Scope of Study

The analyses developed and verified experimentally in Chapters 3 and 4 have been employed to consider two potential vehicle applications for linear induction motors

(1) Use of the ASLIM to provide or supplement propulsion and braking of a rail vehicle with conventional steel rails serving as the secondary

(2) Use of the ALLIM normal force to provide suspension forces for a high-speed (134 m/s) maglev vehicle while simultaneously providing propulsion.

The application of the LIM to rail vehicles considered here is significant in that the LIM does not require the construction of additional rails. In general, vehicle systems using the LIM require the construction of reaction rails, a substantial capital investment. The LIM-vehicle configuration evaluated in this study utilizes the existing conventional steel rails. The penalties incurred by the use of steel rails are an increase in LIM weight and a reduction in efficiency. However, there is considerable design flexibility in which to accommodate the above tradeoffs. The LIM can be designed to produce all the required braking and propulsion of a vehicle or to augment them only.

The first application is assessed by considering the configuration depicted in Figure 5.1. Although the use of existing rails represents a substantial savings in the capital costs of implementing LIM propulsion of a rail vehicle, this benefit must be weighed against the typically lower efficiency and power factor of the ASLIM, when compared to the ALLIM. The lower efficiency is a consequence of the higher slip operation necessary to obtain large thrusts.

The application of the ALLIM to the lift and propulsion of a high-speed maglev vehicle is assessed in the configuration of Figure 5.2. This is a natural variation of the MITRE-CIGGT concept of integrating lift, guidance, and propulsion of a high-speed vehicle with a set of offset LIMs. In this study, the LIM primary is centered with respect to the secondary, since the lateral force is not utilized. This is a more favorable configuration in terms of LIM performance. In addition, a configuration employing the LIM normal force for guidance is considered, as shown in Figure 5.3. For the vehicle configuration of Figure 5.2, guidance electromagnets are still required. Electromagnets for lift are required for the configuration of Figure 5.3. The benefits of the two systems are the elimination of the separate reaction rail for propulsion and some of the drag produced by electromagnets.
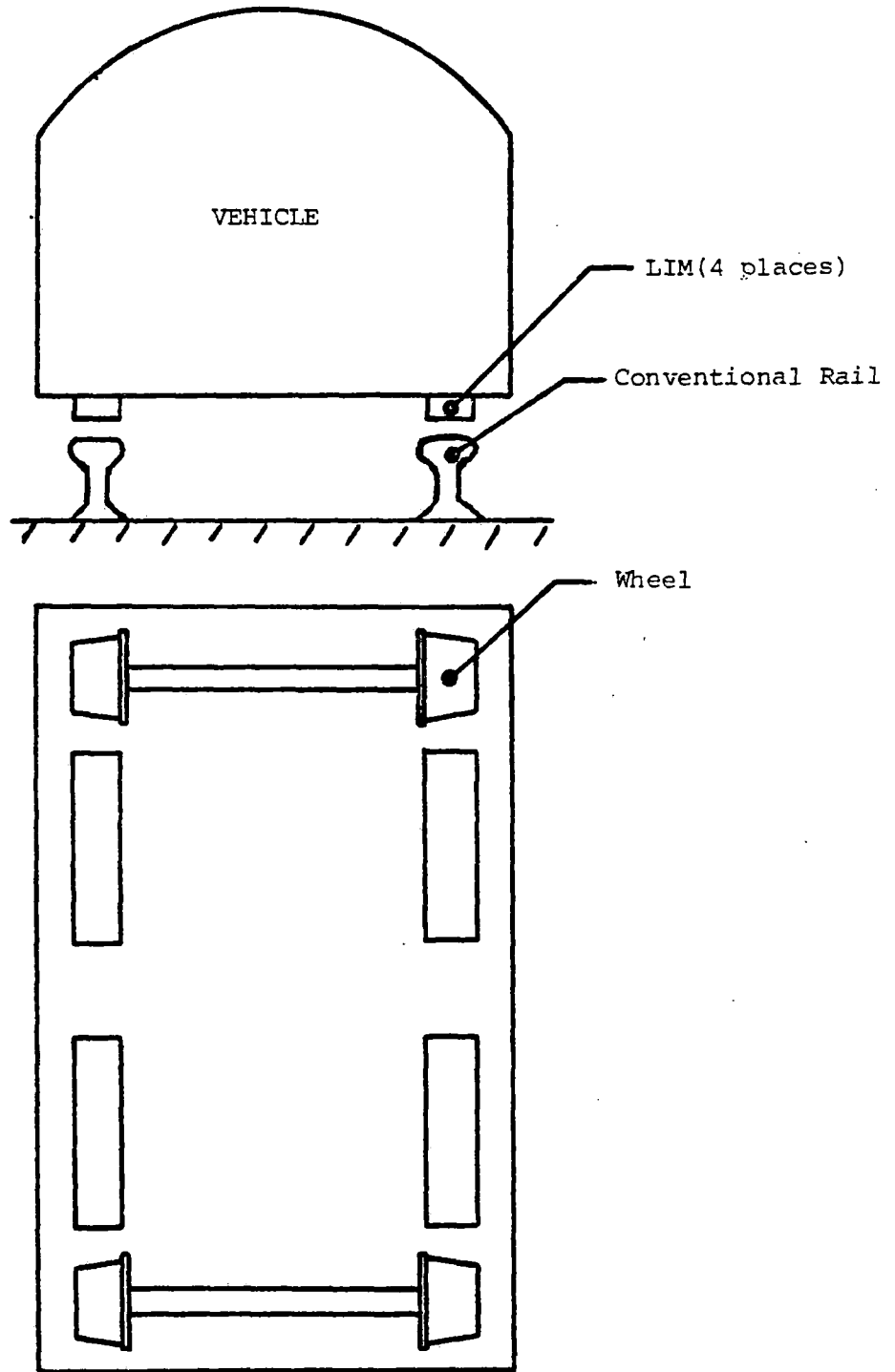
FIGURE 5.1: CONVENTIONAL RAIL USED AS LIM SECONDARY
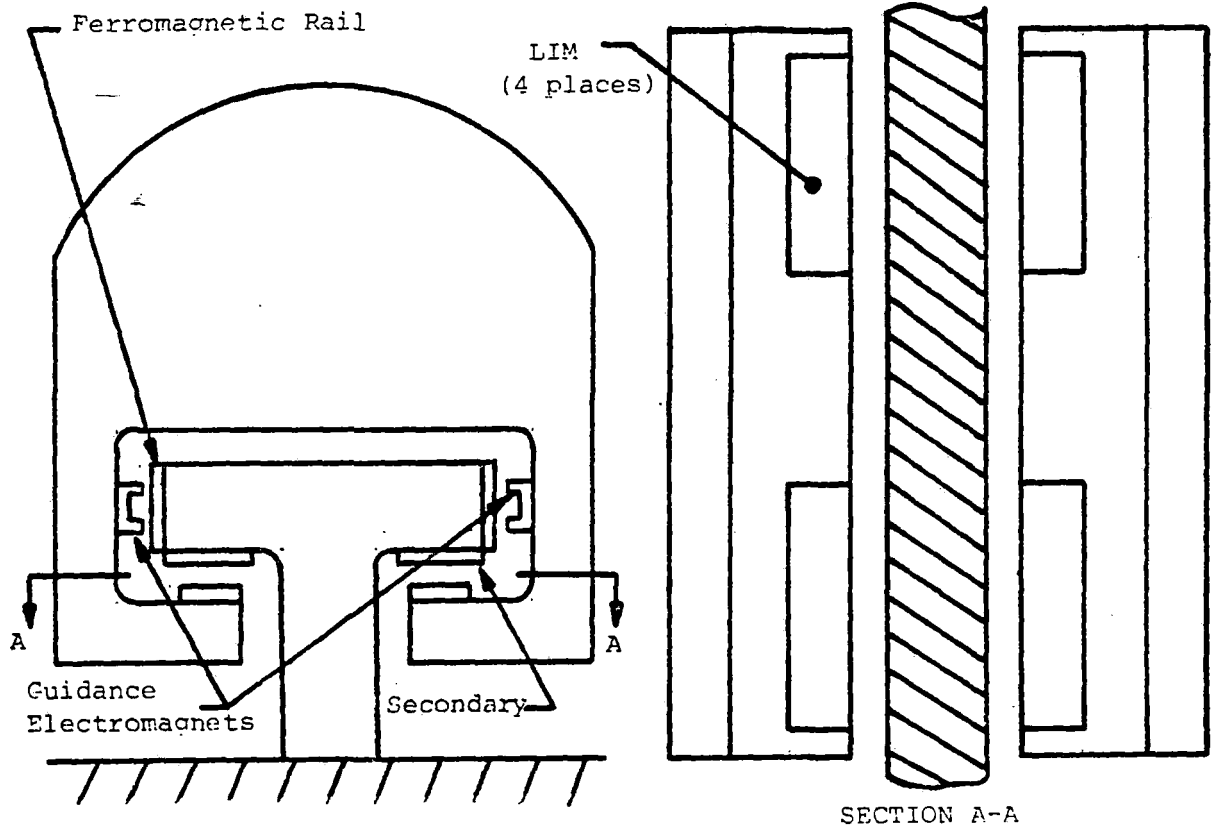
FIGURE 5.2:   LIM USED FOR LIFT AND PROPULSION OF A HIGH SPEED NONCONTACTING
SUSPENSION VEHICLE
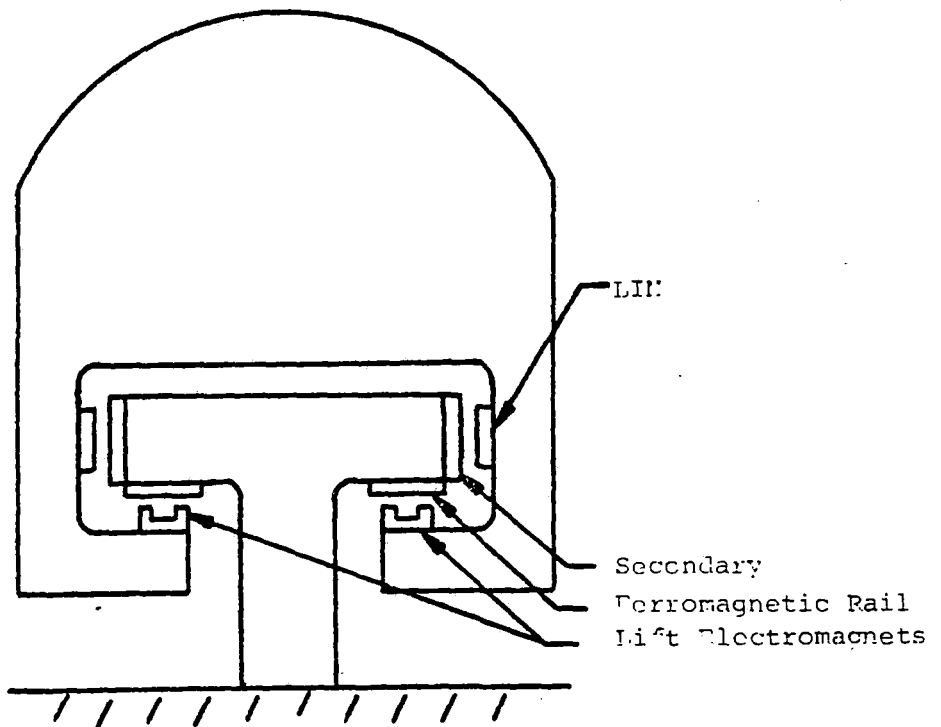
FIGURE 5.3:   LIM USED FOR GUIDANCE AND PROPULSION OF
A HIGH SPEED NONCONTACTING SUSPENSION VEHICLE

5.2 RAIL SYSTEMS

The ASLIM analysis has demonstrated that a LIM interacting with a reaction rail (secondary) made of steel alone can provide significant levels of thrust. This fact suggests that existing conventional rails could be used as the reaction rail for a vehicle LIM. Consequently, the LIM could be applied to a rail vehicle without the construction of additional reaction rails in the manner shown in Figure 5.1. A LIM implemented in this manner could provide several benefits:

   (1)   Provide the total or partial thrust requirements of a vehicle, regardless of wheel-rail adhesion.

   (2)   Assist vehicle braking, independent of wheel-rail adhesion.

   (3)   Reduce the likelihood of vehicle derailment and improve wheel-rail adhesion through application of attractive forces.

Application of the ASLIM has been considered for two rail vehicles:

   (1)   Vehicle A: A 408.97-kN vehicle with a maximum speed of 72.0 m/s (161 MPH).

   (2)   Vehicle B: A 224.38-kN vehicle with a maximum speed of 36.0 m/s (81 MPH).

The size and weight specifications are similar to the specification of the Amcoach [53] and Railbus vehicles, respectively. They are given in Table 5.1.

A range of values may be chosen for the LIM design parameters, and two LIM designs have been considered for each vehicle. The specifications are given in Table 5.2. The primary width, 5 cm, is equivalent to the width of the flat portion of a conventional rail. LIMs 1 and 2 have a synchronous speed of 88.89 m/s (199 MPH) and are considered for application to vehicle A, whereas LIMs 3 and 4 have a synchronous speed of 44.44 m/s (99 MPH) and are considered for application to vehicle B. Each pair of LIMs includes a high frequency-small pole pitch LIM and a low frequency-large pole pitch LIM.

The LIM operating conditions have been selected using data from references [22,27,31,54]. The value selected for the amplitude of the equivalent primary surface current density, J_m, was selected by evaluating J_m for several existing full-scale systems. In general, J_m is limited by the cooling requirements of a LIM. The value chosen for the air gap, g, is a reasonable value based on the tradeoff between mechanical clearance and LIM performance. The two values selected for frequency are in the range of typically suggested values. The operating conditions considered are listed below:

TABLE 5.1: SPECIFICATIONS FOR SELECTED VEHICLES

PARAMETERS	VEHICLE A	VEHICLE B
Weight (kN)	408.97	224.38
Length (m)	26.01	15.24
Frontal Area (m^2)	8.21	9.66
Top Speed (m/s)	72.0 (161.1 MPH)	36.0 (80.5 MPH)

TABLE 5.2: SPECIFICATIONS FOR SELECTED ASLIMs

PARAMETERS	VEHICLE A		VEHICLE B	
	LIM 1	LIM 2	LIM 3	LIM 4
ω(radians/s)	400	800	400	800
Pole pitch (m)	0.70	0.35	0.35	0.17
Synchronous Speed (m/s)	88.89	88.89	44.44	44.44
Primary width (m)	.05	.05	.05	.05

$$J_m = 1.2 \times 10^5 \text{ A/m}$$

$$g = 1.5 \times 10^{-2} \text{m}$$

$$\omega = \begin{cases} 400 \text{ radians/s (64 Hz)} \\ 800 \text{ radians/s (127 Hz)} \end{cases}$$

This study considered the application of the fixed frequency ASLIM, specified above, to vehicles A and B in the following manner.

(1) Establish vehicle thrust requirement, as a function of speed, on level track and on a 2% grade, assuming a drag coefficient of 0.6. [55]

(2) Evaluate thrust capability of various lengths of the specified LIM and compare with the vehicle thrust requirement.

(3) Evaluate the ratio of the LIM-generated normal force to the vehicle weight.

(4) Estimate LIM and power conditioning unit (PCU) weight for each vehicle, LIM type, LIM length, and operating speed.

Figures 5.4 and 5.5 plot the vehicle A thrust requirement and the LIM-generated thrust for LIM designs 1 and 2, respectively, as a function of operating speed. Figures 5.6 and 5.7 plot the vehicle B thrust and the thrust generated by LIM designs 3 and 4. The plots indicate that the ASLIM provides part of or all the vehicle thrust requirements, depending on the operating speed and the length of the ASLIM. The low-frequency-large pole pitch LIM designs, 1 and 3, generate substantially more thrust for a given LIM length and operating speed.

In Tables 5.3 to 5.6 the percentage of the vehicle thrust require- ment generated by the LIM is given for various LIM lengths and operating speeds. The resulting vehicle acceleration, where LIM-generated thrust exceeds the thrust requirement, and the ratio of the LIM-generated normal force to the vehicle weight are also given.

The values in Tables 5.3 to 5.6 lead to several conclusions and tradeoffs:

(1) The ASLIM thrust exceeds or represents a substantial portion of the required thrust, depending on LIM length, pole pitch, operating speed and whether the guideway is level or inclined.

(2) Where the ASLIM thrust exceeds the required thrust, the vehicle acceleration capability of the ASLIM reaches 0.631 m/s^2 for vehicle A with LIM 1 and 0.323 m/s^2 for vehicle B with LIM 3 on level track. This
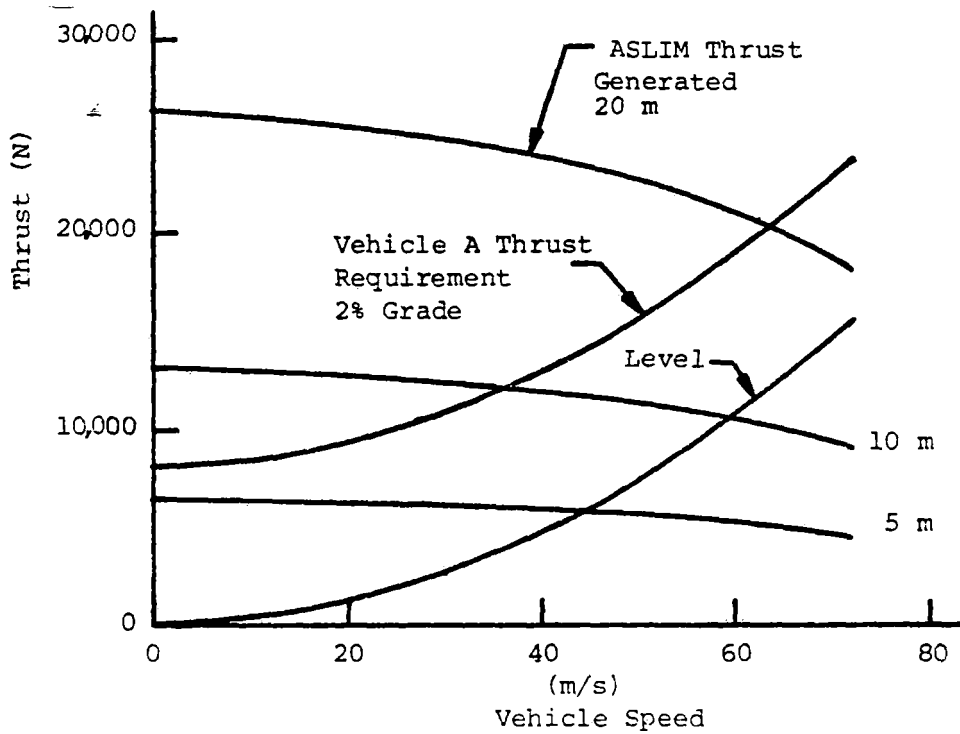
FIGURE 5.4: COMPARISON OF THRUST REQUIREMENT FOR VEHICLE A
AND THRUST GENERATED BY VARIOUS LENGTHS OF LIM
DESIGN 1
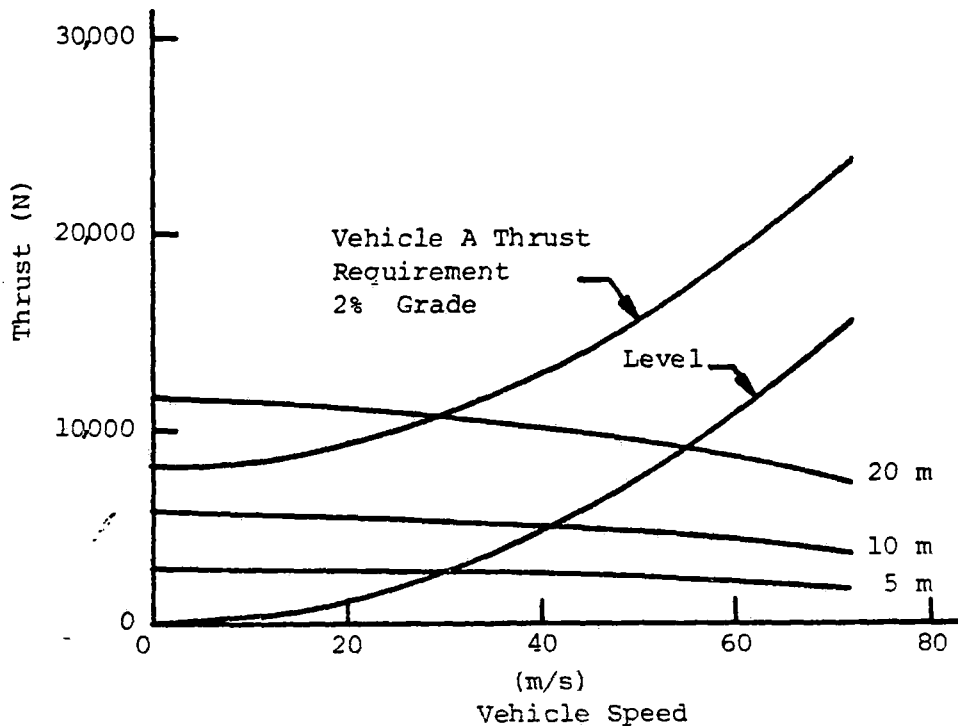
FIGURE 5.5: COMPARISON OF THRUST REQUIREMENT FOR VEHICLE A
AND THRUST GENERATED BY VARIOUS LENGTHS OF LIM
DESIGN 2
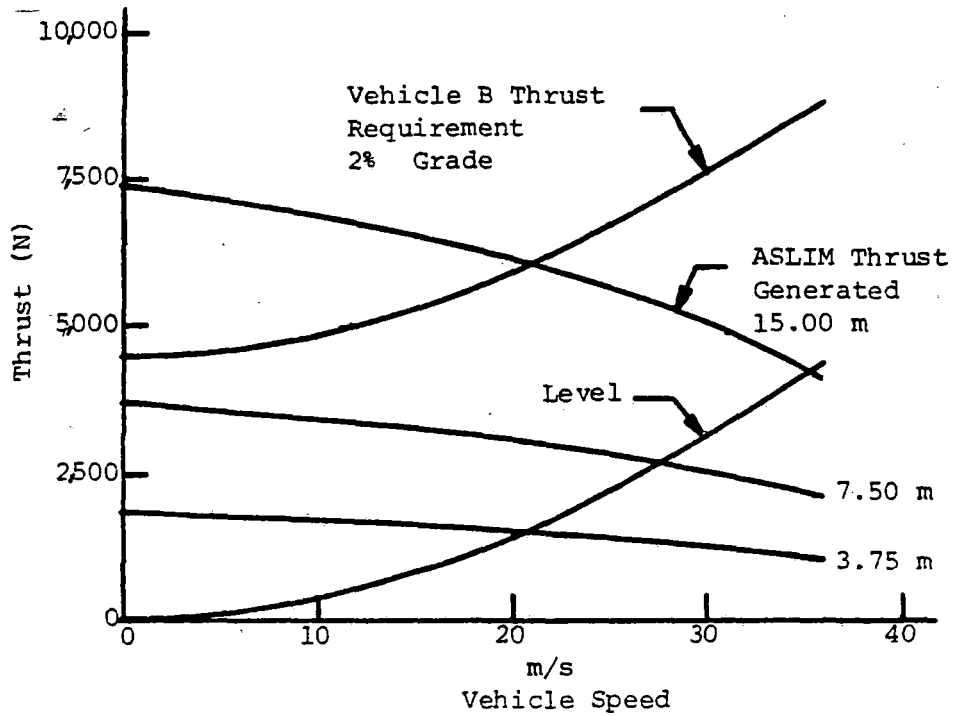
FIGURE 5.6: COMPARISON OF THRUST REQUIREMENT FOR VEHICLE B
AND THRUST GENERATED BY VARIOUS LENGTHS OF LIM
DESIGN 3
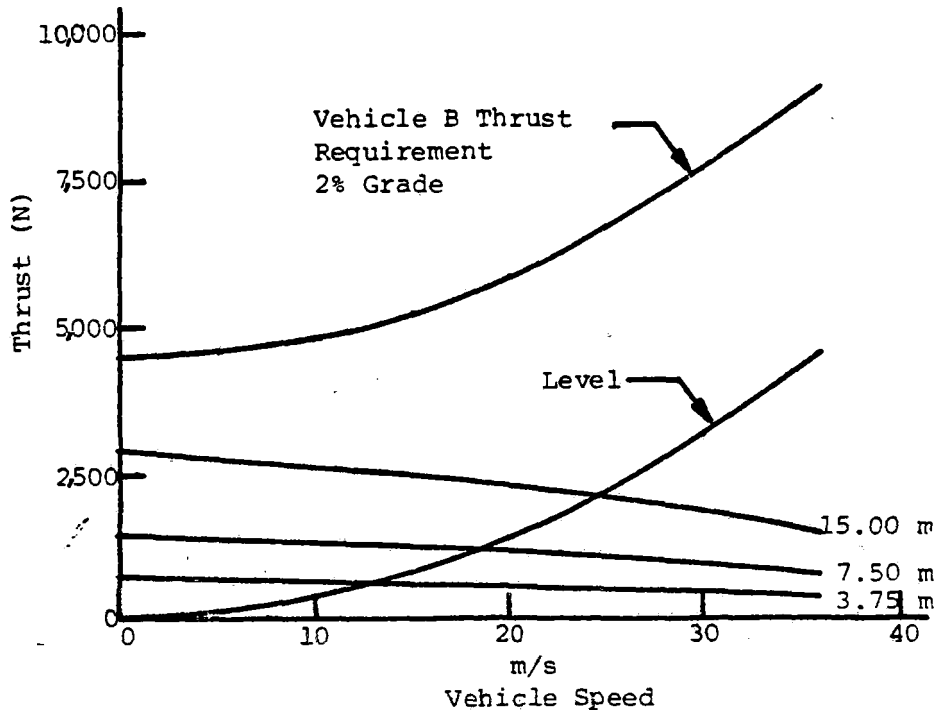
FIGURE 5.7: COMPARISON OF THRUST REQUIREMENT FOR VEHICLE B
AND THRUST GENERATED BY VARIOUS LENGTHS OF
LIM DESIGN 4

TABLE 5.3: VEHICLE A WITH LIM 1 (THRUST, NORMAL FORCE)

LIM LENGTH (m)	OPERATING SPEED (m/s)	PERCENTAGE OF REQUIRED THRUST GENERATED BY LIM		VEHICLE ACCELERATION CAPABILITY OF LIM (m/s^2)		NORMAL FORCE / VEHICLE WEIGHT
		Level	2% Grade	Level	2% Grade	
5.0	0.0	——	80.5	0.158	——	0.25
↓	26.67	291.6	60.6	0.098	——	0.29
	53.33	65.0	33.3	——	——	0.34
	71.11	30.2	19.7	——	——	0.40
10.0	0.0	——	161.0	0.316	0.120	0.51
↓	26.67	583.1	121.2	0.248	0.052	0.58
	53.33	130.0	66.5	0.062	——	0.68
	71.11	60.4	39.3	——	——	0.80
20.0	0.0	——	322.0	0.631	0.435	1.02
↓	26.67	1166.3	242.3	0.548	0.352	1.16
	53.33	260.0	133.0	0.329	0.133	1.37
	71.11	120.9	78.7	0.076	——	1.60

TABLE 5.4: VEHICLE A WITH LIM 2 (THRUST, NORMAL FORCE)

LIM LENGTH (m)	OPERATING SPEED (m/s)	PERCENTAGE OF REQUIRED THRUST GENERATED BY LIM		VEHICLE ACCELERATION CAPABILITY OF LIM (m/s^2)		NORMAL FORCE / VEHICLE WEIGHT
		Level	2% Grade	Level	2% Grade	
5.0	0.00	——	35.8	0.070	——	0.08
	26.67	125.7	26.1	0.013	——	0.09
	53.33	26.9	13.8	——	——	0.10
	71.11	12.0	7.8	——	——	0.11
10.0	0.00	——	71.6	0.140	——	0.16
	26.67	251.4	52.2	0.026	——	0.17
	53.33	53.7	27.5	——	——	0.20
	71.11	24.0	15.6	——	——	0.22
20.0	0.00	——	143.2	0.281	0.085	0.31
	26.67	502.8	104.5	0.053	0.011	0.35
	53.33	107.5	55.0	0.015	——	0.39
	71.11	47.9	31.2	——	——	0.44

TABLE 5.5: VEHICLE B WITH LIM 3 (THRUST, NORMAL FORCE)

LIM LENGTH (m)	OPERATING SPEED (m/s)	PERCENTAGE OF REQUIRED THRUST GENERATED BY LIM		VEHICLE ACCELERATION CAPABILITY OF LIM (m/s^2)		NORMAL FORCE / VEHICLE WEIGHT
		Level	2% Grade	Level	2% Grade	
3.75	0.00	———	41.2	0.081	———	0.13
	13.33	262.8	32.4	0.045	———	0.14
	26.67	54.3	19.5	———	———	0.15
	35.56	23.4	11.7	———	———	0.17
7.50	0.00	———	82.3	0.161	———	0.26
	13.33	525.6	64.8	0.090	———	0.28
	26.67	108.5	39.1	0.009	———	0.30
	35.56	46.8	23.4	———	———	0.33
15.00	0.00	———	164.6	0.323	0.127	0.51
	13.33	1051.2	129.6	0.179	0.066	0.55
	26.67	217.0	78.1	0.129	———	0.61
	35.56	93.6	46.8	———	———	0.66

TABLE 5.6: VEHICLE B WITH LIM 4 (THRUST, NORMAL FORCE)

LIM LENGTH (m)	OPERATING SPEED (m/s)	PERCENTAGE OF REQUIRED THRUST GENERATED BY LIM		VEHICLE ACCELERATION CAPABILITY OF LIM (m/s^2)		NORMAL FORCE / VEHICLE WEIGHT
		Level	2% Grade	Level	2% Grade	
3.75	0.0	———	16.2	0.032	———	0.034
	13.33	101.5	12.5	0.000	———	0.036
	26.67	20.4	7.4	———	———	0.039
↓	35.56	8.6	4.3	———	———	0.041
7.50	0.0	———	32.5	0.064	———	0.068
	13.33	203.0	25.0	0.001	———	0.072
	26.67	40.8	14.7	———	———	0.077
↓	35.56	17.2	8.6	———	———	0.082
15.00	0.0	———	64.9	0.127	———	0.137
	13.33	406.0	50.0	0.002	———	0.144
	26.67	81.7	29.4	———	———	0.155
	35.56	34.4	17.2	———	———	0.165

may be compared to 0.5 m/s^2, the acceleration capability of the Metroliner. [56]

(3)   The low-frequency-large pole pitch LIM designs 1 and 3, produce more than twice the thrust per unit length than the high-frequency-small pole pitch designs, 2 and 4.

(4)   LIM designs 1 and 3 produce nearly four times more attraction force per unit length than LIM designs 2 and 4, respectively.

To provide a complete view of the tradeoff between the high-frequency and low-frequency ASLIM, the power factor, efficiency, LIM weight, and PCU weight are estimated for LIM designs 1, 2, 3, and 4 for various LIM lengths and operating speeds. The computations are performed in thefollowing manner.

(1)   The LIM weight is estimated assuming a primary core thickness of 1/k [57] and a weight density of 76,000 N/m^3.

(2)   The PCU weight is estimated from the apparent power consumed by the LIM (calculated from thrust, speed, efficiency and power factor), an estimated efficiency of 1-S (3-46) and a weight density of 7.5 N/kVA for the PCU. [24] The results are tabulated in Tables 5.7 to 5.10.

The conclusions and tradeoffs indicated by Tables 5.7 to 5.10 are as follows.

(1)   The primary core of LIM 1 or 3 is twice as thick and, hence, twice as heavy as the primary core of LIM 2 or 4, respectively, because of the greater pole pitch of the former.

(2)   The required PCU for LIM 1 or 3 is nearly twice as heavy as the PCU for LIM 2 or 4, respectively.

The above examples suggest that the ASLIM can be applied to a rail vehicle. The contribution of the ASLIM to vehicle propulsion depends on the LIM length chosen. In the example given, the LIM lengths selected were compatible with the vehicle lengths.

The tradeoffs indicate that the ASLIM with a larger pole pitch and lower excitation frequency provides increased thrust and normal force per unit length. However, the large pole pitch-low-frequency ASLIM has a thicker primary core and a heavier PCU weight requirement per unit length than the small pole pitch-high frequency ASLIM. These factors result in the large pole pitch-low frequency ASLIM providing greater thrust and normal force per unit length than the small pole pitch-high frequency ASLIM but approximately the same thrust and normal force per unit PCU and LIM weight.

The estimates of ASLIM efficiency in Tables 5.7 to 5.10 indicate

TABLE 5.7: VEHICLE A WITH LIM 1 (PCU, LIM WEIGHT)

LIM LENGTH (m)	OPERATING SPEED (m/s)	POWER FACTOR	EFFICIENCY	LIM WEIGHT (N)	PCU WEIGHT (N)	LIM WEIGHT & PCU WEIGHT / VEHICLE WEIGHT
5.0	0.0	0.30	0.0	4,222	14,634	0.046
↓	26.67	0.27	0.3	↓	15,445	0.048
	53.33	0.22	0.6		16,894	0.052
↓	71.11	0.17	0.8	↓	18,075	0.055
10.0	0.0	0.30	0.0	8,444	29,267	0.092
↓	26.67	0.27	0.3	↓	30,889	0.096
	53.33	0.22	0.6		33,788	0.103
↓	71.11	0.17	0.8	↓	36,149	0.109
20.0	0.0	0.30	0.0	16,889	58,434	0.184
↓	26.67	0.27	0.3	↓	61,779	0.192
	53.33	0.22	0.6		67,577	0.207
↓	71.11	0.17	0.8	↓	72,299	0.218

TABLE 5.8:   VEHICLE A WITH LIM 2 (PCU, LIM WEIGHT)

LIM LENGTH (m)	OPERATING SPEED (m/s)	POWER FACTOR	EFFICIENCY	LIM WEIGHT (N)	PCU WEIGHT (N)	LIM WEIGHT & PCU WEIGHT / VEHICLE WEIGHT
5.0	0.0	0.24	0.0	2,111	8,136	0.025
	26.67	0.21	0.3		8,650	0.026
	53.33	0.17	0.6		9,039	0.027
	71.11	0.13	0.8		9,369	0.028
10.0	0.0	0.24	0.0	4,222	16,272	0.050
	26.67	0.21	0.3		17,121	0.052
	53.33	0.17	0.6		18,079	0.055
	71.11	0.13	0.8		18,739	0.056
20.0	0.0	0.24	0.0	8,444	32,545	0.100
	26.67	0.21	0.3		34,242	0.104
	53.33	0.17	0.6		36,157	0.109
	71.11	0.13	0.8		37,477	0.112

(m)			
3.75	0.00	0.18	
	13.33	0.16	
	26.67	0.13	
↓	35.56	0.09	
7.50	0.0	0.18	
	13.33	0.16	
	26.67	0.13	
↓	35.56	0.09	
15.00	0.0	0.18	
	13.33	0.16	
	26.67	0.13	
	35.56	0.09	

0.0	1,583	3,420	0.022
0.3		3,454	0.022
0.6		3,513	0.023
0.8		3,890	0.024
0.0	3,167	6,841	0.045
0.3		6,909	0.045
0.6		7,026	0.045
0.8		7,780	0.049
0.0	6,363	13,682	0.089
0.3		13,817	0.090
0.6		14,052	0.091
0.8		15,560	0.098

that efficiency is relatively low at low speeds for a fixed frequency LIM. This consideration is tempered because the thrust power is approximately proportional to the cube of the forward speed of the vehicle. Consequently, the efficiency at low speed is less important. In addition, variable frequency excitation could increase efficiencies at low speeds, if this were deemed necessary.

5.3 PROPULSION/SUSPENSION SYSTEMS

The ROMAG system, developed and tested by Rohr in the early 1970's, integrates suspension and propulsion of a low-speed vehicle with the LIM. The lateral restoring force of an offset LIM is used for guidance of the at-grade ROMAG vehicle; and the attractive normal force provides lift for both the at-grade and elevated vehicles.

An experimental study with the linear induction motor conducted by MITRE [24] at Queen's University in Canada investigated integrating lift, guidance, and thrust at high speeds. It was concluded that the reactive power requirement was excessive because of the required offset configuration of the LIM and the relatively large lift (normal force) required.

This study investigates the normal force generated by a centered LIM providing propulsion for a high-speed vehicle (134 m/s). The specific configuration is shown in Figure 5.2. The LIM normal force is compared with required levels of lift and guidance, in order to assess the feasiblity of employing the LIM for either of these functions.

The vehicle selected for consideration is a high-speed maglev vehicle conceptually designed by Ford in 1974 [58] for the Department of Transportation. Many design specifications were included in the study. Those of interest are listed below

maximum speed = 134 m/s (300 MPH)

required thrust at 134 m/s = 40 kN

capacity = 80 passengers

weight = 366.5 kN

length = 33.7 m

For the configuration shown in Figures 5.2 and 5.3, each LIM must generate 10 kN at 134 m/s i.e., one quarter of the thrust requirement. Consequently, two LIM designs, both capable of generating greater than 10 kN of thrust at 134 m/s are considered for application to the vehicle specified above. The design parameters of each LIM are listed in Table 5.11. LIM 1 has a larger pole pitch than LIM 2. Table 5.12 lists the operating conditions for each LIM at the maximum speed, 134 m/s. The peak phase current, 241.52 A, corresponds to an equivalent primary surface current density of 120,000 A/m, the same value that was used in Section 5.1. Because

TABLE 5.11: LIM DESIGN PARAMETERS

PARAMETER	LIM 1	LIM 2
Primary width (m)	0.2	0.2
Primary length (m)	4.0	5.2
No. of slots per pole	15	15
No. of slots per phase belt	5	5
Slot width (m)	1.6×10^{-2}	8.0×10^{-3}
Slot depth (m)	3.0×10^{-2}	3.0×10^{-2}
Unfilled slot depth (m)	5.0×10^{-3}	5.0×10^{-3}
No. of turns per coil	8	4
Primary wire cross-sectional (m^2)	2.15×10^{-5}	2.15×10^{-5}
Coil pitch	2/3	2/3
No. of poles	10	26
Pole pitch (m)	0.4	0.2
Secondary width (m)	0.35	0.35
Secondary conductor thickness (m)	3.175×10^{-3}	3.175×10^{-3}
Nominal air gap (m)	1.82×10^{-2}	1.82×10^{-2}

TABLE 5.12: LIM OPERATING CONDITIONS AT MAXIMUM SPEED (134 m/s)

PARAMETER	LIM 1	LIM 2
Peak phase current (A)	241.52	241.52
Excitation frequency (Hz)	186.2	360.0
Slip	0.10	0.07
Thrust (kN)	11.0-11.6	10.4-10.6
Normal force (kN)	14.2-24.5	4.4-6.4

of the aluminum sheet, the air gap,* is increased to 1.82×10^{-2} m, in order to maintain a mechanical clearance of 1.5×10^{-2} m. The values in Tables 5.11 and 5.12 were obtained by parameter variation with the ALLIM analysis. The resulting designs are representative of current full-scale LIM designs.

The thrust, normal force, power factor and efficiency of the two LIM designs are plotted as a function of slip in Figures 5.8 to 5.15 and use the ALLIM analysis developed in Chapter 3.

If vehicle lift is provided by the attractive normal force generated by the LIM, a net normal force must be produced equal to the weight of the vehicle at approximately twice the nominal air gap to provide for a full operating range. Table 5.12 indicates, however, that LIM design 1 would be capable of producing between 57 and 98 kN of lift at the nominal gap for the configuration sketched in Figure 5.2. These values represent only 15 to 27 percent of the vehicle weight and, furthermore, they would be substantially reduced at twice the nominal air gap. Design 2 is less satisfactory than the design 1, with respect to providing lift. Design 2 can produce between 17.6 and 25.6 kN of normal force at the nominal air gap, or approximately 5 to 7 percent of the vehicle weight.

The above calculations suggest that the LIM designs considered in this study can provide adequate normal force for lift at 134 m/s, if their lengths are substantially increased and the operating slip at maximum speed is reduced to increase the ratio of normal force to lift. Figures 5.10, 5.11, 5.14 and 5.15 indicate penalties such as reduced efficiencies and power factors are incurred, as well as a substantial increase in LIM and PCU weight. These considerations suggest that the linear induction motor configurations considered in this study are inappropriate for providing lift for a high-speed vehicle. This conclusion agrres with the MITRE-CIGGT findings, [24] although its study considered an offset-LIM configuration rather than the centered-LIM configuration examined in this study.

Since the required forces for guidance of a high-speed vehicle are typically less than those required for lift, the application of the LIM to guidance in the manner suggested by Figure 5.3 may have merit. The ALLIM analysis estimates that design 1 can produce between 8.1 and 12.0 kN of attractive normal force at an air gap of 3.32 cm (twice the nominal mechanical clearance of 1.5 cm) and a slip of 0.10. Whether these values would be sufficient for guidance depends on factors such as the maximum superelevation of the guideway on curves, the smoothness of the guideway and the wind loadings expected. At the maximum allowed lateral derivation, the two LIMs on the side of the vehicle farthest from the reaction rail must produce the entire restoring force.

---

*The term "air gap" includes the secondary conducting sheet thickness if it is present, since for practical purposes, it has a permittivity equivalent to air.
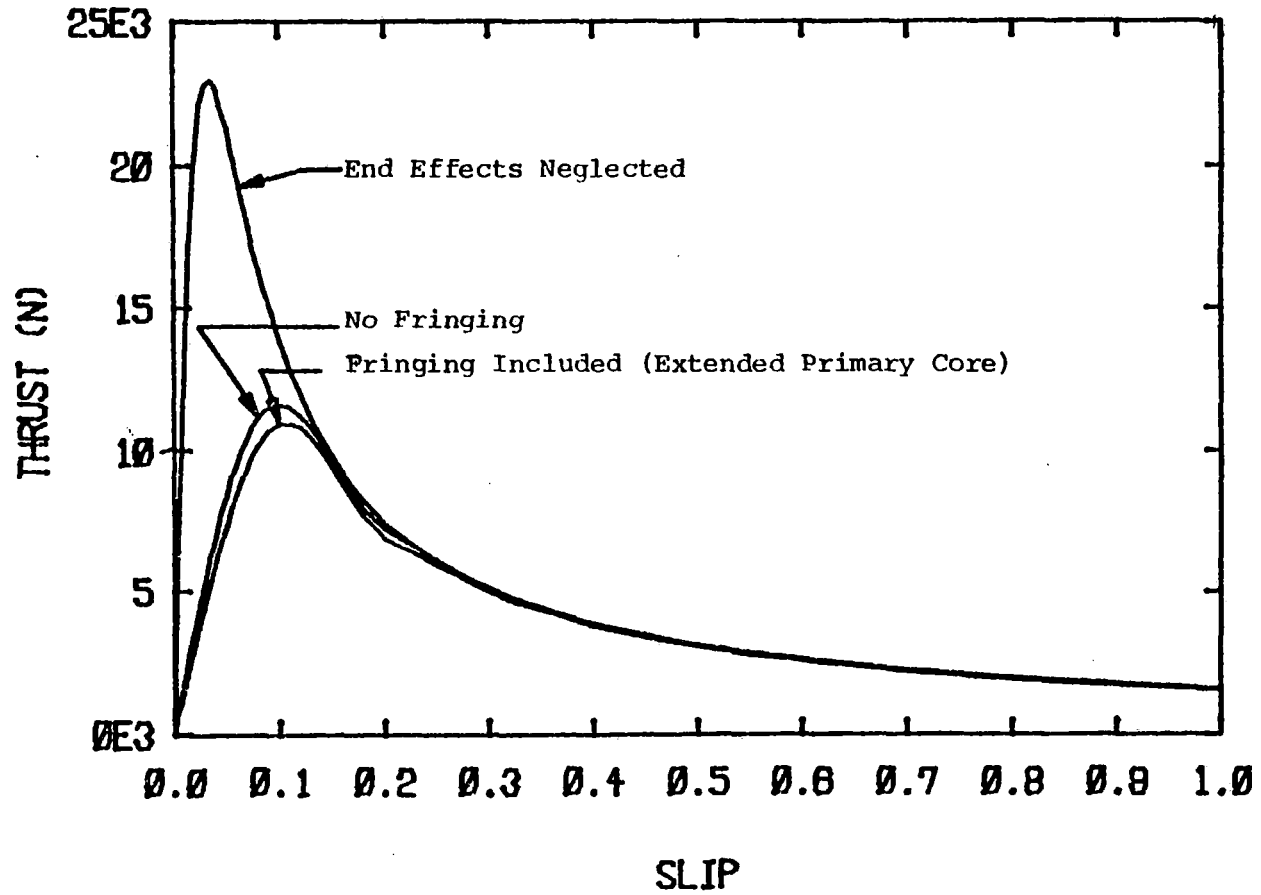
FIGURE 5.8: THRUST VS. SLIP FOR LIM DESIGN 1
(Peak Phase Current = 241.52 A, Excitation Frequency=186.2 Hz)
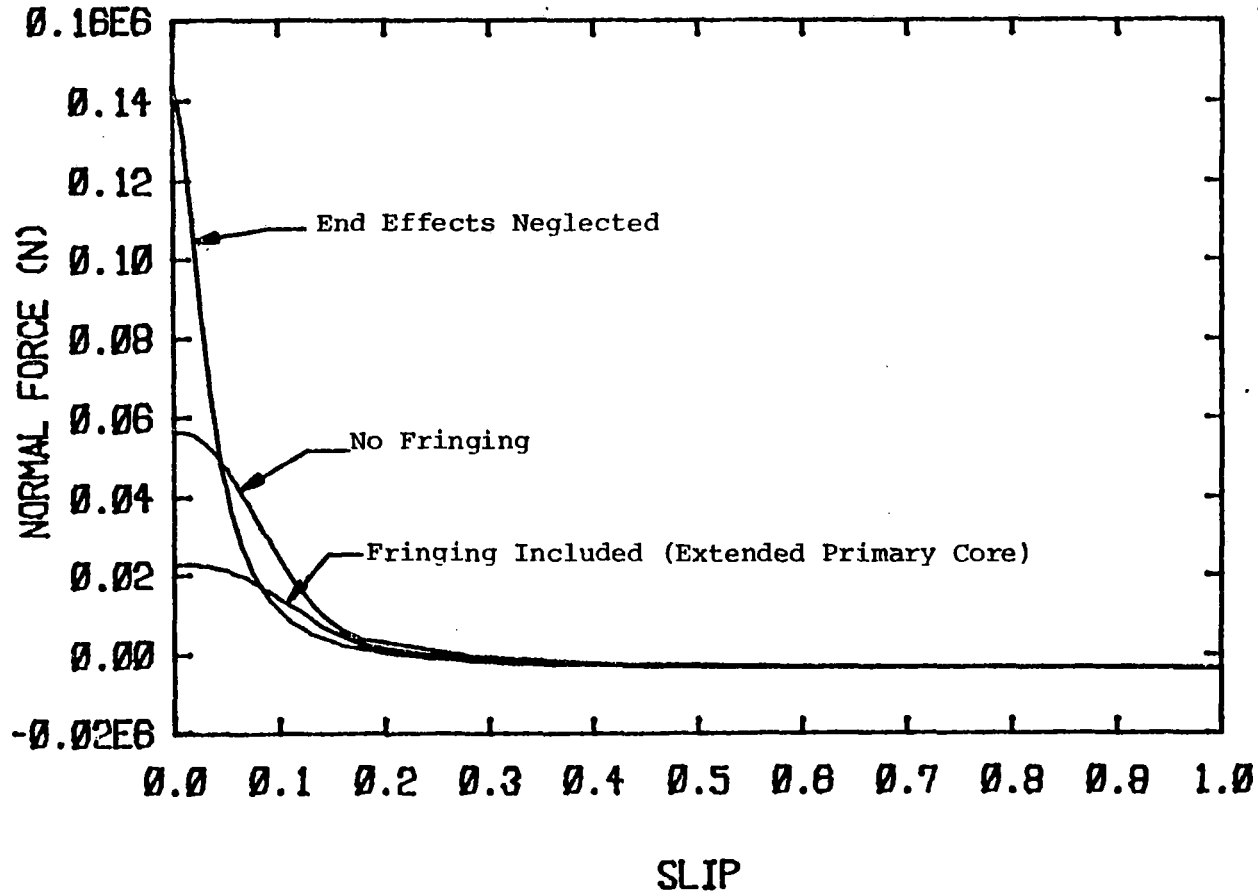
FIGURE 5.9:   NORMAL FORCE VS. SLIP FOR LIM DESIGN 1
(Peak Phase Current = 241.52 A, Excitation Frequency=186.2 Hz)
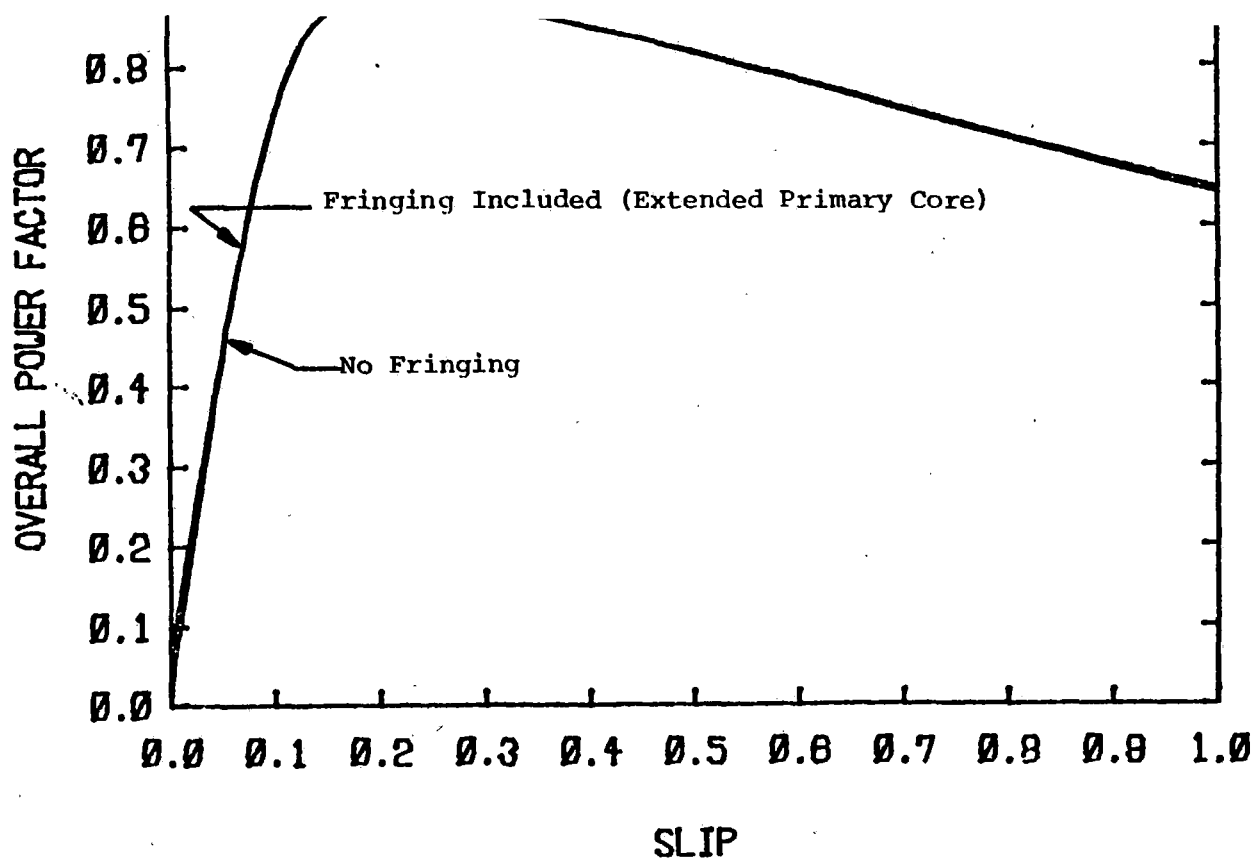
FIGURE 5.10: POWER FACTOR VS. SLIP FOR LIM DESIGN 1
(Peak Phase Current=241.52 A, Excitation Frequency=186.2 Hz)

FIGURE 5.11: EFFICIENCY VS. SLIP FOR LIM DESIGN 1
(Peak Phase Current=241.52 A, Excitation Frequency=186.2 Hz)
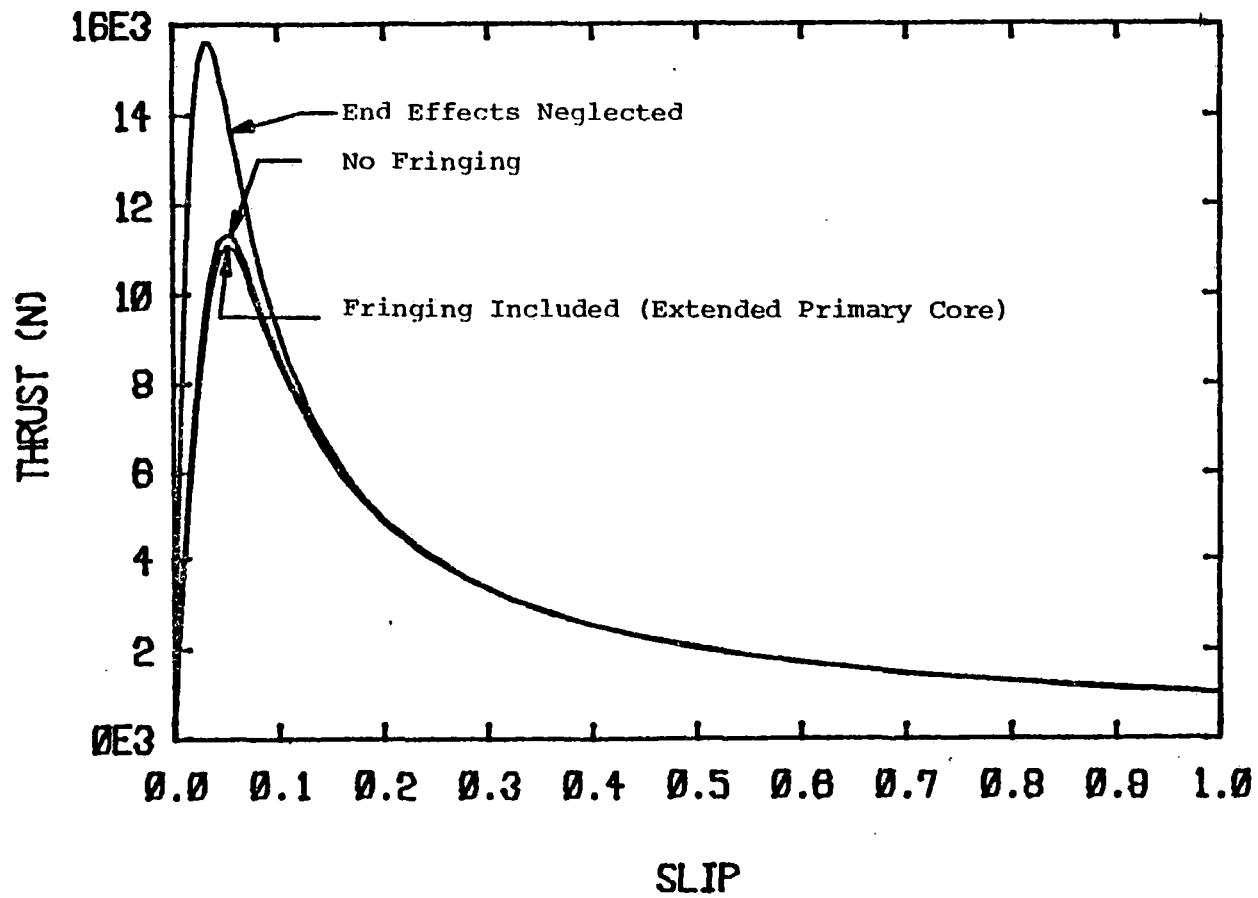
FIGURE 5.12: THRUST VS. SLIP FOR LIM DESIGN 2
(Peak Phase Current=241.52 A, Excitation Frequency=360.0 Hz)
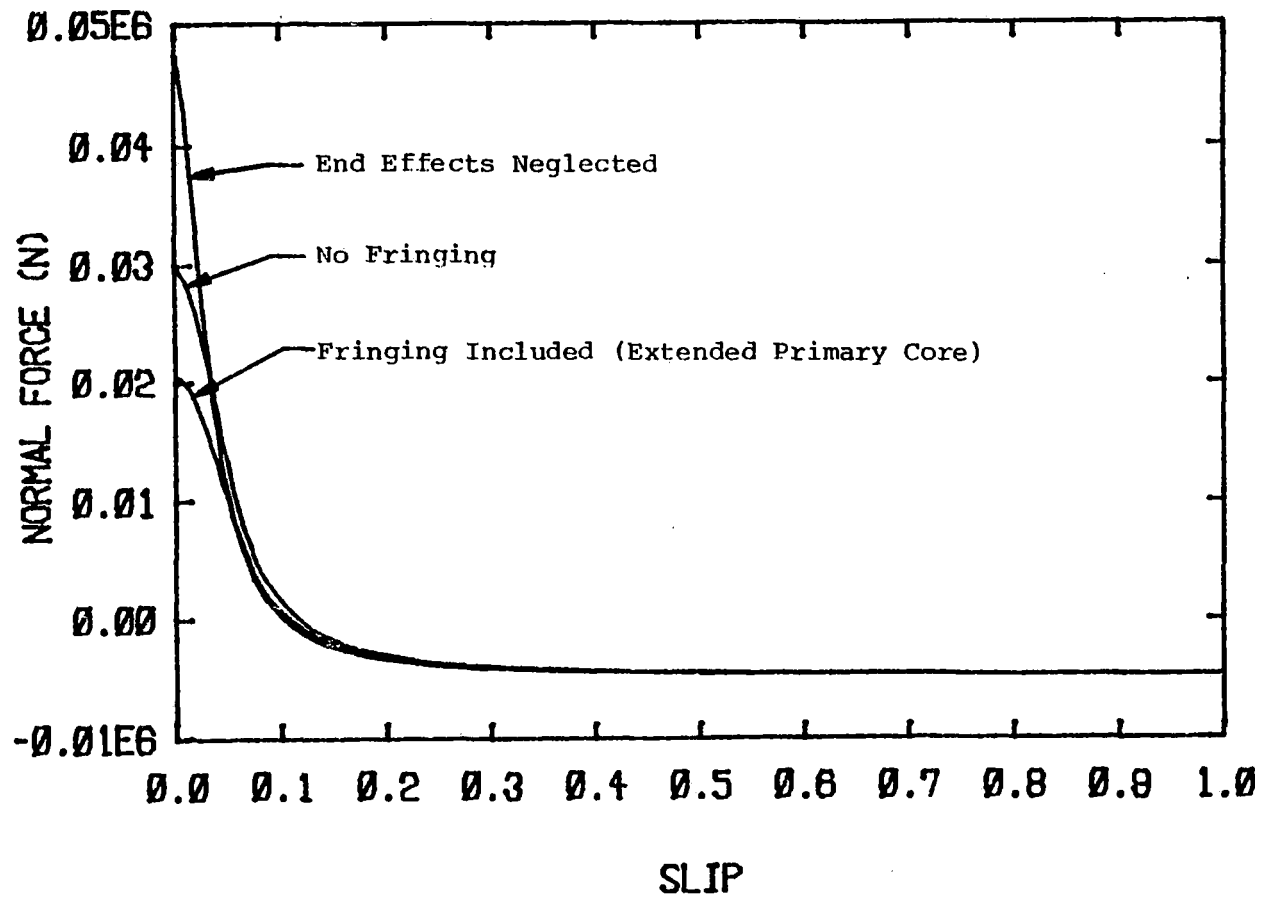
FIGURE 5.13: NORMAL FORCE VS. SLIP FOR LIM DESIGN 2
(Peak Phase Current=241.52 A, Excitation Frequency=360.0 Hz)
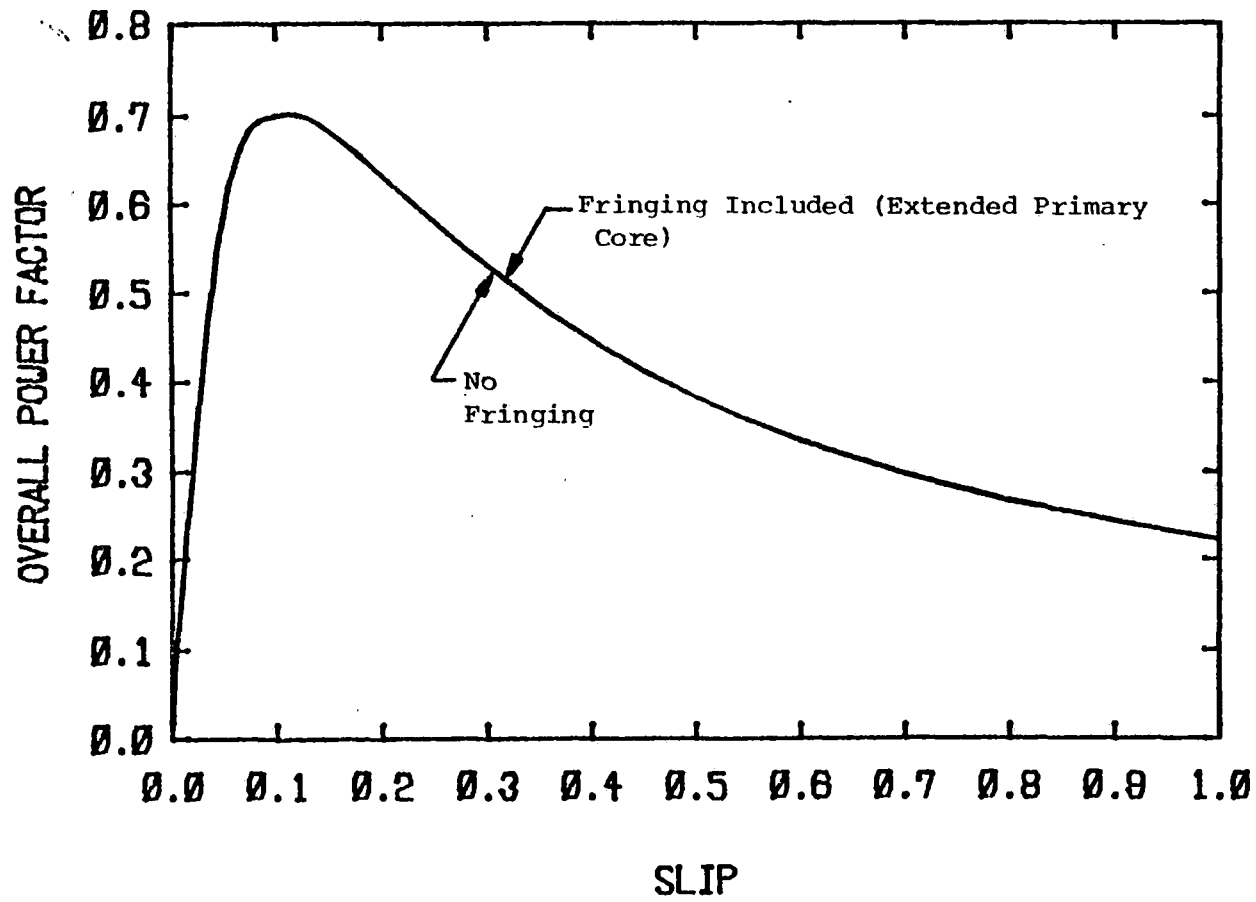
FIGURE 5.14: POWER FACTOR VS. SLIP FOR LIM DESIGN 2
(Peak Phase Current=241.52 A, Excitation Frequency=360.0 Hz)
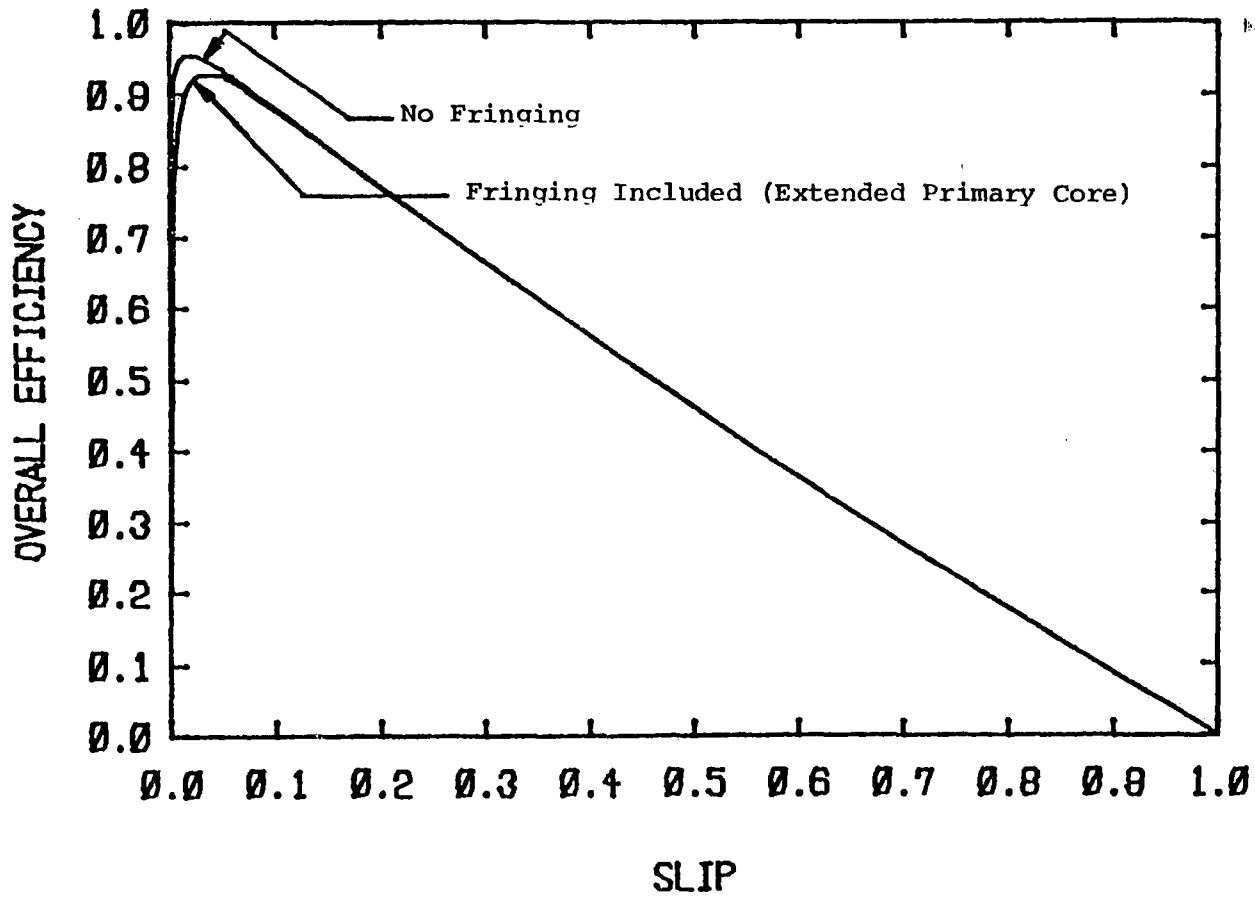
FIGURE 5.15: EFFICIENCY VS. SLIP FOR LIM DESIGN 2
(Peak Phase Current = 241.52 A, Excitation Frequency=360.0 Hz)

6. SUMMARY

6.1 SUMMARY

In this study, research has been performed to accomplish the following objectives.

(1) To review past and present high-speed TLV systems and recent low-speed AGT systems employing both noncontacting suspension and propulsion and conventional rail technology

(2) To review development of the linear motor as a means of vehicle propulsion

(3) To develop and verify experimentally, models for linear induction motors employing all-steel reaction rails (ASLIM) and aluminum clad steel reaction rails (ALLIM)

(4) To assess, using the model for the ASLIM, the feasibility of providing a supplementary propulsion and braking of a conventional rail vehicle with a LIM interacting with existing rails.

(5) To consider application, for the ALLIM, of the normal force generated by a LIM interacting with an aluminum clad, steel reaction rail to suspension of a high-speed maglev vehicle.

The review of high-speed maglev systems has led to a classification of these systems into two groups: the electromagnetic suspension systems developed in West Germany and the electrodynamic suspension systems developed in Japan. The EMS system uses the attraction force generated by feedback-controlled electromagnets; the EDS system uses the repulsion force produced by superconducting magnets moving over a conductor. Research on high-speed EMS technology includes vehicle power pickup, on board PCU size reduction, and activation of the guideway for active track systems. Research in EDS systems is examining reduction of the weight of on-board cryogenic hardware, the reduction of the drag inherent in EDS systems, and the need for increased suspension damping.

In recent years attention has focused on low-speed systems that use automation, small headways, and the combined technology of conventional rail and maglev systems. Several systems built in the United States, Canada, France, West Germany, and England have been reviewed.

The utilization of the linear motor for vehicle propulsion has been reviewed. Linear motor propulsion may be classified into three categories:

(1) Passive track with linear induction motor propulsion

(2) Active track with linear synchronous motor propulsion

(3) Passive track with linear synchronous homopolar
motor propulsion

Research and development of additional types of linear motors for
vehicle application have been outlined.

The review of advanced systems has shown that no fundamental techni-
cal barriers exist to prohibit implementation of advanced, high-
speed systems; however, for each system further engineering devel-
opment is required before it is ready for revenue service. While
a number of the technical issues normally associated with the
development of a new technology remain to be solved, the princi-
pal issues related to implementation concern the economic aspects
of new systems and in particular the large capital investment re-
quired of a new system.

This economic factor coupled with the development of advanced rail
systems have tended to decrease the research and development in-
terest in tracked, levitated systems in many countries, with the
exceptions of West Germany and Japan.

Performance models for the linear induction motor interacting
with an all-steel secondary (ASLIM) and an aluminum clad steel
secondary (ALLIM) have been described. These models predict
thrust, normal force, power factor, and efficiency, as a function
of the operating conditions and LIM design parameters.

A scale-model LIM test facility has been utilized to obtain LIM
performance data.

For an all-steel secondary, the model for the ASLIM has correctly
predicted the trends of the measured performance. The numerical
agreement between theory and experimental values is satisfactory
for the purposes of this study.

For a track in which an aluminum sheet has been bonded to the
steel, the trends of the predicted and measured performance are in
agreement. The numerical agreement is adequate for the purposes
of this study.

Two applications of the LIM to vehicle systems have been considered.
The first application utilizes LIMs interacting with existing con-
ventional rails, to provide or supplement thrust and braking of a
CR vehicle. This system is notable because it avoids the sub-
stantial cost of added aluminum-clad, steel reaction rails.
Furthermore, the generated propulsion or braking forces are inde-
pendent of the wheel-rail adhesion limit.

The second application utilizes the normal force generated by the
LIM to provide suspension forces for a high speed (134 m/s) maglev
vehicle. The potential benefits include elimination of suspension
magnets and the propulsion reaction rail.

The ASLIM model suggests that a configuration involving LIMs
attached to the underside of a rail vehicle could be feasible.
LIMs interacting with conventional rails can provide part or all

of the vehicle thrust requirements, depending on the operating conditions and LIM length. The power factor, efficiency, LIM weight, and PCU weight are estimated for two rail vehicles employing the LIM in this manner.

Investigation of the feasibility of utilizing the normal force generated by a LIM interacting with an aluminum clad steel reaction rail for vehicle lift indicates that a LIM designed to produce adequate lift as well as propulsion would be prohibitively heavy. The potential for application of the LIM normal force to the typically smaller guidance force requirements is also discussed. A configuration with two LIMs on each side of the vehicle is considered.

6.2 POTENTIAL OF LINEAR MOTORS FOR ADVANCED APPLICATIONS TO CONVENTIONAL RAIL

The application of the LIM to conventional rail vehicles in the manner described above merits further consideration. Several areas need to be investigated.

A study of the application of the ASLIM to rail vehicle braking is suggested. The LIM produces a braking force when the primary and traveling air gap waves are moving in the same direction relative to the reaction rail. This occurs in two instances.

(1) The vehicle (primary) is moving faster than the synchronous speed of the LIM ($S < 0$).

(2) The air gap traveling wave is moving in the same direction relative to the vehicle (primary) as the vehicle is moving relative to the reaction rail ($S > 1$).

Both cases can be modeled with the analysis developed by inserting the slip values of interest.

Experimental measurements of ASLIM performance with an actual rail should be performed to confirm that adequate performance is achievable with the material and cross-section of a conventional rail. There is a possibility of increasing the effective width of the LIM by fabricating the primary to conform with the shape of the upper rail surface.

Additional experimental work is required to ascertain that the model developed here would be valid for the full range of operating conditions. End effects are neglected in the ASLIM model. Furthermore, the correction factor for the secondary resistivity may have to be altered when the widths of the secondary and primary differ.

The effects of the substantial normal force should be considered. The potential benefits include improved stability and wheel-rail adhesion. However, the increased wheel and rail wear may outweigh these benefits.

7. REFERENCES

(1) Katz, R.M., "TLV Status Report," MTR-7599, The MITRE Corporation, McLean, Virginia, October 1977.

(2) Katz, R.M., Swanson, C., del Cid, L., "Non-Contacting Suspension and Propulsion Systems for Transportation Applications," Report No. DOT/RSPA/DPB25/81/16, MTR-80W376, The MITRE Corporation, McLean, Virginia, May 1981.

(3) Glatzel, K., Schulz, H., "The Research and Development Program of Magnetically Suspended Transport Systems in the Federal Republic of Germany," The 1980 International Conference on Cybernetics and Society, Cambridge, Massachusetts, October 8-10, 1980.

(4) Glatzel, K., Khurdoch, G., Rogg, D., "The Development of The Magnetically Suspended Transportation System in the Federal Republic of Germany," IEEE Transactions on Vehicular Technology, Vol. VT-29, No. 1, pp. 3-17,

(5) Yamashita, H., "Progress of Research and Development on Repulsive Levitation Railway in JNR," Japanese National Railways Quarterly Reports, Vol. 19, No. 3, pp. 99-105, 1978.

(6) Publication by Japan-U.S. Transportation Research Panel on Magnetic Levitation," Department of Transportation, 1980.

(7) Gaede, P., "An Air Cushion System in Comparison to an Electromagnetic Suspension for High Speed Ground Transportation," Krauss-Maffei Report, June 1974.

(8) Hikasa, Y., Takeuchi, Y., "Detail and Experimental Results of Ferromagnetic Levitation System of Japan Air Lines HSST-01/02 Vehicles," pp. 35-41, February 1980.

(9) Nakamura, S., Aizawa, H., Eno, S., "Test Results of HSST Maglev System," Japan Air Lines, The 1980 International Conference on Cybernetics and Society, Cambridge, Massachusetts, October 8-10, 1980.

(10) MacKinnon, Duncan, "Japanese Tokyo/Narita-Haneda Airports High Speed Maglev Transportation System," Memorandum at the Department of Transportation, April 1976.

(11) Gottzein, E., Meisinger, R., Miller, L., "The 'Magnetic Wheel' in the Suspension of High Speed Ground Transportation Vehicles," IEEE Transactions on Vehicular Technology, Vol. VT-29, No. 1, pp. 17-23, February 1980.

(12) Koerv, P., "Control Systems for Operating the Long Stator Maglev Vehicle TR05," IEEE Transactions on Vehicular Technology, Vol. VT-29, No. 1, pp. 23-34, February 1980.

(13) Klapas, D., et al., "Electric Arc Power Collection for High-Speed Trains," Proceedings of the IEEE, Vol. 64, No. 12, December 1976.

(14) Conversation with Donald Shulsinger concerning current DOT-sponsored research being conducted by Professor John Kassakian and Donald Shulsinger at M.I.T.'s Electri Power Systems Engineering Laboratory, April 1980.

(15) Fujiwara, S., "Damping Characteristics of the Repulsive Magnetic Levitation Vehicle," Japanese National Railways Quarterly Reports, Vol. 21, No. 1, pp. 49-52, March 1980.

(16) Miyazaki, K., "The Magnetic Levitation Railway-Results of the Miyazaki Tests and Future Plans," Japanese Railway Engineering, Vol. 20, No. 9, 1981.

(17) Kasai, K., "Test Results in the Miyazaki Test Track for Magnetic Levitation Vehicle," Japanese National Railways Quarterly Report, Vol. 21, No. 1, March 1980.

(18) "Intermediate Capacity Transportation System," Publication by Urban Transportation Development Corporation, Ltd., Toronto, Canada.

(19) Rule, R.G., Gilliland, R.C., "Combined Magnetic Levitation and Propulsion: The Mag-Transit Concept," IEEE Transactions on Vehicular Technology, Vol. VT-29, No. 1, pp. 41-49, February 1980.

(20) Jayawant, B.V., "Passenger Carrying Vehicles Using Controlled DC Electromagnets," University of Sussex, The 1980 International Conference on Cybernetics and Society, Cambridge, Massachusetts, October 8-10, 1980.

(21) May, Hardo, "Controlled Permanent Magnet (CPM) Configurations Generating Forces for Lift, Guidance and Thrust," University of Braunschweig, The 1980 International Conference on Cybernetics and Society, Cambridge, Massachusetts, October 8-10, 1980.

(22) Yamamura, S., "Theory of Linear Induction Motors," John Wiley & Sons, University of Tokyo Press, 1972.

(23) Kliman, G.B., Mischler, W.R., Oney, W.R., "Performance of a Single-Sided Linear Induction Motor with Solid Back above and with Various Misalignments," General Electric Co., Report No. FRA/ORD-80/53-1, September 1980.

(24) Katz, R., "Integrated Suspension and Propulsion of Guided Ground Transportation Vehicles with a SLIM," The MITRE Corporation, Report No. UMTA-VA-06-0035-79-1, January 1979.

(25) Eastham, A.K., Dawson, G.E., Pringle, D.M., Davidson, J.A., "Comparative Experimental Evaluation of the Performance of a SLIM with a Solid-Steel Reaction Rail and with an Aluminum-Capped Reaction Rail," Canadian Institute of Guided Ground Transport, Transport Canada Report No. TP2909, January 1981

(26) Yamazoe, H., "Analysis and Experiments of Single-Sided Linear Induction Motor," Japanese National Railways Quarterly Report, Vol. 22, No. 3, pp. 118-122, 1981.

(27) Poloujadoff, M., "The Theory of Linear Induction Machinery," Oxford University Press, 1980.

(28) Rummich, E., "Synchronous Linear Machines," Bull. Assoc. Suisse Electr., Vol. 63, No. 23, pp. 1338-1344, November 11, 1972.

(29) Levi, E., "Linear Synchronous Motors for High Speed Ground Transportation," IEEE Transactions on Magnetics, Vol. MAG-9, No. 3, pp. 242-248, September 1973.

(30) Levi, E., "Preliminary Design Studies on Iron-Cored Synchronously Operating Linear Motors," Polytechnic Institute of New York, Performed for Federal Railroad Administration, May 1976.

(31) Mischler, W.R., Nondahl, F.A., "Performance of a Linear Synchronous Motor with Laminated Truck Poles and with Various Misalignments," General Electric Co., Report No. FRA/ORD-80/ 5-21, September 1980.

(32) Slemon, G.R., Dewan, S.B., Burke, P.E., Straughen, A., Bhatice, R., "Study of an Analytical Model of the Homopolar Linear Synchronous Motor," University of Toronto, Transport Canada, Report No. TP2856E, January 1981.

(33) Dawson, G.E., Unteregelsbacker, E., "A Transverse Laminated Linear Synchronous Homopolar Machine," IEEE/AIS Annual Meeting Conference Record, Cincinnati, Ohio, October 1980.

(34) Balchin, M.J., "Operating Characteristics of a Heterpolar Linear Synchronous Motor," IEE Colloquiam on Advanced Ground Transportation Schemes, Digest No. 1979/27, 1979.

(35) El-Portably, A.M., et al., "Steady State Performance Characteristics of Linear Reluctance Motors," IEEE Transactions on Magnetics, Vol. MAG-15, No. 6, November 1979.

(36) Umemori, F., et al., "Development of D.C. Linear Motor-Fundamental Construction and Feasibility," IEEE Transactions on Power Apparatus and Systems, Volume PAS-98, No. 4, July/ August 1979.

(37) Umemori, F. "Construction and Characteristics of DC Linear Motor," Japanese National Railways Quarterly Reports, Vol. 21, No. 1, pp. 22-28, March 1980.

(38) Slemon, G.R., et al., "A Linear Synchronous Motor for Urban Transit Using Rare-Earth Magnets," Digest of the 1978 Intermag Conference, Florence, Italy, May 9-12, 1978.

(39) Weh, H., "Linear Synchronous Propulsion with Permanent Magnet Excitation," University of Braunschweig, The 1980 International Conference on Cybernetics and Society, Cambridge, Massachusetts, October 8-10, 1980.

(40) Ross, J.A., "ROMAG Transportation System," Proceedings of the IEEE, Vol. 61, No. 5, pp. 617-620, May 1973.

(41) Katz, R.M., Eastham, A.R., Dawson, G.E., Atherton, D.L., Schwalm, C.L., "Integrated Magnetic Suspension and Propulsion of Guided Ground Transportation with a SLIM," IEEE Transactions on Vehicular Technology, Vol. VT-29, No. 1, pp. 61-64, February 1980.

(42) Nene, V.D., "Use of Linear Motors for Conventional Railroad Applications," The MITRE Corporation, Technical Report MTR-79W00369 for the Federal Railroad Administration, December 1979.

(43) Usami, Y., et al., "Linear-Motorized Yard Automation System," Japanese National Railways Quarterly Report, Vol. 14, No. 4, pp. 207-213, 1973.

(44) Sweet, L.M., Caudill, R.J., Garrard, W., "Improvement in Rail Vehicle Dynamic Performance Through Control of Linear Motor Lateral and Normal Forces," Draft Final Report for Phase One, Prepared for Department of Transportation, September 26, 1980.

(45) Oda, Kazuhiro, "Comparative Evaluations for Linear Motor/Vehicle Configurations In Order to Improve Rail Vehicle Dynamic Performance," S.M. Thesis, Princeton University, December 1980.

(46) Sweet, L.M., Caudill, R.J., Garrard, W., "Improvement in Rail Vehicle Dynamic Performance Through Control of Linear Motor Lateral and Normal Forces," Quarterly Report No. 5, Prepared for Department of Transportation, September 1981.

(47) "New French Railroad Will Take Steep Slope in its Stride," The New York Times, February 22, 1981.

(48) "Shinkansen," Publication by Japanese National Railways, International Department, January 1981.

(49) Boocock, D., Newman, M., "The Advanced Passenger Train," The Institution of Mechanical Engineers, Proceedings 1976, Vol. 190, 62/76.

(50) "Analysis of Intercity Passenger Transportation Alternatives for Mobility and Energy Savings," Aerospace Corporation Technical Report, ATR-79(4848), December 1979.